Polyelectrolyte Multilayer Growth Factor Delivery: Mediating Tissue/Device Interactions

by

Mara Lee Macdonald

B.S. Chemical Engineering
University of Colorado, Boulder (2002)

SUBMITTED TO THE HARVARD-MIT DIVISION OF HEALTH SCIENCES AND TECHNOLOGY IN PARTIAL FULFILLMENT OF THE REQUIREMENTS FOR THE DEGREE OF

DOCTOR OF PHILOSOPHY IN CHEMICAL AND BIOMEDICAL ENGINEERING
AT THE
MASSACHUSETTS INSTITUTE OF TECHNOLOGY

JUNE 2010

Signature of Author: _____
Mara Macdonald
Harvard-MIT Division of Health Sciences and Technology
, 2010

Certified by: _____
Paula T. Hammond
Bayer Professor of Chemical Engineering
Thesis Supervisor

Certified by: _____
Robert Langer
Institute Professor
Thesis Supervisor

Accepted by: _____
Ram Sasisekharan, Ph.D.
Director, Harvard-MIT Division of Health Sciences and Technology
Edward Hood Taplin Professor of Health Sciences & Technology and Biological Engineering

Polyelectrolyte Multilayer Growth Factor Delivery: Mediating Tissue/Implant Interactions

by

Mara Lee Macdonald

Submitted to the Harvard-MIT Division of Health Sciences and Technology
on May 10, 2010 in Partial Fulfillment of the Requirements for the Degree of
Doctor of Philosophy in Chemical and Biomedical Engineering

Abstract

This thesis focuses on the use of ultrathin therapeutic protein delivery films to control host tissue/medical device implant interactions, thereby reducing complications that lead to implant failure. The Layer by Layer (LbL) deposition platform was used to fabricate conformal, tunable, micron scale reservoirs for the controlled release of a wide variety of proteins including enzymes, growth factors, and antibodies that were shown to be capable of directing cells *in vitro* to desired outcomes including proliferation, differentiation, and quiescence. Film release profiles were controlled through rational polymer design, tuning film composition, and varying film architecture. In studies with a model protein lysozyme, 100% retention of protein function was observed, underscoring gentle process conditions. *In vitro* experiments with Fibroblast Growth Factor-2 (FGF-2) and Bone Morphogenetic Protein -2 (BMP-2) showed that released growth factors are *more* active than growth factors supplemented in medium, suggesting a surface concentration mechanism and/or specific growth factor interactions with LbL film components. Anti-VEGF releasing LbL films afforded new opportunities to modify cancer therapy nanoparticles for multitherapeutic release, and provided an important switch to turn *off* the cellular response to growth factors. Using an orthopedic hip implant model as a test case, the first LbL film with enough growth factor load to direct *in vivo* host cell response was demonstrated. BMP-2 releasing LbL films were used to direct MC3T3 pre-osteoblast differentiation *in vitro*, and the differentiation of host mesenchymal stem cells in a rat quadriceps model *in vivo* to form bone tissue in a first generation model for remediating orthopedic hip implant complications. Preliminary data on second generation, multifunctional drug delivery films are promising. These studies contribute to the mechanistic design of protein LbL films and show promise for a wide variety of clinical applications, opening avenues for multifunctional drug delivery from LbL films.

Thesis Supervisor: Paula T. Hammond, Bayer Professor of Chemical Engineering
Thesis Supervisor: Robert Langer, Institute Professor

Thesis Supervisors

Paula T. Hammond, Ph.D
Bayer Professor and Executive Officer of Chemical Engineering
Massachusetts Institute of Technology

Robert S. Langer, Sc.D
Institute Professor
Massachusetts Institute of Technology

Thesis Committee

Myron Spector, Ph.D (Chair)
Professor of Orthopedic Surgery
Harvard Medical School

Sangeeta N. Bhatia, M.D., Ph.D
Professor of Health Sciences and Technology
Professor of Electrical Engineering and Computer Science
Massachusetts Institute of Technology

Acknowledgments

I have been blessed to have the support and encouragement of many phenomenal people during my doctoral work at MIT and Harvard, without whom I could not have accomplished the thesis I present here today.

I am grateful to my advisors, Paula Hammond and Bob Langer for their myriad contributions to my training. Beyond presenting world class challenging and fascinating research concepts, contributing to my professional development, and providing excellent mentors and role models, they are two of the kindest people I know in academia.

I am thankful to my thesis chair Myron Spector and my thesis reader Sangeeta Bhatia for their attention and the rigor they have brought to my thesis. I have enjoyed intellectually stimulating and exciting conversations with each of them, and count myself fortunate to have been honored by their presence on my thesis committee. I would also like to thank two other mentors here. I thank Mary Bee Chan of Nanyang Technological University for welcoming me to her lab in Singapore for my Fulbright research. Finally, I most gratefully thank Xuedong Liu, my undergraduate senior thesis advisor and a truly excellent mentor, who started me down this amazing path and has stood behind me staunchly ever since. Through all of these people's invested time and belief in me, I have flourished.

I cannot imagine two better lab groups to be a part of than the Hammond and Langer groups. I thank Kris Wood and Helen Chuang for mentoring me as I was establishing my thesis area in the Hammond group. I have counted Dan Kohane in the Langer lab as a friend and mentor from the early days in Boston. I am thankful for all of the wonderful, unique individuals of the LbL drug delivery and linear dendritic block-copolymer subgroups in the ISN. In particular, Anita Shukla and Renee Smith have been my sounding boards and partners. Kevin Krogman is my unofficial "angel" at the ISN, helping me with everything from finding a screwdriver to building spray LbL machines. Finally, last but not least, I am forever in the debt of Ray Samuel, who has contributed enormously to both my understanding of science and the process of becoming a PhD.

Much of the richness of my PhD experience has come from the wonderful friends I have made while here. In a big part this is a shout out to all of the HST PhDs and MDs (you know who you are), who have danced, laughed, cried, rallied, bummed around, ran around, skied, camped, climbed, and generally shared the unique angst of being PhD (or MD) students with me. HST's wealth is in you guys. MIT Chemical Engineering has yielded another wonderful group of friends. I would also like to thank Tamahine o'Tairi and in particular Beth Sievert, as well as Christopher Zebo and the Salsa Crew (Ravi Purushotma, Rahmat Cholas, Grace Kim, Ashley Evans, and Divya Bolar), for giving me reasons to dance. While in Singapore, I

counted on Becky Snyder, Dana Hornbeak, Philip Stenberg, and Margaret Tay. You have all made my life so rich.

I am incredibly grateful to the amazing administrative staff that make MIT and Harvard run. Christine Preston, Linda Mousseau, Connie Beal, Ilda Thompson, and Bethany Day are the ones who made my MIT function. Patty Cunningham at Harvard is amazing. I am grateful to Kim Benard for her fantastic support in helping me get the Fulbright, and to Julie Greenberg and Traci Anderson for all that they do in the HST office for the students. There will always be a special place in my heart for Cathy Modica, who cannot be easily classified in terms of her role in my life. Cathy for me will always be the heart of HST.

This fantastic ride of a PhD at MIT and Harvard has been made so much sweeter by meeting Divya Bolar, my boyfriend of 3 years. During the ups and downs and the learning processes I have encountered here (and while on my Fulbright fellowship), he has been a sounding board, a teacher and a friend. It is always difficult to describe love, but simply put, he has my love, and I treasure our time together. I am lucky to have the happiness that we share.

I dedicate this thesis to my family. This is to my Mom for sharing her particular brand of mother's love, passion for life and education, the outdoors, and medicine with me while instilling in me a strong sense of justice, and also for percussing me starting from an early age. To my Dad for ingraining a good work ethic, high standards, an ability to look at the big picture, and the confidence to throw it all to the wind and start from scratch – and for his own particular brand of love. To my sister for being my earliest friend, one of my best teachers, providing the counterpoint of my scientific point of view, and expanding my horizons, both intellectually and geographically. To my brother for being a punk and a partner in hurtling off cliffs, both physical and intellectual, and for reminding me that nothing in life is worth doing at less than full steam. To my aunts and uncles on both sides for their support and love, and finally, last but not least, to the four incredible people who are my grandparents. Two notes of interest here: MIT has been instrumental in my mother's family history from the time that they emigrated from China during World War II; I am thankful to my grandfather H.Y. Fan for the scientific culture of my family (as well as for his love!) and honored to carry on the tradition. A special loving thought goes out here to Li Nien Bien Fan, my last living grandparent, who turned 90 this February, and to Hilda Macdonald, who has passed away, but whom I remember with fondness. I'm so proud of you all, and love you deeply.

MARA LEE MACDONALD

Massachusetts Institute of Technology and Harvard Medical School,
May 10, 2010

Financial support for this work is gratefully acknowledged from Deshpande Center grant 009216-1 and the National Institutes of Health grant 1-R01-AG029601-01. M. Macdonald is thankful for a National Science Foundation Graduate Research Fellowship and a Fulbright Fellowship to Singapore. This work made use of MRSEC Shared Facilities supported by the National Science Foundation under Award Number DMR-0213282, and was partially supported by a Singapore Ministry of Education Tier 2 Grant (M45120007)

Contents

Figures

Tables

Introduction

In recent years, probing the qualities of the cellular microenvironment has been an area of intense research focus. One overarching theme that has emerged is that both mechanical cues including shear stress, matrix stiffness, surface roughness, and geometry, as well as chemical cues including sequence of therapeutic drugs, pH, and matrix composition strongly influence the behavior of cells. This increasing understanding of the microenvironment provides novel handles to manipulate the cellular response in human health and disease.

One arena that has a high potential to benefit from this enhanced understanding is that of implantable medical devices. From hip implants to stents to heart valves, these remarkable devices have the ability to improve the quality of life and lifespan over a vast range of diseases through simple, typically mechanical, interventions. Unfortunately, these life-saving mechanical improvements can be blunted by unintended host tissue responses (or lack thereof) to the implanted devices. Mechanical heart valves require lifelong systemic anti-coagulation therapy (quite dangerous in itself) to prevent clot formation on the device that could lead to heart attacks and strokes; reactive proliferative response to intraocular lens placement leads to proliferation of cells on the lens, clouding it and leading to secondary cataracts. The case of drug eluting stents is particularly powerful here: as a forerunner device using drug eluting coatings, it was hailed as a medical breakthrough. However, we now know that we need complex control over multiple cell types and multiple

time windows to get the integrated host tissue response necessary for implant success. Thus, the ability to control the host tissue response to the implant becomes crucial in implant technologies.

Local delivery is commonly preferred for such implant applications (preferably directly at the point of contact between the implant and host tissue). Either because of systemic side effects or off-target effects caused by systemic administration, or to avoid dilution of the potent signals necessary for a response, traditional injections fail here. Although pioneering work with delivering small molecules from implant surfaces has increased our understanding of how drug/device systems affect the disease process, therapeutic protein release from such implanted medical devices has lagged clinically behind small molecules. Because therapeutic proteins are capable of evoking extremely diverse responses from the tissues they interact with, this presents a powerful opportunity to increase implant/tissue integration. Furthermore, the ability to locally release therapeutics from *several* classes of therapeutic agents, including antibiotics, anti-inflammatory agents, and growth factors, or, alternatively, to release several growth factors from the same class, from a micron-scale coating to mediate the host tissue response therefore becomes a compelling problem that requires a novel, surface coating solution.

All of the advantages of sequentially released growth factors in implant applications are equally powerful in the area of tissue engineering and regenerative medicine. Here, being able to decouple the mechanical properties of a porous matrix from the drug release properties allows for much more flexible and tunable systems so that a simple coating system that could be applied in a combinatorial fashion to matrices of different mechanical properties. Thus, such a co- or sequential releasing growth factor coating that could be applied to the intricate geometry of such a scaffold would open many avenues of discovery both in terms of basic science and in clinically focused applications.

In this thesis, I have focused on the incorporation of growth factors and other therapeutic proteins in a surface coating drug reservoir for the tunable local sustained drug delivery of these fragile but potent molecules based on Layer-by-Layer (LbL) assembly. LbL has many attractive features discussed at length in Chapter 1, but one unique capability worth highlighting here is the potential to release multiple therapeutics, together or in sequence, from the film, placing it on the cutting edge of discoveries now into the combinations of growth factor and immune system cues necessary to successfully mediate stem cell progression and implant/tissue interactions. However, before such sequential modalities can be explored, LbL must first be characterized in terms of single entity release profiles, which form the basis for my thesis here.

Chapter 1 motivates the application of a local controlled drug delivery LbL solution in the area of drug/medical device applications in general, and for the specific case of orthopedic implants. This chapter provides an overview of the LbL technique, the current state-of-the art in LbL drug and growth factor delivery and the major limitations facing the field today.

In Chapter 2, a synthetic polymer LbL system designed to hydrolytically degrade to release a model protein, lysozyme is described. Although synthetic polymer LbL has many attractive advantages discussed in Chapter 1, before my arrival on the project, our lab had not tried to incorporate proteins into our LbL system, and we were unsure if the films would even construct properly. We thus needed to rapidly and inexpensively test the LbL system properties, which was possible using lysozyme as a "model protein". With this simple and versatile system it is shown that protein loading on the milligram scale (orders of magnitude more than that needed for biological response to growth factors), the ability for continual release over 1 month, the tunability of release through several important parameters, and retention of biological activity of protein through film construction and release are possible. These characteristics showed promise, leading to studies in growth factor and antibody systems

Chapter 3 explores the release of Fibroblast Growth Factor 2 (FGF-2), an important mitogen active in bone tissue formation, from LbL films. In this application, increasing the cellular proliferation response of progenitor cells is desired to allow for a bigger pool of cells capable of differentiating into bone. The release of biologically relevant amounts of FGF-2 from an LbL thin film reservoir is shown, which retains its activity *in vitro*.

Although the majority of this thesis details LbL fabricated through dipping the scaffold of interest in polymer solutions, in Chapter 4 the properties of sprayed LbL growth factor delivery films are explored with both lysozyme and FGF-2. Spray LbL is attractive because it is amenable to roll through, continuous processing (vs. a batch process with dipped films), and because fabrication time can be decreased from 25-50 fold compared with dip systems. Sprayed films are found to have different properties; they are thinner, and thus have lower overall drug loads and release times, although on a per-thickness basis they perform equally with dipped films. Lysozyme maintains 100% activity upon release from sprayed films, suggesting that the shear induced by the system does not affect the protein function. FGF-2 sprayed films are applied to an electrospun three dimensional polycaprolactone mat, and are observed to increase proliferation of cells exposed to the matrix, indicating that growth factor activity is maintained through the spray process.

In Chapter 5, an alternative approach to mediating cell response is explored. In this chapter, an unwanted growth factor signaling response is turned off, providing a powerful handle to interact with host tissue growth factor signaling processes. Anti-Vascular Endothelial Growth Factor (Anti-VEGF) delivery from LbL films is examined for potential use in normalizing tumor vasculature in cancer therapy, as a pertinent example of how antibodies from this growing class of therapeutics might be employed to control tissue response in another application of the LbL protein delivery platform. Anti-VEGF readily incorporates in LbL films and can be released in microgram quantities. Bioactivity knocking down HUVEC proliferation in response to VEGF is maintained.

The classic bone growth factor for inducing increased bone tissue formation is Bone Morphogenetic Protein 2 (BMP-2). In Chapter 6, *in vitro* and *in vivo* studies of BMP-2 delivery from LbL synthetic films is discussed. Here, LbL films are shown to be conformal to the complex surface of a model delivery cell scaffold. BMP-2 release from LbL films shows activity *in vitro* and *in vivo*, indicating that a micron-scale drug reservoir is capable of directing cellular microenvironment cues to enhance bone tissue growth in a living system. Release of microgram-scale quantities of growth factor from LbL films is unprecedented, but necessary for clinical intervention; the ability to grow bone in an ectopic site shows unequivocally that the bone formed is in response to the released growth factor. An introductory treatment of finding the fractional protein functionality in growth factor LbL films is also discussed. Such bone tissue regeneration is an important metric of the success of orthopedic implants.

Chapter 7 provides insights into a second project of interest done in this thesis during time spent abroad in Singapore on a Fubright Fellowship. While following the same themes of directing tissue interactions through mechanical and chemical means, the application here is patterning of diverse cell types according to pre-arranged surface signals to direct and template complex tissues through early interventions in cell organization. By first microcontact printing a fibronectin pattern on a cell resistant PDMS surface, endothelial cells can be patterned in vessel-like patterns in two dimensions. The addition of a three dimensional matrix (Matrigel™) seeded with smooth muscle cells shows that the smooth muscle cells will migrate towards and align themselves with the endothelial cell pattern, yielding vessel-like forms in three dimensions precipitated through a single template cue of spatial organization. This work dovetails with the LbL work in that all of these techniques probe the cellular microenvironment to precipitate desired cell behaviors and integrations with our test devices.

The ability to create complex temporal or spatial release profiles of multiple drug compounds is important in all fields of drug delivery, but has particular significance in the

context of protein delivery from implant surfaces. The advancement of developmental biology shows that such complex profiles of different growth factors directs the growth, differentiation and functionality of cells within the embryo; for regenerative medicine to be successful, it will likely need to recapitulate such profiles. Similarly, encouraging cellular acceptance and integration of medical devices through growth factor signaling is likely to be a key functionality that decreases implant failure rates. This thesis describes the first steps taken towards achieving these important goals.

Chapter 1

Background and Significance

1.1 Controlled Local Delivery

Controlled local delivery can be defined as the delivery of therapeutic drug only to discrete target sites within the body for prolonged periods of time required to produce the desired pharmacologic outcome[1]. Although the first clinically employed controlled release system was introduced less than 35 years ago, advanced drug delivery systems have quickly grown to a multi-billion dollar market annually[2]. Compared with traditional routes of entry such as oral or intravenous delivery, controlled release systems can yield several distinct advantages[3], especially when considering delivery systems for biologic molecules such as recombinant therapeutic growth factors and antibodies:

1. ***Safety and efficacy can be improved.*** Most drugs possess a "therapeutic window" in which the desired response of therapy is effectual; above this window there is a region of drug toxicity, which is crucial to avoid, and below this window the drug is not effective. Controlled delivery can sustain concentrations in the therapeutic range, whereas oral and intravenous routes typically yield wide fluctuations in concentration that are in turn dangerous or ineffectual[1, 4]. Furthermore, local delivery can reduce the incidence of off-target effects in other body compartments, lowering toxicity and decreasing secondary effects, such as antibiotic resistance.
2. ***New drug entities require controlled delivery.*** Many biologic drugs, such as recombinant therapeutic growth factors cannot be effectively delivered by oral or intravenous routes; digestion of orally consumed proteins renders them ineffective, while intravenous or intramuscular injections are rapidly cleared (on the order of 7-

16 minutes in some cases[5]) rendering them ineffective[6]. Local, sustained release is necessary for therapeutic effect in many of these applications[7].

3. ***Controlled delivery can increase bioavailability.*** The current cost to develop a new molecular entity has been estimated at $800M USD[8], and it is estimated that 40% of failures in drug development can be attributed at least in part to in abilities to deliver the therapeutic effectively[9]. Advanced drug delivery can thus salvage useful therapeutic drugs with poor bioavailability profiles and enhance the properties of already approved drugs. Furthermore, the prolonged exposure possible with local delivery is attractive and in cases only accessible through a controlled delivery strategy.

4. ***Controlled delivery can lower costs.*** Biologic therapies are typically much more expensive than small molecule drugs; thus decreasing the amount of these expensive materials employed, especially that portion that would be lost through degradation, filtration, or larger off target body compartments would bring these highly effective therapies' price to a more clincically feasible price point that would allow quick adoption.

As a result, local drug delivery strategies have been employed in therapies for a wide variety of conditions including thrombosis, ocular diseases, infection, inflammation, osteomyelitis, and cancer[1-3, 10].

1.2 Local Controlled Delivery in Drug/Implant Combination Devices

1.2.1 Overview

Local controlled delivery is central to the success of drug/implant combination devices. The Food and Drug Administration defines a combination device as comprising "two or more regulated components, i.e., drug/device, biologic/device, or drug/device/biologic, that are

physically, chemically, or otherwise combined or mixed and produced as a single entity; or two or more separate products packaged together in a single package or as a unit and comprised of drug and device products, device and biological products, or biological and drug products" [1]. By mediating or augmenting the host tissue response to the implanted device directly at the device/tissue interface, such combinations have decreased the incidence of device failure related to infection or poor tissue response. Drug/implant combination devices can outperform the administration of the same drug and device in their conventional, separate forms[1, 11, 12], and can be cost-effective due to decreased complication rates and shorter hospital stays[13], in addition to reductions in morbidity and mortality. As such, the market for these products is expected to reach $9.5 billion USD in 2009[1]. Examples of FDA approved drug/device combinations include drug eluting stents, such as the Cordis CYPHER™ (Johnson & Johnson) and the TAXUS Express[2]™(Boston Scientific), the central venous catheters ARROWgard™ (Arrow International) and BioGuard Spectrum™ (Cook Critical Care), urinary catheters such as LubriSil I.C.™ by C. R. Bard, and bone cement Simplex P™ by Stryker Osteonics[1], the spine fusion agent Infuse™ (Medtronic), and the non-union fracture device OP-1™ (Stryker). The successes seen with these implantable devices can hopefully be replicated across many implant technologies where interfacing with host tissue is important; as this important idea spreads it is likely that delivery of biologics from coatings will become central to this goal, due to the myriad, relatively precise effects that therapeutic proteins, DNA, and other biologic products have on cellular responses.

The drug/device technologies of today largely release small molecule drugs, which are more stable than biologics in the face of harsh processing conditions. In the cases that biologics are employed, such as in Infuse™ and OP-1™, the use of an imperfect collagen carrier limits their application. For example, Infuse™ works by delivering 12 mg of BMP-2 from a bulk collagen sponge carrier for spine fusion applications at an estimated cost of $5,000-10,000 per application[14]. There are two major issues with this strategy: (1) there are well known issues with the collagen carrier, which dumps 40-60%[15] of the very costly 12 mg

dose within 3 hours ($t_{1/2}$ outside of the carrier is 7-16 minutes[5]), contributing to a clinical cost that can be difficult to justify[14]; (2) Such a collagen carrier would also be difficult to apply in instances that require a *conformal coating* to a complex implant geometry, such as in the case of most implantable medical devices such as stents, or hip implants. Here, we hope to introduce the ability to release fragile protein therapeutics, which do not respond well to traditional fabrication methods, from implantable medical devices. Simultaneously, however, we can also exploit other advantages that the LbL system holds over other methodologies.

Currently, most implant coatings are created through either (i) surface adsorption, absorption, or covalent drug attachment strategies or (ii) through encapsulation in a bulk polymer release system. While each method has merits, these systems have drawbacks that prevent full clinical utility from being achieved. Surface technologies suffer from area limits on the achievable drug load, a large burst release profile in the case of ad- and absorption strategies, and potential decreases in bioactivity with covalent drug attachment. It is also difficult to tune the release profile, loading, and time span of release of even a single therapeutic agent. Bulk polymer release systems afford greater control over release and a larger potential reservoir, but are difficult to coat on intricate, medically relevant geometries, and typically employ harsh solvents or high temperatures during polymer casting that can inactivate fragile protein therapeutics. Finally, acidic degradation products from bulk releasing films can lead to very low pH profiles within the polymer system, which can inactivate fragile proteins[16]. Finally, regardless of the incorporation strategy typically employed, there is no clear methodology to allow for *sequential, tunable* release profiles. In order to both gain access to the ability to encapsulate fragile protein therapeutics in implant coatings and also to allow for sequential release, a new methodology must be employed.

1.2.2 Orthopedic Implants: Successes and Opportunities

A particular case of in which both therapeutic protein release and sequential release are of high interest is that of the orthopedic hip implant, which we have focused on as the first implant system to test with our platform technology. In the following section, particular areas of concern and the specific focus of this thesis are discussed.

Over one million joint replacements worldwide, and half a million joint replacements in the United States, are implanted every year[17]; this number is expected to grow as the baby boomers age, younger patients such as athletes become candidates for surgery, and emerging markets have capital to spend on health improvement. Patients typically report high levels of satisfaction with such interventions, which reduce joint pain, increase range of motion, and increase quality of life. Unfortunately, approximately 10% of joint replacements fail, typically due to either joint loosening or infection[18]. Revision arthroplasty can involve up to two additional surgeries and six weeks of hospital stay, leading to significant patient morbidity and mortality and a cost of over $1 billion annually in the U.S.[19]. In these joint replacement surgeries, a well-known host of problems arise over a well known typical series of time spans; pain and inflammation are high over the first few days, implant related infections typically occur over the first two weeks, and loosening can happen over the lifetime of the implant. However, systemic drug administration cannot effectively resolve issues that arise, which makes a local delivery approach attractive and effective compared with systemic routes.

An ideal drug delivery coating would be one in which multiple therapeutic agents, either co-released or sequentially released, could be tuned to release over the time spans of these complications. However, to date, the ability to release highly controlled, highly bioactive multicomponent drug schedules from a conformal, non-planar, easily fabricated system is unprecedented. Thus as an overarching goal, we propose to create multilayered

sequentially releasing coatings that will elute the following agents over the time spans that each problem is known to arise:

1. Anti-inflammatory Agents
2. Antibiotics
3. Bone/Angiogenic Growth Factors

However, before such a combination film can be produced, each therapeutic system must be studied. *Thus, in the work presented here, my objective has been to understand and manipulate the release of fragile biologic molecules from implant surfaces to recruit and collaborate with the host tissue to enhance clinical outcomes of implant surgeries.* It is predicted that the ability to deliver bone growth factors directly from the implant surface would lead to enhanced tissue/prosthesis integration, one of the important metrics of good outcome for biologically fixated implants[20].

Our specific goals in this research have been to develop a widely applicable platform controlled delivery system capable of delivering a wide range of therapeutic proteins that can be applied to existing implanted medical devices, regardless of the size, shape, or surface chemistry of the device. The Layer-by-Layer directed self-assembly technique is employed in this work due to its unique capabilities, which are described below.

1.3 Layer-by-Layer (LbL) Drug Delivery

1.3.1 LbL Deposition

In the Layer-by-Layer deposition technique, an activated surface is sequentially dipped in aqueous solutions of chemical species with complementary functional groups which adsorb to create a nanolayered film. While the initial applications of LbL in the 1990s were done with positively and negatively charged polymers dipped sequentially on a charged surface of interest[21, 22], LbL is also possible with complementary hydrogen bonding moieties [23-25] and

Van der Waals attractions[26]. With the adsorption of each electrostatic polymer layer, the surface charge is reversed, and thus leads to self-repulsive forces that limit further adsorption; the architecture in the film can therefore be controlled with a nanometer precision that is attractive in many applications. LbL allows a high degree of flexibility of materials used, including polymers, polysaccharides[27-29], proteins[30-33], small molecules[34, 35], uncharged molecules[36, 37], carbon nanotubes[38], and dendrimers[39] while the surface the film is applied to can have virtually any surface chemistry or geometry. LbL has therefore contributed to varied applications including glucose sensors, semi-permeable membranes, electrochromic devices, gene transfection surfaces, solar cells and fuel cells[40, 41]. Finally, LbL is also compatible with existing surface patterning and templating techniques[42] and nanoencapsulation strategies[43], opening interesting possibilities in exploring the cellular response to protein exposure in localized micro-environments.

1.3.2 LbL Drug Delivery

LbL has been examined by multiple groups interested in exploiting LbL's attractive characteristics for drug delivery. Particularly in drug delivery, LbL has the advantages of being conformal to complex geometries to the nano-scale, utilizing fragile therapeutic-friendly aqueous baths (compared with the harsh solvents typically employed in bulk polymer systems) likely to preserve drug activity, and being amenable to incorporating many therapeutics and thus allowing a platform technology with multiple applications. Most crucially, because of the nano-architectured nature of the films, LbL allows a mechanism to sequester different therapeutics in different layers and thus allowing for sequential release though surface erosion[44, 45].

Early work in LbL drug delivery focused on the incorporation of model dyes[46, 47], but rapidly spread to include the incorporation of antibiotics[34, 35], anti-inflammatory agents[36], proteins and growth factors[30, 44], anti-coagulants[45], steroids[48], and DNA[49, 50], among others.

Several approaches have been taken to release drugs from LbL films. Early experiments with hydrogen bonded films showed that they fall apart rapidly at near-neutral pH, allowing a rather instantaneous method of drug release[47]. However, such release is impossible to tune, and on a shorter time span than most controlled drug delivery applications require. In a similar approach, drugs will occasionally be adsorbed electrostatically to the surface of a LbL film, with similar problems with release duration and lack of tunability[51].

Another approach is to pre-construct LbL films out of inert polymers and then load drug into the permeable network for diffusive or pH induced release[46, 52, 53]. While such porous LbL systems work well for the delivery of small molecules, the delivery of substantially larger protein therapeutics is difficult, as the therapeutic gets trapped in the polymer mesh and cannot diffuse out.

LbL films can be disrupted by submersion in high ionic strength or high pH solutions[54-56]. However, such conditions of 0.6 M or pH 8 or greater are scarce in the human body, relegating these systems to a choice few applications.

Another technique has been the coating of microcapsule templates with LbL films. Therapeutic drugs can either be encapsulated in the core, or in the LbL film surrounding the core itself[57]. Drugs in the core can either be crystalline drug which therefore is ready for solubilization and release after LbL coating[48, 54], encased in a polymer which is subsequently leached out[37, 58], or absorbed into the capsule once the template core is dissolved[59]. However, as non-degradable polymers are typically used, release is diffusive in nature and thus not easily tuned, and such microcapsules do not take advantage of the conformal nature of LbL in the implant setting.

With all of the above systems, there is no clear mechanism allowing for sequential release, and the coating is permanent. These limitations can be overcome by the inclusion of biodegradable materials into the LbL films to allow surface erosion of compartmentalized films and complete dissolution of the film after therapeutic release. FDA-approved

biopolymers, such as poly-(L-lactic acid) (PLLA) and poly(L-lysine) are attractive for such applications and have been utilized in LbL. However, these polymers also suffer from inherent limitations; these molecules cannot be tuned or altered *and hence the drug delivery characteristics cannot be modified for the application of interest*. Furthermore, particularly in the realm of protein release, it is known that such polymers create acidic byproducts that can lower the pH several units below neutral and potentially denature fragile protein therapeutics[16]. It is therefore of interest to find a degradable, biocompatible polymer with easily tuned drug release characteristics. Thus, the approach of employing biocompatible, biodegradable synthetic polymers which can be tuned becomes very attractive, and is described below in Section 1.3.3. In Table 1-1, the capabilities of each LbL drug delivery strategy is summarized.

Table 1-1: Capabilities of LbL Drug Delivery Strategies

Delivery system	Sustained release	High Load	Tunable release	Sequential release
H-bonded Film	**No**	**No**	**No**	**No**
Surface Adsorption	**No**	**No**	**No**	**No**
Post Construction Absorption	**Yes**	**Yes**	**Yes**	**No**
Microcapsule	**Yes**	**Yes**	**Yes**	**No**
Degradable Biopolymers	**Yes**	**Yes**	**No**	**Yes**
Biodegradable Synthetic Polymers	**Yes**	**Yes**	**Yes**	**Yes**

1.3.3 Biodegradable Synthetic Polymers: Poly (β-aminoester)s in LbL

The approach taken in this thesis is to incorporate a cationic polymer from the class of poly(β-aminoester)s (PBAEs)[60]. These polymers are created through the simple Michael addition of two commercially available classes of starting materials; a combinatorial library can be created with different polymer characteristics[61]. Work in our group has shown PBAEs readily incorporate in LbL films[62], and that the drug delivery characteristics of PBAEs from

LbL can be varied through varying the polymer architecture[63, 64]. In particular, increasing the hydrophobicity of the region directly next to the ester linkage is predicted to decrease water access to the bond, therefore leading to a more slowly degrading polymer. However, this hydrophobicity has the dual feature of making slower-releasing films and decreasing the charge group density along the polymer backbone. It was found that increasing the hydrophobicity in LbL films led to extended release up until a critical point, at which the films would quickly fall apart and release all of the film contents due to film instability[64]. Taken together, the ready incorporation of PBAEs in LbL films combined with our deep understanding of the tunability of these polymers represent an excellent opportunity to allow synthetic polymer tuning of drug release profiles from LbL films[62]. However, PBAE protein LbL delivery films had not been explored prior to this thesis, although protein LbL systems of other varieties did exist.

1.3.4 Protein LbL Systems

Early LbL protein encapsulation was focused on creating sensors for biological substrates by embedding enzymes in a film to create a colored detection product. The enzymes glucose oxidase and peroxidase were incorporated as layers in a non-degradable LbL film. In this work, it was shown that these enzymes could retain functionality and perform their catalytic function while embedded in the film[33]. Later work with enzymes, both for their own applications and as model protein systems for growth factor delivery, continues to this day[65, 66].

Later on, work with Protein A, a potent stimulator of macrophages, proved that proteins embedded in LbL films could be constrained to distinct layers within a degradable film, and that the timing of their release could thus be controlled[30]; this work represents an important precursor to the sequential release of proteins from structured LbL films.

The field of therapeutic growth factor delivery from LbL films is still in its infancy. There are a few notable model systems. Two groups have employed the method of pre-

constructing an LbL film without growth factors and then adsorbing or absorbing the growth factors. Muller et al adsorb Vascular Endothelial Growth Factor (VEGF)[51] through electrostatic interactions to a non-degradable LbL film and show retention of bioactivity. Crouzier et al first pre-construct an ultrathin, crosslinked LbL reservoir, and then absorb Bone Morphogenetic Protein 2 (BMP-2)[53] into it. In both cases, hundreds of nanograms are released, an amount which allows reasonable *in vitro* activity assays to be performed, but below critical limits to see *in vivo* stimulation of host tissue cells. These systems also have the drawbacks of having limited reservoirs based on surface area and thickness, and loosing the important modality of sequential release.

There is only one known *in vivo* LbL growth factor system to date. Benkirane-Jessel et al have used biological polyions to construct LbL films where the growth factors Transforming Growth Factor β (TGF-β) and BMP-2 were encapsulated in spatially distinct layers, allowing for sequential release. These systems were deployed *in vitro*[44] and *in vivo*[67] by application to exogenous-sourced stem cells to show the differentiation of stem cells to the bone lineage. This work is encouraging, in both the possibility of sequential release retained by the LbL system and the in vivo effectiveness. However, the doses loaded are very small (undetectable by ELISA[67]), and utilized exogenous stem cells, which introduce possibilities such as graft vs. host disease, introduction of feeder layer cells in implantation, and the introduction of other pathogens to affect a cellular response, and do not allow for a dose large enough to manipulate a host tissue response. It is possible that polymer carrier limitations due to the inherent drug delivery profiles of the polyions use, disallow larger doses from being employed. Most importantly, in applications in which host cell response must be modified, much larger drug delivery loads are required. Thus, none of these systems retains the ability to sequentially release multiple growth factors at doses that can stimulate native host stem cells.

1.3.5 Synthetic LbL Growth Factor Delivery

Thus, in this thesis, a novel and powerful approach is taken to achieve biologic delivery from thin, polymeric coatings. This unique LbL approach allows:

- nano- to micro-scale thin films
- fabrication with an aqueous process likely to preserve fragile protein activity
- conformal coating of complex medical geometries
- tunable through synthetic PBAE chemistry, as well as multiple other handles
- sequential delivery through compartmentalization of the fabricated film
- powerful co- and sequential release schemes when combined with antibiotic and anti-inflammatory systems under development in the Hammond lab

Next-generation medical implant coating design necessitates a deeper understanding of how to deliver multiple therapeutics to interact with multiple cellular processes from the same implant coating, work that is discussed in this thesis.

Chapter 2

Explorations with the model protein lysozyme

2.1 Introduction

Layer-by-layer (LbL) deposition[21, 62], a technique in which nanoscale layers of polyanions and polycations are dipped onto a charged surface from aqueous baths, constitutes a powerful tool with applications ranging from electrochemical thin films to biocatalysis[41, 68]. LbL's many advantageous characteristics in the context of drug delivery coatings include nano-scale film architecture allowing fine control of film loading and release of multiple drugs, ability to conformally coat difficult geometries, adherence to many surface chemistries, and ease of fabrication. Particularly relevant to protein delivery, LbL deposition has the advantage of utilizing mild aqueous baths which have the potential to preserve fragile protein activity in comparison with the harsh organic solvents typically employed to fabricate protein delivery devices. When LBL films are constructed with surface eroding poly(β-aminoesters), it is furthermore possible to avoid more acidic degradation products of PLGA and PLLA (forerunner polymers in the field) and resultant low pH erosion conditions that cause proteins to denature and deactivate[16]. Finally, LbL enjoys the advantage of being compatible with existing surface patterning and templating techniques[42], opening interesting avenues to explore the cellular response to protein exposure in localized micro-environments. However, to reach the high potential of LbL in the exploration of protein-surface-cell interactions, more must be done to understand the characteristics of protein-releasing LbL films.

Original research in the LbL drug delivery field focused upon the diffusive release of low molar mass drugs from uniform, non-degradable films. While demonstrating a clear scalability of drug loading with increased numbers of layers, diffusion- or bulk dissociation-

based release typically yields "burst" profile characteristics with high drug elution at the beginning of the time course, and very low levels at the end [46]. Rarely is diffusion controlled release from LbL films sustained for more than a few hours. One notable exception to this trend was the use of nanoporous multilayer films to sequester hydrophobic drug, which resulted in release times of up to multiple days in certain cases at room temperature[52]. However, because the release time is impacted by the affinity of the drug for water, it is directly related to the hydrophobic nature of the drug, rather than an externally controlled parameter, and therefore is not a useful strategy for more hydrophilic macromolecules, such as proteins.

A few mechanisms of protein release from LbL films do not require diffusion. It is possible to coat a crystal of protein with a non-diffusive LbL shell for release under significant pH (pH 8 or higher) or ionic strength changes[54], [56] under which the shell dissipates, releasing the protein; however this is impractical for many medical applications in which such large deviations from physiological conditions would be deadly. In other cases, enzymatic breakdown of biological polymers renders release over a period of several hours[30, 69, 70]; in one case time-dependent release was shown to be possible[30], which is a positive step towards time-delayed release of protein therapeutics. However, release is dependent on specific cellular adhesion and interaction with the surface, and the loading and release of protein can be influenced by a combination of diffusion and enzymatic degradation that is more difficult to tune for sustained periods. Rather than relying upon diffusion, bulk release, or large pH changes, we hypothesized that a more linear release profile could be attained by utilizing hydrolytic surface degradation of biocompatible and degradable polymers.

The concept of using degradable synthetic polyions in LbL films addresses many of the inherent difficulties encountered with above systems while affording new, very desirable characteristics. These polymers retain biocompatibility and biodegradability while allowing tunability of polymer degradation and therefore release rates, and may have the additional

benefit of avoiding the low pH release environment of PLGA or PLLA. Surface erosion allows the possibility of linear release profiles and therefore the ability to exert stronger control over the drug release characteristics of the system. Finally and crucially, through the combination of the nanoscale architecture possible with LbL deposition with surface eroding poly(β-aminoester)s[62, 71], it is possible to create sequentially releasing devices in which the composition of individual layers changes through the thickness of the film; different proteins are released as the film erodes from the top down and dissolves layers of differing compositions, yielding exquisite control of the release profile of each incorporated protein. The widespread opportunities in tissue engineering and drug delivery available with sequential delivery require controlled, surface erosion based release, and are inaccessible with diffusion or bulk degradation based release systems.

Degradable poly(β-aminoesters) such as Poly1 and Poly2, shown in Scheme 2-1, are attractive for this purpose due to their ability to slowly degrade via ester hydrolysis at physiologically relevant pH [60], their positive charge (which allows for film construction), and because such poly(β-aminoesters) have been shown to be biocompatible in a number of different applications [71, 72, 73]. Previous work with poly(β-aminoesters) has yielded devices capable of delivering anticoagulants (heparin sulfate), anti-inflammatory agents (chondroitin sulfate[29, 45], DNA for gene therapy[49], and demonstrated proof of concept for sequential delivery[45, 74]. Attempting to incorporate proteins in such films is a natural next step; proteins delivered from synthetic LbL films would benefit from the mild processing conditions, elimination of polymers using acidic byproducts, fine control of protein incorporation, and ease of fabrication. This approach is also strongly motivated by a well-recognized need in the fields of tissue engineering and implantable medical devices to sequentially release growth factors, which can be achieved with surface erosion from LbL films. In this work, lysozyme was utilized as a model protein due to its similarity in size and shape to many growth factors. Lysozyme has a molar extinction coefficient of 38,010 and molecular weight

of 14.4 kDa, and a high isoelectric point (pI 9), and also has the advantage of being a well studied biomolecule with many assays for detection of concentration and functionality.

Finally, both lysozyme and Poly1 are cationic, necessitating a tetralayered repeat unit architecture with an anionic polymer in between Poly1 and lysozyme. Two anionic biopolymers, heparin sulfate and chondroitin sulfate, were investigated as candidates for film construction. Heparin was selected due to its well known anti-clotting properties. This is a potentially useful characteristic for a delivery device or implant coating, as clotting is a serious concern with any device that may be put into contact with the bloodstream (ie stents). Failure to address this concern may lead to myocardial infarction, stroke, or ischemia of other vital organs. However, in applications where anticoagulation would be problematic (ie at wound sites), alternative functionalities could become desirable. For example, by providing a matrix-like environment which cells can utilize to begin proliferating, it may be possible to speed the integration of an implanted device with the surrounding host tissue. Chondroitin, a native extracellular matrix component with anti-inflammatory properties, was used with this intent.

Thus here we describe for the first time the construction of polyelectrolyte multilayer films that incorporate a synthetic, hydrolytically degradable polymer capable of controlled release and a model protein of interest, constructed for the purposes of drug delivery and tissue engineering. The incorporation of protein within such constructs is examined, and the subsequent hydrolytic degradation and release of proteins from these films is described. We demonstrate tuned and sustained release of significant protein quantities from micron scale conformal thin films over periods of several days to several weeks at body temperature. Finally, the activity of the protein is addressed upon release. Such films may become significant in the sectors of tissue engineering and medical device coating technology, as increased cellular interactions with devices are sought, and the delivery of therapeutic factors at specific times during the implant lifetime become necessary.

2.2 Materials and Methods

2.2.1 Materials

Linear poly(ethylenimine) (LPEI, Mn = 25000) was bought from Polysciences, Inc (Warrington, PA) and poly(sodium 4-styrenesulfonate) (PSS, Mn = 1000000) was purchased from Sigma-Aldrich (St. Louis, MO). Chondroitin sulfate sodium salt (Mn = 60000) was obtained from VWR Scientific (Edison NJ) and heparin sodium salt was obtained from Celsus Laboratories (Cincinnati, OH). Poly1 was synthesized as previously described[60]. Poly2 was synthesized in a similar manner to Poly1, substituting a 1,6 heptane dioldiacrylate for the 1,4 butane dioldiacrylate used to synthesize Poly1. Lysozyme and Micrococcus lysodeikticus bacteria were obtained from Sigma Aldrich (St. Louis MO). All commercial polyelectrolytes were used as received without further purification. A micro-BCA assay was obtained from Pierce (Rockford, IL) and used according to manufacturer instructions. Glass and quartz slides (substrates) were obtained from VWR Scientific (Edison NJ). Deionized water (18.2 MΩ, Milli-Q Ultrapure Water System, Millipore) was used for all washing steps. Dulbecco's PBS buffer was prepared from 10x concentrate available from Invitrogen (Frederick, MD).

2.2.2 Preparation of Polyelectrolyte Solutions

LPEI and PSS were dissolved in deionized water to a concentration of 10mM with respect to repeat unit and pH adjusted to 4.25 and 4.75 respectively. Heparin, chondroitin, Poly1 and Poly2 were prepared in sodium acetate buffer (pH 5.1, 100mM) at a concentration of 2mg/mL. Lysozyme was prepared at a concentration of 0.5 mg/mL in sodium acetate buffer pH 5.1, 100 mM.

2.2.3 Film Construction

Glass substrates or quartz slides (1" x ¼") were rinsed with methanol and deionized water, dried under a stream of dry nitrogen, and plasma etched in oxygen using a Harrick PDC-32G

plasma cleaner on high RF power for 5 minutes. Ten base layers of (LPEI/PSS) were deposited upon plasma etched substrates to create a surface area 0.75"x 1/4" with a Carl Ziess HSM series programmable slide stainer according to the following protocol: 5 minutes of dipping in LPEI, followed by three washes (10, 20, 30s respectively) in deionized water, followed by 5 minutes in PSS and three deionized water washes (10, 20, 30s) for 10 repetitions. On top of the base layers, tetralayers were stepwise built stepwise, adding a layer of PolyX (+), polyanion (-), lysozyme (+), and polyanion (-) to the surface to create the following architecture: $(PolyX/polyanion\ /Lysozyme/polyanion)_n$ where the PolyX is either Poly1 or Poly2, the polyanion is either heparin or chondroitin, and n refers to the number of tetralayers deposited on the substrate. A typical dipping protocol is 10 minutes in a solution of Poly1 dissolved in 100 mM sodium acetate buffer, pH 5.1, 3 washes (10, 20, 30 s) in deionized water, 7.5 minutes in heparin dissolved in 100 mM sodium acetate buffer, pH 5.1 with 3 washes (10, 20, 30s) in deionized water, 10 minutes in lysozyme in 100 mM sodium acetate buffer with 2 washes (20, 30s) in deionized water and 7.5 minutes in heparin in 100 mM sodium acetate buffer with 3 deionized water washes. Films were controlled to be 0.75 inches x 0.25 inches in size, or roughly 1.2 cm^2. Note that by changing the contents of a dipping bath, different molecular species can be loaded in different layers of the film, allowing sequential release. Once a film is constructed, placement in phosphate buffered saline triggers hydrolytic degradation of the poly(β-aminoester), allowing release of protein.

2.2.4 Film Characterization

Varying numbers of tetralayers were dipped onto clean quartz substrates pre-treated with 10 base layers. Three techniques were used to analyze buildup. The thickness of the resulting films was measured by scoring the samples to the base of the film with a razor blade and measuring the step height using a profilometer (P10 Surface Profiler) with a 2um tip radius stylus. Protein incorporation in the film was measured by UV-Vis spectroscopy. A profile was taken of each sample on a Cary 6000i spectrophotometer from 200-800 nm.

Proteins absorb light at 280 nm due to tryptophan, tyrosine, and cystine, and intensity of absorption can then be correlated to protein buildup within the film. The absorbance value at 320 nm (baseline) was subtracted from the absorbance value at 280 nm and plotted according to number of tetralayers. Instantaneous release was used to quantify the total protein concentration in the film by using 1 mL of 1M NaOH for 1 hour, which disrupts film architecture and releases all incorporated protein. A 50 uL sample was quenched in 1X PBS and read using a micro-BCA Protein Assay Kit (Pierce Biotechnology, Rockford IL). Briefly, bicinchoninic acid can be used to quantify protein concentration by detecting a reduction of copper by the protein of interest in an alkaline environment. A color change can be monitored and compared to a constructed standard curve. Triplicate 100 uL aliquots of standards and samples were run in 96 well plates according to the manufacturer's protocol and read on a microplate reader (PowerWave XS, BioTek, Winooski VT).

2.2.5 Release Characterization

Samples were released into phosphate buffered saline pH 7.4 at either room temperature or 37 degrees Celsius in a microcentrifuge tube containing 1 mL of PBS. At a series of different time points, 0.5 mL of sample was removed and 0.5 mL of fresh PBS was introduced to the sample container. Samples were frozen at -20C until analyzed. Two methods were used to detect release of lysozyme into the solution. A micro-BCA Protein Assay Kit (Pierce Biotechnology, Rockford IL) was used to detect the total amount of protein released during a time point. To track the functionality of the released protein, bacterial lysis experiments were performed[75]. A cloudy suspension of bacteria lysed by lysozyme will lead to clearing of the solution, which can be tracked as a decrease in absorbance at 450 nm. This work is done as a kinetic plate reading assay, in which the slope of the graph of [absorbance at 450 nm versus time] calculated for samples and standards is proportional to the concentration of enzyme present in the solution. A standard curve of [concentration vs slope] from 200-0 μm is constructed (which is linear over this concentration range), and the concentrations of the

unknown samples interpolated based on the slope of each individual sample. In these tests, 290 uL of a 0.25 mg/mL solution of Micrococcus lysodeikticus was mixed with 10 uL of samples and standards performed in triplicate and read in a 96 well plate at 450 nm every 15 seconds for a total of 10 readings. The readout from the assay is a concentration of enzyme present based on the lysing ability of the sample, and thus represents the concentration of functional protein present in the sample. Error bars for all figures in this paper represent a 99% confidence interval calculated from triplicate repeat samples of 2 independent trials (total of 6 data points).

2.3 Results and Discussion

2.3.1 Film growth characteristic implications for loading, release, and interdiffusion

Films were constructed using pH 5 sodium acetate baths of heparin, lysozyme, and Poly1 and washed with deionized water to create films with the architecture (Poly1/heparin/lysozyme/heparin). Film buildup was tracked by monitoring thickness, protein incorporation, and instantaneous protein release (Figure 2.1, Table 2.1). After a brief induction period where little protein incorporation, film thickness, or protein release is achieved (approximately 10-20 tetralayers), all three methods indicate that the films build and incorporate protein in a roughly linear fashion.

Table 2-1: Comparison of film characteristics of the three types of film discussed herein. Thickness of the films was measured using profilometry, and film protein incorporation was measured indirectly with UV-Vis measurement of absorbance at 280 and directly through instantaneous dissolution of films and quantification of the released protein.

	Film thickness in um	UV-Vis absorbance of film at 280 nm	Total protein incorporated (ug/cm^2)
(Poly1/chondroitin/lysozyme/chondroitin)$_{50}$ film	2.73	0.24	133
(Poly1/heparin/lysozyme/heparin)$_{50}$ film	7.92	1.24	650
(Poly 2/heparin/lysozyme/heparin)$_{50}$ films	13.23	1.52	800

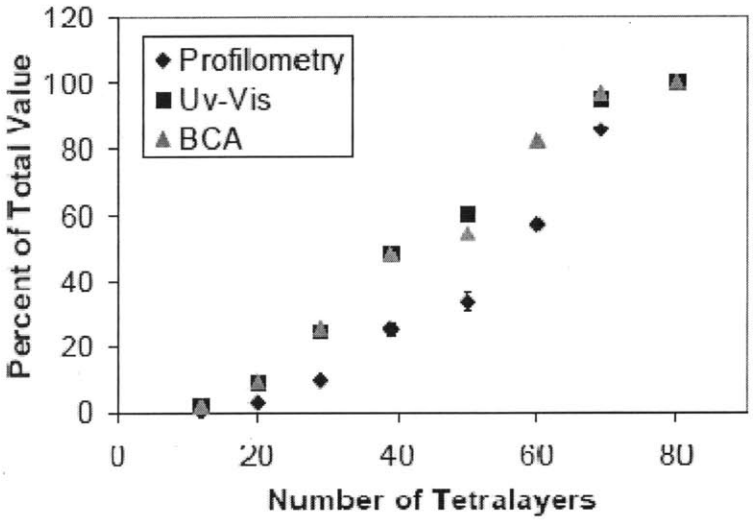

Figure 2-1.1: Film characterization of (Poly1/heparin/lysozyme/heparin) tetralayers by UV-Vis spectroscopy, profilometry and instant dissolution methods. Percent of value at 80 tetralayers is plotted vs. number of tetralayers to allow comparison of curves. Agreement is seen in the three methods of detecting film building indicating that the films are growing in thickness and incorporating protein.

An induction period for multilayer growth is typical of many LbL systems and has been reported in the literature[76, 77]. In this initial period, surface effects are hypothesized to influence the buildup of the LbL film until complete surface coverage is achieved after

several adsorption cycles. In comparing the two techniques which measure protein content (UV-Vis, and BCA) and that which measures total film buildup (profilometry), it appears that protein incorporation becomes linear after approximately 10 tetralayers, whereas the thickness increase becomes linear at approximately 20 to 30 tetralayers. The thickness per tetralayer repeat unit in the linear growth regime is approximately 0.42 μm, which is large in comparison with typical electrostatic multilayer systems that exhibit 0.01 to 0.03 μm per bilayer pair, and suggests that although protein incorporation is substantial after just 10 tetralayers, the polymer composition in the film may be changing in a nonlinear fashion during this initial period. This regime of superlinear growth is hypothesized to be due to intermolecular interdiffusion of macromolecules into the film during the adsorption process, which leads to increasingly thick films[77, 78] until a constant repeat unit thickness is ultimately achieved[76]. However, unlike asymptotic growth films, eventually a steady state, linear growth trend is established.

This second, linear regime is hypothesized to be created by a "front" in which diffusion of polymers into the bulk film is possible (vastly increasing the amount of protein able to be incorporated in each dip step compared to the initial steps when the film and therefore the front are thinner), underneath which is a "reorganized" layer which is impermeable to diffusion, retaining the linearity of the film[76-80]. The diffusive character of the front and therefore of the film are affected by a number of factors including hydrophilicity of the polymer backbone, charge density of the polyions, and molecular weight of the polymers involved. The buildup characteristics seen in Figure 2-1 are very consistent with the growth patterns of other films containing poly(β-aminoesters) and polyanions such as heparin[29].

In general, there is strong agreement between the three measurement techniques, indicating excellent protein incorporation in the films, with linear build-up after an initial induction period. This linearity makes it simple to predict the additional amount of protein incorporated by adding subsequent tetralayers, as the amount incorporated increases linearly with the additional number of tetralayers dipped. For

[Poly1/heparin/lysozyme/heparin]80 films, a UV-Vis signal of 2.064 units at 280 nm corresponded with a profilometry thickness of 23.78 μm or approximately 1137.5 $\mu g/cm^2$ of loaded lysozyme.

2.3.2 Release Characteristics

Once it was established that films could be built with excellent protein incorporation, the release characteristics of the films were examined. Films were released at 37º C in PBS to approximate physiologic conditions and analyzed using a micro-BCA kit. In Figure 2A, the release curves show that lysozyme can be released with a linear trend over a period of approximately 14 days, releasing approximately 650 $\mu g/cm^2$ of incorporated protein. Although caution must be taken with extending the utility of these results too far, since these experiments are idealized simulations of body conditions that lack enzymes, cellular reactions, and complex mass transfer profiles likely to be encountered *in vivo*, the linear release trend is encouraging from multiple perspectives. First and foremost, if this release trend was extrapolated to in vivo conditions, it would be very desirable for the drug delivery applications it is designed for, because it allows for constant, low levels of protein to be released from the surface. Compared to burst release profiles in which most of the protein is released instantly and is therefore lost to a greater body volume and cleared before therapeutic action can take place with only a minority of the protein incorporated being controlled in release, nearly all of the release in these films occurs in a controlled fashion in a constant, easy to predict (and therefore dose) fashion. This controlled delivery has significant advantages over pill or bolus injection methods to keep the concentration at the local site of interest within a therapeutic window between an upper limit of toxicity and a lower limit of effectiveness. This method therefore represents a new modality for the timed local release of proteins within the body where the expense or size of a dose was previously prohibitive. It is simple to load more drug by increasing the number of tetralayers used and also simple to predict the additional amount incorporated. It is also encouraging that, even

in a mid-range number of built tetralayers (films from 10 to 80 tetralayers were examined) very large amounts of protein can be incorporated

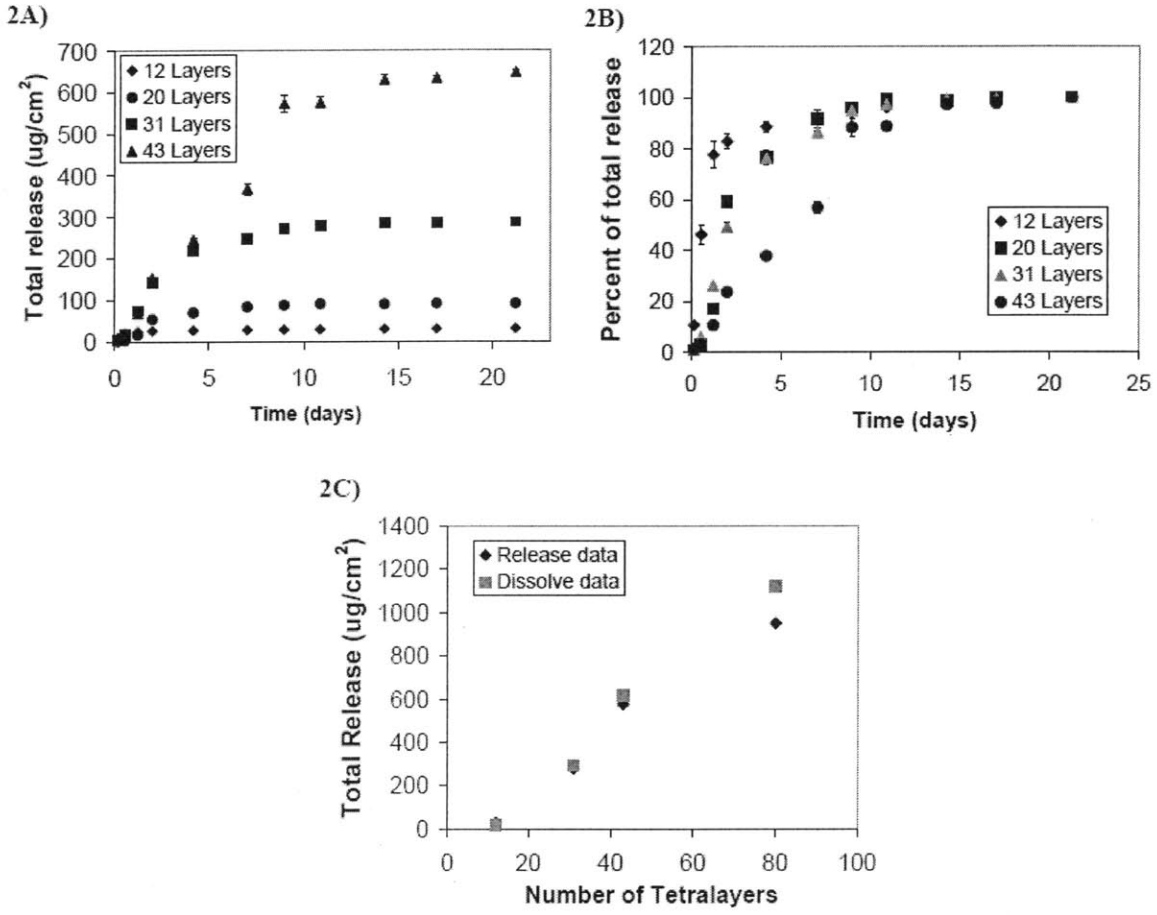

Figure 2-2: Total release and release time span are affected by number of tetralayers. 2A) Replicate samples were dipped with the architecture (Poly1/heparin/lysozyme/heparin)n and released at 37ºC. Total release in µg/cm2 is plotted vs. time in days. Note that both the amount of protein incorporated and the time to total release are increased with increasing numbers of tetralayers, suggesting surface erosion as a mechanism of release. 2B) The signal value for each timepoint was taken as a percentage of the signal at the last timepoint to allow comparison of release kinetics. Percent of total value is plotted vs. time in days. 2C) Fractional release of lysozyme is 85-95%. Films of various tetralayers of (Poly1/heparin/lysozyme/heparin) films were either instantaneously released as described in materials and

methods or allowed to elute into PBS at 37ºC. Total protein loaded or released protein are plotted versus number of tetralayers

while most growth factor applications require only nanogram/mL concentrations of protein. This suggests that these films have copious loading capacity for the applications of tissue engineering and drug delivery.

In addition to these advantages, the controlled and linear release profile suggests a surface erosion mechanism for release, which is consistent with previous work showing ester hydrolysis to be the driving force behind release from LbL films created with poly(β-aminoesters)[81]. While burst release was also considered, burst release profiles tend to have a power law shape in which most of the release occurs at the beginning, unlike this linear release. Similarly, release can be seen due to ionic interactions with the film when release buffer has high ionic strength (greater than 0.5 M)[81, 82], but due to the mild difference in ionic strength of the assembly and release conditions (0.1 vs. 0.2 M) and the release span of months rather than seconds, this mechanism of release is also unlikely.

2.3.2.1 Lysozyme loading as a function of n, the number of tetralayers

A second, important characteristic is the change in loaded dose with increasing numbers of layers. Also in Figure 2-2A, a family of release curves for films with (Poly1/heparin/lysozyme/heparin) architecture and varying numbers of tetralayers is striking for the observation that with increasing numbers of tetralayers, both the total amount of protein released and the time span of release are increased, in good agreement with the hypothesized mechanism of surface erosion. Films with 20 tetralayers released 100 ug of protein over 7 days while films with 43 tetralayers released 650 $\mu g/cm^2$ of protein over 14 days. Bulk releasing films would possibly have increased loading with increasing numbers of tetralayers, but release the entire load over the same amount of time independent of the number of tetralayers. This in turn suggests, when taken with the linear buildup and release of the film, that a surface erosion mechanism of release (rather than bulk diffusion) is

responsible, as demonstrated and discussed in previous publications[29, 62]. To allow for comparison of release kinetics, these values have also been plotted as percent of total release (taking release at the last time point to be total release) in 2- 2B. As can be seen in this figure, films with more tetralayers take longer to release their entire payload of protein, again reinforcing the mechanism of surface erosion.

2.3.2.2 Fractional film release

To address the question of fractional release (the fraction of the drug loaded into the film that is released) two sets of films were constructed with the architecture (Poly1/heparin/lysozyme/heparin) and varying numbers of tetralayers. One set of films was released at 37ºC and the other was instantaneously released as described in the Materials and Methods section. The total release was calculated in each instance, and plotted in Figure 2-2C. In this figure, nearly 95% release or higher is observed at low numbers of tetralayers (50 tetralayers and below). At 80 tetralayers, approximately 85% release is achieved. Because this is a fully degradable system, it is anticipated that eventual recovery of the remaining 15% would happen over a long course of time. It is likely that the thickness of the film and incomplete degradation of overlying polymer networks hinders further release of protein from the film.

2.3.2.3 Effect of polycation choice on loading and release

One of the advantages of using a synthetic erodable polymer is that the drug delivery from the device can be tuned through additional mechanisms over those already discussed by modifying the molecular structure of the polymer used. Poly1 is only one of a large family of poly(β-aminoesters) that can be used in these films; by tuning the composition of the polymers used for this purpose, one can alter the degradability of the ester bond and therefore decrease or increase the time scale over which the film degrades. A second poly(β-aminoester), Poly2, was used to explore the effect of the kinetics of ester hydrolysis on protein release from the constructed multilayers (see Scheme 1). Poly2 differs from

Poly1 in that it has an additional two methylene units in the backbone next to the ester bond, making Poly2 more hydrophobic and making the ester bond less susceptible to hydrolysis. This in turn is predicted to decrease degradation and therefore increase time span of release. Thus, characterization and comparison between Poly1 and Poly2 films yields further interesting information on the erosion of these films as well as allowing demonstration of the ability to tune release by tuning the characteristics of the synthetic polymer used.

Comparing buildup data of P2 compared to similar films for P1 (Figure 2-3A), there is similar agreement between the three measurement techniques, suggesting that linear film buildup and incorporation occur around 20 tetralayers. However, compared with similar films containing Poly1 instead of Poly2, two interesting differences are uncovered. In Figure 2-3B,

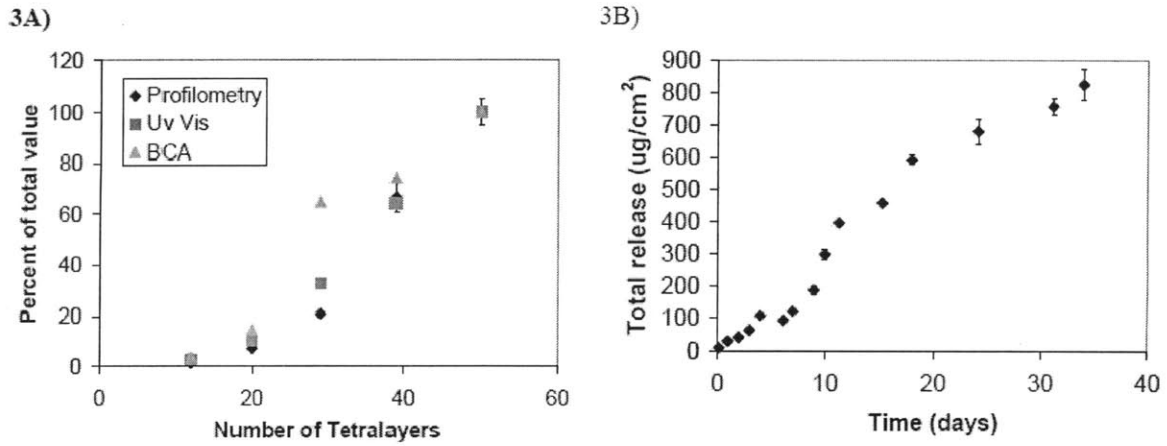

Figure 2-3: Poly2 Film Characterization 3A) The signal recorded at each point of construction is taken as a percent of the signal at 50 tetralayers and plotted against the number of (Poly2/heparin/lysozyme/heparin) tetralayers to allow comparison of curves. By comparison of curves, it is possible to see the transition from exponential to linear building regimes. 3B) When Poly2 is layered in the architecture [(Poly2/heparin/lysozyme/heparin)$_{50}$], and released at 37ºC, release of over 34 days is achieved, showing the tunability of this system in response to a designed synthetic polymer. Total release in μg/cm^2 is plotted vs. time in days

release of a film with the architecture (P2/heparin/lysozyme/heparin) demonstrates that the time period of release is successfully modified by tuning the degradable polymer used. Over 34 days of release are observed with Poly2 films, indicating a 2x increase in release time using the more hydrophobic polymer. This suggests that surface erosion occurs more slowly due to decreased hydrolysis of the polymer and therefore releasing protein for a longer span of time. The second interesting difference is noted by comparison of thickness and total protein incorporation of Poly1 and Poly2 films in Table 1. The more hydrophobic films are capable of increased protein loading as well as increased time span of release. This can be understood on the nano-level to be due to a modification in the film morphology or architecture. Because of the added two methylene units, the distances between the positively charged units along the backbone increases, leading to lower polycation charge density. This lower charge density, along with the fact that hydrophobic chain segments can yield less extended, more coiled chain conformations in solution and upon adsorption, results in the adsorption of thicker, loopier polyelectrolytes. Thus the Poly2 films are anticipated to be thicker , and therefore have a larger volume with which to store loaded protein and other charged species which interdigitate into the forming film during assembly.

2.3.2.4 Effect of polyanion choice on loading and release

As another modality for changing release behavior, a different polyanion, chondroitin, was explored in films of the architecture [Poly1/chondroitin/lysozyme/chondroitin] with varying numbers of tetralayers. In Figure 2-4A, profilometry, UV-vis and instantaneous release curves are plotted in manners similar to Poly1-heparin-lysozyme and Poly2-heparin-lysozyme films. Contrary to the film building behavior for heparin, chondroitin buildup is characterized by an extended period of time in the first, superlinear surface modification portion of the buildup regime. Even by 50 tetralayers it is unclear whether the films are beginning to build linearly or not. Values at 50 tetralayers are much lower than those of

Poly1/heparin or Poly2/heparin films. UV-vis absorbance at 280 is 0.236 units, the thickness of the film is 0.027 μm, and the film was loaded with approximately 133 $\mu g/cm^2$ of protein (values for each film construction are summarized in Table 1). The release from these films reflects the difference in incorporation rates, showing power law dependence, less incorporation and faster time to completion of release (Figure 2-4B). Kinetic data of the same samples are given in Figure 2-4C. Because there is a more burst-like release profile, it is not surprising that the kinetic plots overlay each other, showing that the timescale of release is independent of the amount released. However, in alternative applications in which a burst at the beginning is desirable with low levels of sustained release following, these films might be useful. In addition, the same trend of increased loading and time to complete release is seen with these films as is seen in the case of Poly1/heparin and Poly2/heparin films.

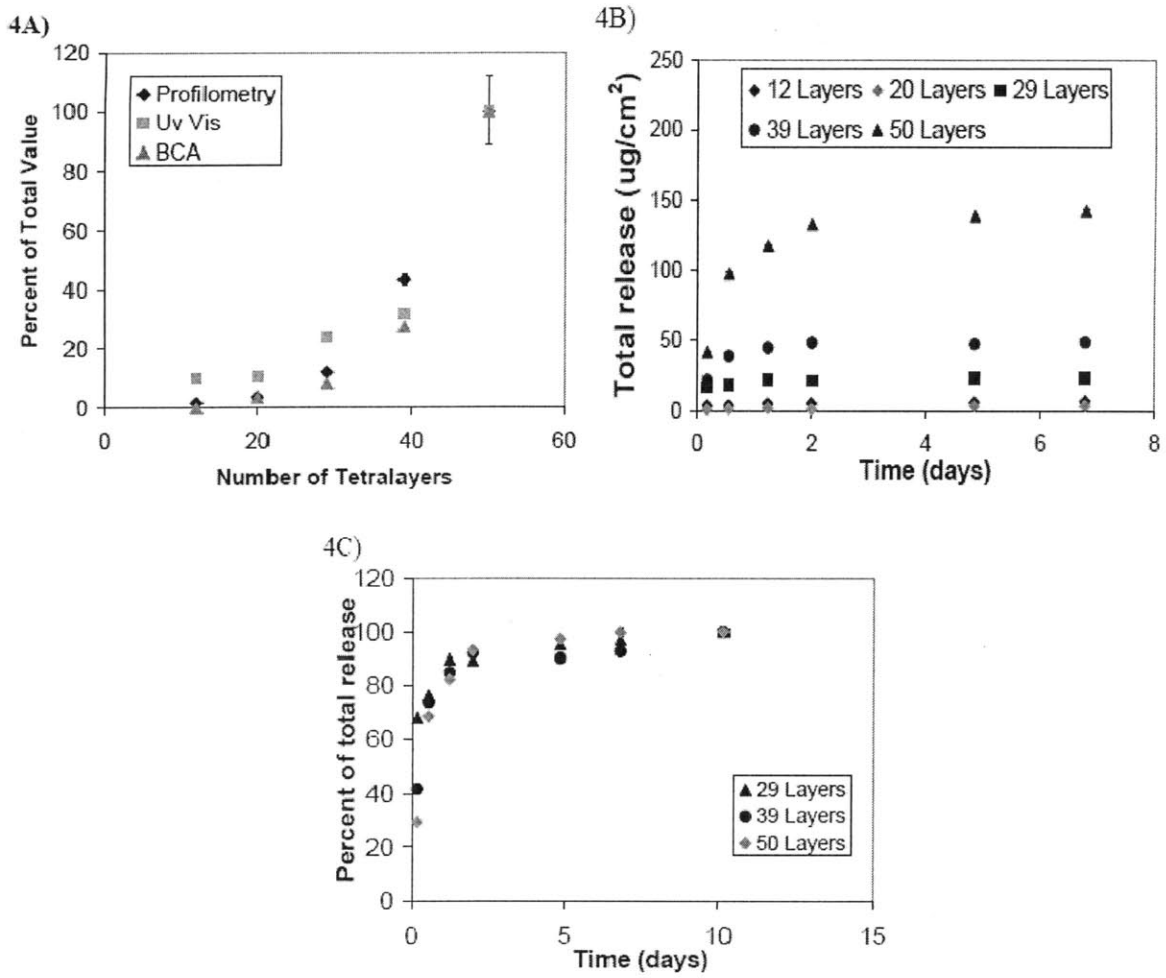

Figure 2-4: Chondroitin film characterization. 4A) The signal recorded at each point of construction is taken as a percentage of the signal at 50 tetralayers and is plotted against the number of (Poly1/chondroitin/lysozyme/chondroitin) tetralayers to allow comparison of the curves. It is possible to see agreement of different measurement techniques and an exponential pattern of growth. 4B) Release of films constructed with lysozyme and chondroitin. Total release in μg/cm^2 is plotted vs. time in days. Note increased loading with increased numbers of tetralayers. 4C) The signal value for each timepoint was taken as a percentage of the signal at the last timepoint to allow comparison of release kinetics between films with different numbers of tetralayers. Percentage of total release is plotted vs. time in days. Results at 12 and 20 tetralayers included large error in measurements corresponding to very low release rates and were therefore omitted from the plot

2.3.3 Protein activity is preserved through fabrication and release

The ultimate concern in encapsulating proteins for drug delivery is whether the processing conditions will destroy the activity of the encapsulated component. Layer-by-layer deposition is a likely candidate for the preservation of activity of encapsulated proteins due to the aqueous baths used in the process as well as the mild pH, which can be adjusted to biological conditions. To quantify the functionality of released enzyme, activity assays of lysozyme were performed. Lysozyme's native activity is to cleave bacterial cell walls; one can detect the amount of functional protein in solution by a kinetic reduction in turbidity of a bacterial solution. In Figure 2-5, results of the micro-BCA assay for typical films are plotted in tandem with the results of a functional assay which reports the concentration of active enzyme present in a given sample.

Figure 5

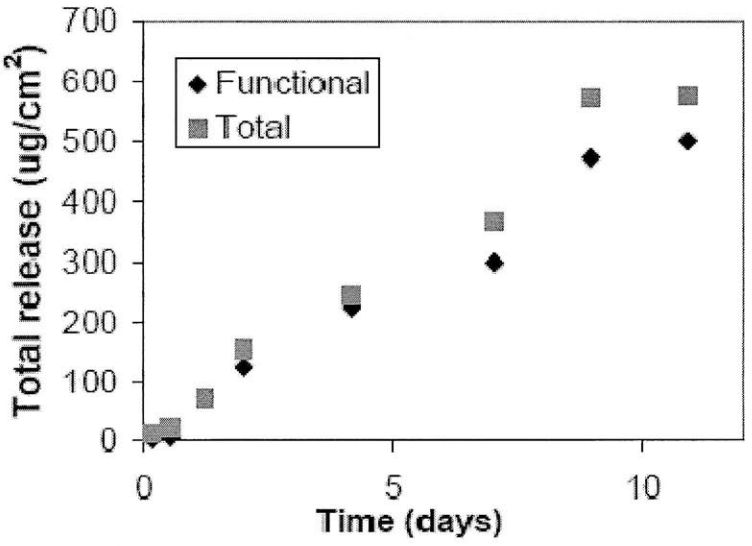

Figure 2-5: The total amount of protein detected using the micro-BCA kit (total protein) was plotted with the total amount of protein detected using the kinetic functional lysozyme assay (functional protein) to elucidate the functionality of the released protein. The amount of total protein released (ug) and functional protein released (ug) is plotted against time in days. This [(Poly1/heparin/lysozyme/heparin)$_{43}$] film shows nearly 100% maintenance of enzyme activity

Encouragingly, 80%-100% of activity is preserved within the films throughout the length of the trial. These rates of activity compare favorably with those of protein release from LbL films in the literature. In the case of Derbal et al[83], activity at physiologic pH was possible, but long term activity of the enzyme (over a period of months) dropped to levels of approximately 30% of their original value. In the case of Caruso and Tiourina[54, 56], excellent retention of activity was possible, ranging from 70 to 100%; however, the capsules required a high pH to release, which is unattainable for many medical device release applications, and underwent a burst style of release. By combining hydrolytic degradability in a polyion directly with the protein of choice in LbL assembly, it is possible to protect and retain protein for long periods of time while sustaining the ability for extended release at biologically relevant conditions.

2.4 Conclusions

In this paper, a new method of protein encapsulation is described using layer by layer deposition to release active proteins in a method that is applicable to objects of any desired geometry and size scale. The protein rate and timescale of release from the film are tunable by choosing the anion to be used, the properties of the degradable polymer, as well as the number of tetralayers that are deposited upon the surface of interest. Additional film properties such as anticoagulant activity or providing matrix material for cell proliferation can be chosen through the polyanion used. In particular, creating films with heparin leads to a linear release profile that is sustainable over 34 days of release at body temperature with the ability to tune release time span and loading. This system combines the useful characteristics of other approaches including high functionality of released enzyme, as well as the ability to release at physiological pH and temperature, making it a widely applicable system that can be tailored to a growing number of release applications.

Chapter 3
Fibroblast Growth Factor 2 (FGF-2) Studies in Multilayer Films

3.1 Introduction

Fibroblast Growth Factor-2 (FGF-2) is a potent biologic capable of helping to direct the stem cell differentiation and proliferation of cells as diverse as hepatocytes[84, 85], neurons[86, 87], cartilage[88], and bone. The presentation of FGF-2 to control cell response therefore represents a tremendous potential opportunity in affecting clinical outcomes across a number of different medical conditions in which exogenous cell transplantation, or the recruitment of native stem cells, is a possible strategy. In particular, there is a clear need for enhancing bone creation and regeneration. A bone defect that is too large to bridge can occur in response to trauma, during treatment of bone non-union, or when resecting bone tumors, leading to a lesion which cannot heal[89]. In reconstructive surgery, frequently the need for allograft bone tissue outstrips the supply available[44], particularly in elderly and pediatric populations, limiting therapeutic intervention. In both of these circumstances, it has been found that the introduction of FGF-2 can greatly enhance the rate of healing and the ability of natural bone to bridge defects[90-93] due to its ability to promote proliferation both in pre-osteoblast cell populations to increase bone production[94], and also in endothelial cell populations which enhance blood supply to the growing tissue[95]. FGF-2 has further bone

forming roles in increasing inorganic phosphate transport[96] and in stimulating VEGF secretion[97]. However, bolus injections of growth factor are rapidly cleared, leaving little time to exhibit therapeutic effects[6, 98]. Furthermore, supraphysiologic doses of growth factor are needed for injections due to growth factor dilution in a larger body volume (opening the possibility of off-target side effects), loss of growth factor activity on exposure to blood, and clearance from the blood stream. There is therefore a need for a biomaterial that will locally release sustained low levels of active growth factors for long periods of time.

One means of accomplishing this is to create polymer coatings that can safely contain and release even sensitive biologic drugs in an active form within nanolayered film architectures for controlled release directly from implanted surfaces. Such release from implant surfaces calls for new, surface based methodologies that allow coating of a current mechanical device rather than traditional bulk polymer encapsulation methods. This can be achieved using Layer-by-Layer (LbL) assembly[21]; in this technique, positively and negatively charged polymers are adsorbed sequentially onto a charged surface to build a film. LbL assembly is advantageous in that the films are created through a gentle, aqueous process that preserves fragile drug activity[30, 34, 44], while the resulting films can be made to be biodegradable, thin, and completely conformal to the device of interest, with easily tunable drug incorporation and film architecture[29, 34, 70]. Furthermore, LbL opens the possibility of sequestering multiple drugs in different layers of the film and creating the opportunity to sequentially release several growth factors or other therapeutic agents such as antibiotics or

anti-inflammatory agents[45, 99] through surface erosion of the film. Finally, because conformal LbL deposition is possible on a wide variety of biomedically relevant materials, including titanium, ceramic, polymer, and glass, there are many potential medical applications of LbL.

Although proteins, and in particular growth factors, have been incorporated in LbL films[30, 31, 70], it is not typical for these LbL films to incorporate synthetic polymers that are designed to allow biodegradability and growth factor release, which can sometimes hamper efforts to tune drug release due to the constraints of existing biopolymers[63]. Here, release from the film is controlled through the incorporation of a degradable poly(β-amino ester) (PBAE)[60]. PBAEs are synthetic, hydrolytically degradable polycations that are readily incorporated into LbL multilayers[62, 63], and allow surface erosion of the film and gradual release of the incorporated FGF-2.

A negatively charged polyanion is also required for film construction. Heparin sulfate and chondroitin sulfate were chosen to exploit advantageous interactions each of these molecules has with FGF-2. Heparin is well known to highly increase the mitogenic potential of FGF-2 by assisting its receptor binding[100, 101] while preserving FGF-2 from heat, pH changes, and proteolysis[102]. Specific binding sequences[103] have been discovered which allow FGF-2 to bind and be sequestered in heparin [104], leading to a developing body of work on the use of heparin for controlled delivery[105-108]. However, because it is difficult to modify and optimize biopolymers such as heparin as a release material, there are challenges in

addressing their inherent materials limitations, such as undesirable release profiles or unintended side effects. Chondroitin, a natural extracellular matrix biopolymer found in cartilage with anti-inflammatory properties has also been shown to enhance FGF-2 mitogenic activity[109]. In addition, in a previous study the ability to tune the release profile[63] from LbL films has been demonstrated, and chondroitin has potential synergism in creating bone and cartilage[110-112].

The aim of the present work is to investigate the characteristics of this novel FGF-2 carrier film that combines the advantages of biopolymer enhancement of FGF-2 mitogenic activity with the fine control over release afforded by synthetic polymers, with a focus on creating a conformal thin film that can be coated on implanted medical devices to enhance tissue growth once implanted *in vivo*.

3.2 Materials and Methods

3.2.1 Materials

Linear poly(ethylenimine) (LPEI, Mn = 25000) was bought from Polysciences, Inc (Warrington, PA). Poly (sodium 4-styrenesulfonate) (PSS, Mn = 1000000) and chondroitin were purchased from Sigma-Aldrich (St. Louis, MO). Heparin sodium salt was obtained from Celsus Laboratories (Cincinnati, OH). Poly 1 and Poly 2 were synthesized as previously described[60]. Fibroblast Growth Factor-2 (17.2 kDa, pI = 9.6) and FGF-2 ELISA kits were

obtained from Peprotech (Rocky Hill, NJ). Glass slides (for substrates) were obtained from VWR Scientific (Edison NJ).

3.2.2 Preparation of polyelectrolyte solutions

LPEI and PSS dipping solutions contained 10mM polymer with respect to repeat unit, adjusted to pH 4.25 and 4.75 respectively. Dipping solutions were prepared in sodium acetate buffer (pH 5.1, 100mM) in the following concentrations: heparin, chondroitin, Poly 1 and Poly2 prepared at 2mg mL^{-1}, and FGF-2 prepared at 1.65 μg mL^{-1}.

3.2.3 Film construction and characterization

For dipping experiments, glass substrates (1" x ¼") were plasma etched with room air using a Harrick PDC-32G plasma cleaner on high RF power for 5 minutes. Ten base layers of (LPEI/PSS) were deposited upon plasma etched substrates to create a surface area 3/4"x 1/4" with a Carl Ziess HSM series programmable slide stainer with 5 minutes of soaking per polymer followed by 3 rinses in deionized water. On top of the base layers, layers of polymers and growth factors to the surface to create the following tetralayer architecture: $(PolyX/heparin/FGF\text{-}2/heparin)_n$ where the PolyX is either Poly1 or Poly2 and n refers to the number of tetralayers deposited on the substrate. A typical dipping protocol is 10 minutes in Poly 1 solution, 3 washes, 7.5 minutes in heparin solution, 3 washes, 10 minutes in FGF-2 solution, 2 washes and 7.5 minutes in heparin solution with 3 washes (all washes were performed with non-pH adjusted deionized water). The thickness of films was measured by

scoring the samples with a razor blade and measuring the step height using a P10 Surface Profiler with a 2um tip radius stylus.

3.2.4 Release characterization

FGF-2 films were released into 1 mL of 1% serum medium, consisting of αMEM supplemented with 1% fetal bovine serum and 1% penicillin streptomycin (Invitrogen, Carlsbad CA) at 37ºC. At a series of different time points, 0.5 mL of medium and eluted material was removed and 0.5 mL of fresh release medium was replaced. Samples were analyzed using ELISA development kits and cell proliferation assays (see below) according to manufacturer instructions. At the conclusion of the experiment, residual film was scraped from the surface with a razor blade and analyzed with ELISA to determine the total FGF-2 load and fractional release.

3.2.5 Cell culture

MC3T3 E1S4 (ATCC, Manassas, VA) were maintained in growth medium consisting of α-MEM supplemented with 10% FBS and 1% penicillin/streptomycin. Cells were split when subconfluent and used until passage 15.

3.2.6 FGF-2 activity assay

750 MC3T3 cells were seeded in 96 well plates in 100 uL of growth medium and allowed to attach overnight. The medium was changed to 1% serum and after 24 hours 10 uL of eluted material from each sample or control was mixed with 90 uL of 1% serum and applied in triplicate to the wells. After 72 hours, BRDU was placed in the release medium (BRDU kit,

Roche Applied Science, Indianapolis, IN) for 4 hours. Similar to [^{3}H] thymidine assays, BRDU is incorporated into the DNA of proliferating cells only, which is later analyzed using ELISA detection at 370 nm according to manufacturer instructions.

3.3 Results and Discussion

3.3.1 Film assembly characterization

Multilayer films with a tetralayer architecture were created by alternately dipping FGF-2, which exhibits a net positive charge under physiological conditions (isoelectric point = 9.6), with a non-cytotoxic polyanion and a hydrolytically degradable polycation from a series of poly(β-amino-esters). Figure 3-1 depicts a schematic of the LbL dipping process and resulting tetralayer architecture of the films, which is denoted through this chapter as [PolyX/Polyanion/FGF-2/Polyanion]$_n$, where the term in brackets represents one repeat unit (tetralayer) of film and n represents the number of repeat units deposited on the substrate.

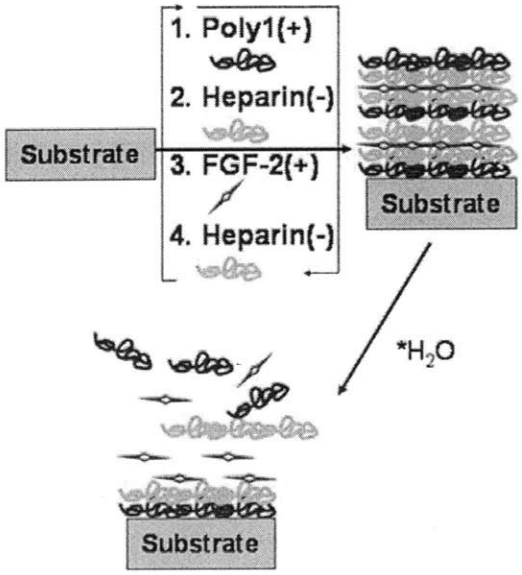

Figure 3-1: Schematic of the Layer-by-Layer tetralayer architecture employed in this paper and potential mechanism of release, in which surface erosion through polymer hydrolysis allows for sustained, local delivery of growth factor.

Two poly(β-amino-esters), Poly1 and Poly2, were utilized in this work; they are identical structurally save for two additional methylene units in the backbone of Poly2. Figure 3-2 shows the structure of both polymers. Previous work [63, 64] has shown that in drug delivery applications, use of Poly2 typically results in longer release periods than Poly1. This has been attributed to increased hydrophobicity from the methylene units adjacent to the hydrolytically cleavable ester bond, which decreases water access to the bond and results in longer degradation times than Poly1 [63, 64].

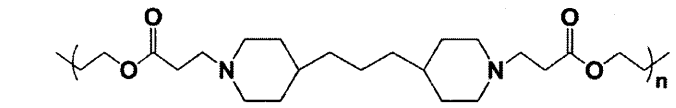

Poly 1

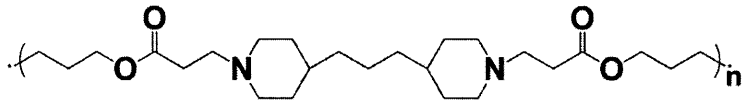

Poly 2

Figure 3-2: The poly(beta-aminoester)s used in this paper, denoted Poly1 and Poly2, have the same structural characteristics, save for the addition of two methylene units in the backbone of Poly2, increasing the hydrophobicity in the region next to the ester bond which is hydrolytically cleaved and therefore decreasing degradation.

LbL films were successfully constructed varying both the polyanion and polycation, resulting in the three following architectures: [P2/chondroitin/FGF-2/chondroitin], [P2/heparin/FGF-2/heparin], and [P1/heparin/FGF-2/heparin]. The correlation between thickness of the films and number of tetralayers deposited was tracked with profilometry for the three film formulations in Figure 3-3. All film architectures tested exhibited a two-regime buildup behavior with a brief period for which thin films with nanometer scale thicknesses are formed, followed by a linear building regime. This characteristic growth pattern is has been observed in many LbL systems reported in the literature[63, 76, 77].

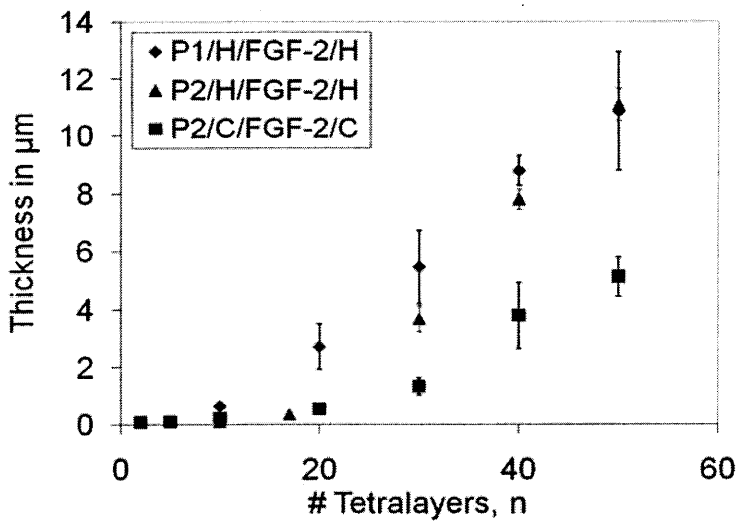

Figure 3-3: Film growth is monitored by profilometry. A typical two regime building process is observed in all film formulations, indicating superlinear building and therefore good drug loading potential. In the figure above P1 and P2 = Poly 1 and 2 respectively, H = heparin, and C = chondroitin. Duplicate films were assayed 3-5 times each with profilometry. Error bars represent standard deviation.

When the film is composed of a few tetralayers (10-20 tetralayers or less), an exponential or superlinear growth behavior is observed in which each additional tetralayer incorporates more material than the previous layer due to interdiffusion of the polymers into the film during deposition. This regime gives way to the second, diffusion-limited linear growth regime, which grows by approximately 200 nm per tetralayer; it is thought that this linear thickness increase is the result of diffusion limitations over the timeframe of the adsorption/absorption step from interdiffusion behavior.

This film growth behavior is typically observed in LbL systems for which one or more of the film components can diffuse into the film during the dipping process, and has been attributed to film rearrangement due to this diffusive process during dipping[63, 76-79]. This is

typically true of biological systems in which lower polymer backbone charge density prevails, or in cases when small, rapidly diffused molecules are entrapped in a film[113]. Such exponential buildup can be advantageous for drug delivery applications, due to the rapid buildup and incorporation of drug compared to linearly building LbL films. The thickness per tetralayer of film, 100 to 200 nm, is an order of magnitude larger than typical values for electrostatic multilayer systems.

3.3.2 FGF-2 loading and release

After ensuring that FGF-2 containing films would assemble properly, the release characteristics and drug loading of the films were tested. Figure 3-4 shows the cumulative release of FGF-2 release samples incubated at 37°C in 1% serum cell medium from 50 tetralayer films of each film formulation of interest. All three films exhibit a high level of release over the first 24 hour period, followed in the case of Poly2 films by a sustained low level of release over a period of about 5 days. These results are interesting from several perspectives.

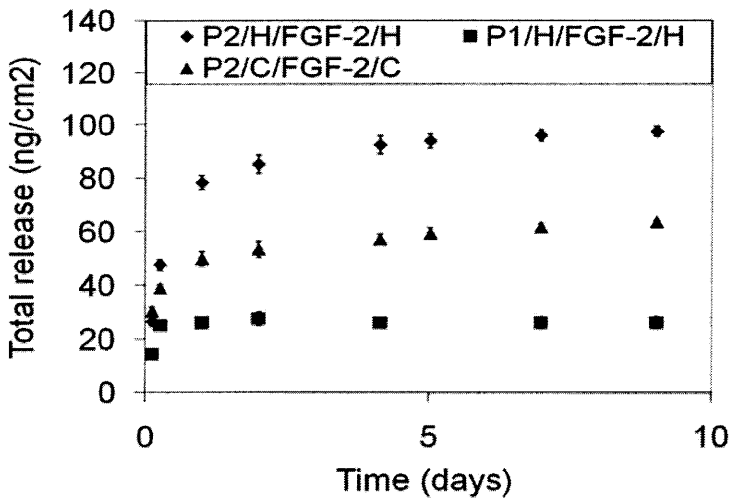

Figure 3-4: Release profiles for different 50 tetralayer LbL film architectures.

3.3.3 Release Mechanism

Unlike the linear release observed in lysozyme architectures studied in Chapter Two, these release curves have a classic burst phase followed by a sustained phase, which is neither linear when plotting release vs time, which would suggest surface erosion as a mechanism of release[36, 63], nor linear when plotting release vs. square of time, which would suggest classic Higuchi diffusion[114]. It is likely that multiple mechanisms of release contribute to the profiles seen here.

It is known that in exponentially growing films such as those seen here, interdiffusing species can partition towards the top of the film leading to nonuniform drug distribution[76]; this would naturally yield increased drug release at the beginning of the film's erosion due to a higher concentration of drug in the top layers. This could certainly play a role in the release profile seen.

Classic models of a passive, homogeneous drug/polymer blend [115, 116] based on comparing the characteristic time scales for water diffusion into the polymer matrix and the degradation rate of polymer by chain scission suggest bulk degradation. Not to be confused with bulk erosion, in which chunks of film dissolve from the surface and quickly release their loads, bulk degradation here suggests that the polymer degradation rate is substantially slower than the diffusivity of water within the film, and therefore that polymer chain scission by ester hydrolysis could happen at any depth within the film, rather than being confined to the top surface eroding area. Epsilon[116], a dimensionless number that indicates bulk erosion when much less than one, surface erosion if much greater than one, and no conclusive evidence at values equal to one was estimated using available data, with the result that epsilon is much less than one. (For this calculation, the diffusivity of water was taken to be 10^{-12} m^2/s, which has been found to be a reasonable estimate for a broad range of polymer matrices[115], gamma, equal to the first order rate constant k was taken from a $t^{1/2}$ measurement in literature[117], and Lcritical equal to 10 microns (the thickness of a typical growth factor LbL film), as an estimate. Epsilon was found to be 6E-8.)

However, the models that have been developed to describe bulk release of drugs are likely too simple to predict release from LbL films; the non-uniformity induced by film rearrangement described above, for example, leads to a non-homogeneous film; electrostatic interactions that lead to soluble polyanion complexes with FGF-2 upon release would increase the FGF-2's apparent molecular weight, increasing the pore size necessary for escape, and such electrostatic interactions could also act to retard drug escape from the film compared to a passive polymer matrix[118] due to the presence of ionic interactions. The homogeneous model

of drug release is interesting in the perspective that with very thin films made of polymers designed to degrade slowly, bulk erosion must almost certainly take place; thus sequential release strategies that employ two compartments with different polymer degradation rates are predicted to be more successful than two compartments sharing a common release polymer. However, the substantial limitations on the model when applied to LbL systems make it impossible to conclude anything definitively here.

Another interesting phenomenon has been observed in that polymer species "ejection" is possible if the film is constructed at one pH and released at a second pH. In this case, the ionic crosslink balance and density can shift with the isoelectric points of the weakly acidic or basic polymers during construction and release, leading to a charge imbalance within the film that is corrected by polymer ejection. The ejection event leads to film rearrangement that again confounds simple modeling, but is known to rearrange the internal architecture of the film. Polymers of up to 350 kDa were observed to be ejected over the first 8 hours of film immersion in a new pH environment[118]. Although this work was done in a different system, if the same were true here, it would not be impossible for chondroitin to be ejected from these films.

Taking all of these effects into account, it seems likely that the burst release seen in our release profiles is due to film rearrangements introduced during non-linear layer growth and possible pH related polymer ejection, while the sustained release phase can be attributed to the slow ester hydrolysis of the PBAE. This area is one of increased interest in the

Hammond group today, as it is anticipated that a clearer understanding of release mechanism will likely be needed to understand how to achieve sequentially releasing systems.

The drug loading is affected by both the polycation and polyanion used, with maximum loading observed with P2/H (100 ng/cm^2), and minimum loading with P1/H (35 ng/cm^2). Comparing first the effect of the polycation, it is seen that P2/H contains three times as much FGF-2 as did P1/H. This may be due in part to the increased hydrophobicity along the P2 backbone, combined with a slightly lower charge density, resulting in a lower effective ionic crosslink density within the film, and hydrophobic pockets within the film that may increase secondary interactions with FGF-2. It has been posited that a lower ionic crosslink density can lead to looser, loopier polymer chain conformations within the film that may also more readily accommodate protein sequestration within the multilayer, and, indeed, model protein Poly2 films are thicker and load more protein than their Poly1 equivalents[63]. To compare release profiles, the released amounts are plotted as percent of total release in Figure 3-5; here it is seen that Poly2 containing films exhibit the same general release behavior regardless of the polyanion used, releasing 80% of their load in the first day with a sustained release of the remainder over the following eight days. In contrast, the Poly1 film releases 95% of its contents in the first day with sustained release for an additional day. This supports the notion that, because Poly2 is more hydrophobic and thus less degradable by ester hydrolysis, it takes longer for the film to erode and release its contents.

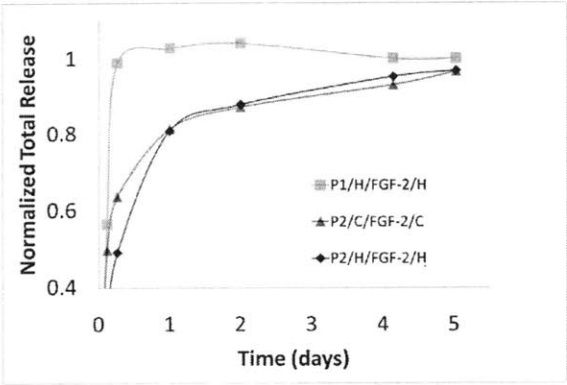

Figure 3-5: Release from different 50 tetralayer LbL architecture films plotted as a fraction of total release show overlapping release profiles for P2 films which have a slower release rate than the release from a P1 film.

The polyanion also affects film loading. Comparing P2/H and P2/C films, total drug loading capacity of the films is affected, with P2/C films loading approximately 60% of the FGF-2 loaded into the P2/H film. One contributing factor is likely the specific interaction between FGF-2 and heparin, which allows more FGF-2 to be incorporated. However, studies with the model protein lysozyme, which has similar isoelectric point and molecular weight to FGF-2, also showed that P1/H films loaded more lysozyme than P1/C films, indicating that specific binding interactions are not the only contributing factor. In that work, it was posited that specific interactions allow better film packing and increased drug density[63]. However, interestingly, the same release behavior (Fig 2B) is observed for P2/H and P2/C films, suggesting that specific binding activity has affected drug loading, but does not necessarily affect release rate from the film.

In Figure 3-6, [P2/heparin/FGF-2/heparin] films ranging from 10 to 50 tetralayers thick were released to generate a family of curves, showing that the delivered dose and the time span of release of FGF-2 from these LbL films can be easily tuned simply by changing the number of tetralayers used.

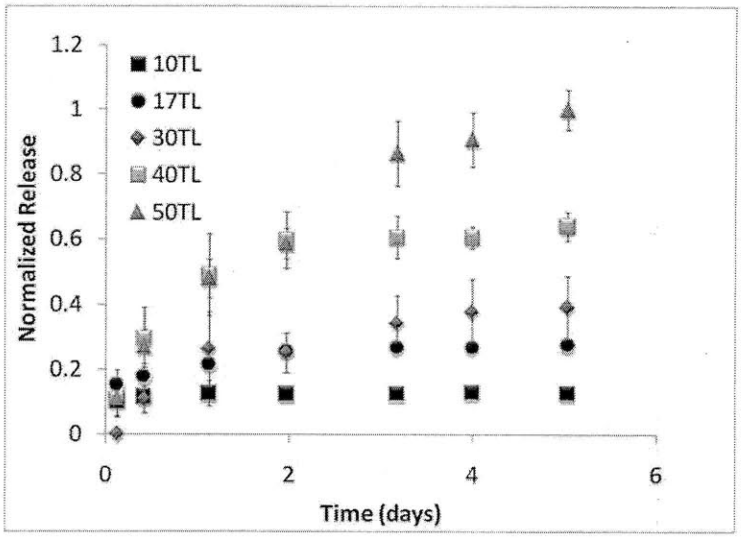

Figure 3-6: Release is tunable with number of tetralayers, using [P2/Heparin/FGF-2/Heparin] film as an illustration. Duplicate films were assayed in triplicate; error bars represent a 95% confidence interval.

Finally, it was of interest to pursue the fractional release from the film. After 10, 20, 30, 40, and 50 tetralayers were done releasing as detected by ELISA, any remaining visible film was scraped from the surface with a razor blade and vortexed in collection medium. The resulting, non released fraction was run on ELISA to detect unreleased FGF-2 in the polymer matrix. In all cases, the fractional release was 95% or higher of the total drug load (Table 3-1).

Table 3-1: Fractional release of [P2/heparin/FGF-2/heparin] films of varying numbers of tetralayers. Greater than or equal to about 95% release is seen at all numbers of tetralayers, suggesting that all FGF-2 incorporated is released.

# Tetralayers	Percent released
50	98.8
40	100.0
30	94.8
17	95.7
10	99.5

3.3.4 In vitro assessment of activity

FGF-2 is known to be a potent mitogen for the pre-osteoblastic MC3T3 cell line[119, 120], as well as for human osteoblasts[119], which increases the population of pre-osteoblast cells available to become bone cells *in vivo*. The FGF-2 released from the film was tested in a BRDU proliferation assay (Figure 3-7). In this assay, proliferating cells are labeled with BRDU which is later detected by ELISA. FGF-2 released from all three film formulations of interest (P2/C, P2/H, P1/H, Fig 7A, B, C, respectively) shows robust (three or more fold) increases in proliferation over control cells which received no FGF-2. This released FGF-2 maintains proliferative activity far past the period of release from the film, as proliferation rates are elevated for up to 12 days in culture, indicating that FGF-2 retains high levels of activity while in the film. Concentrations of free FGF-2 (100, 50, 5, 0,5 and 0 ng/cm^2) introduced into the medium show a dose dependence on FGF-2 (Figure 3-8). Interestingly, FGF-2 released from LbL films demonstrate increased ability of up to eight fold negative control values to enhance proliferation compared to the free FGF-2 (about 2 fold), which may be due to the co-

release of heparin or chondroitin sulfate. Both heparin and chondroitin are known to increase the mitogenic activity of FGF-2[109], and thus represent a synergistic addition to the film.

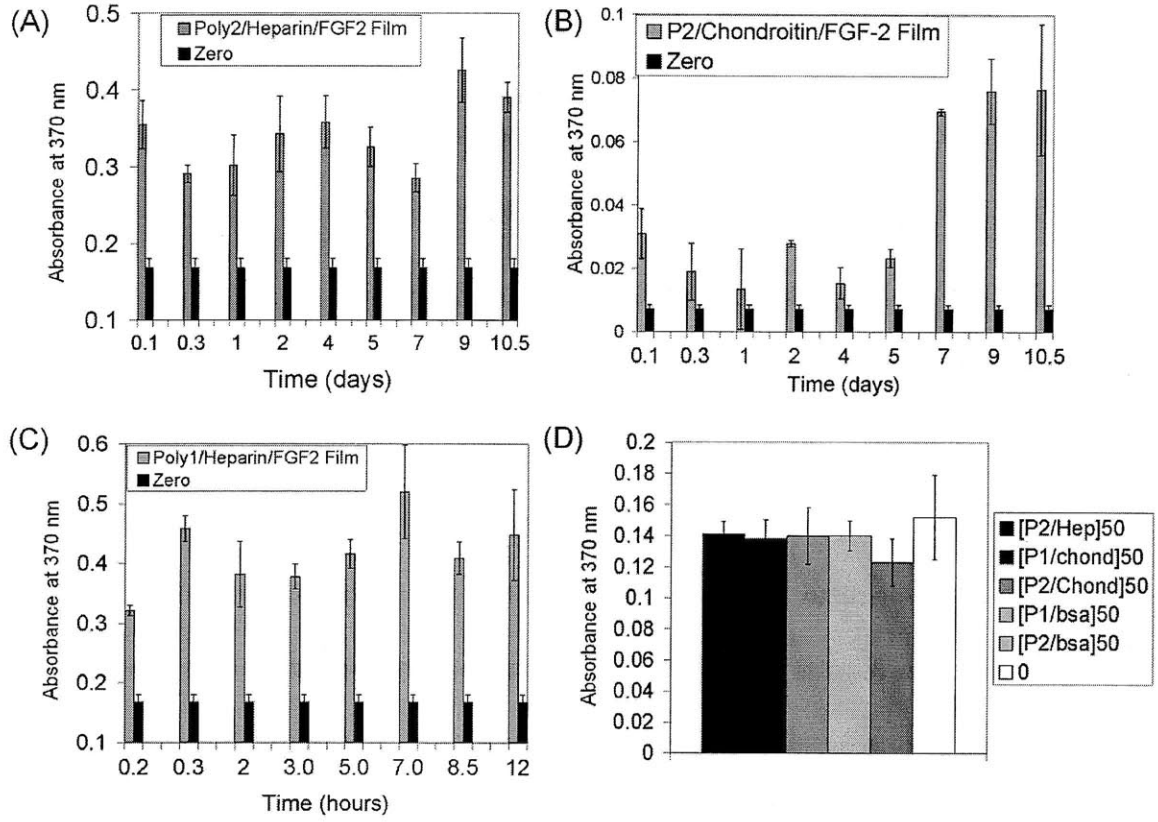

Figure 3-7: Released FGF-2 from LbL films retains proliferative effect on MC3T3 cells, as detected by BRDU ELISA at 370 nm detection wavelength. BRDU, which is incorporated in proliferating cells' DNA, shows a marked increase in proliferation in cells exposed to FGF-2 from films compared with control cells which were not exposed to FGF-2 from the films ("zero" in (A), (B), (C)). (D) All film components tested other than FGF-2 show no positive or negative effect on proliferation compared with control cells not exposed to LbL films. Error bars are standard deviation on triplicate assays of films.

components tested other than FGF-2 show no positive or negative effect on proliferation compared with control cells not exposed to LbL films.

To rule out the possibility that heparin, or another film component released from the film, could increase proliferation alone by helping native FGF-2 present in the cell medium serum bind to MC3T3, films were created without FGF-2 (only inactive components) and were released

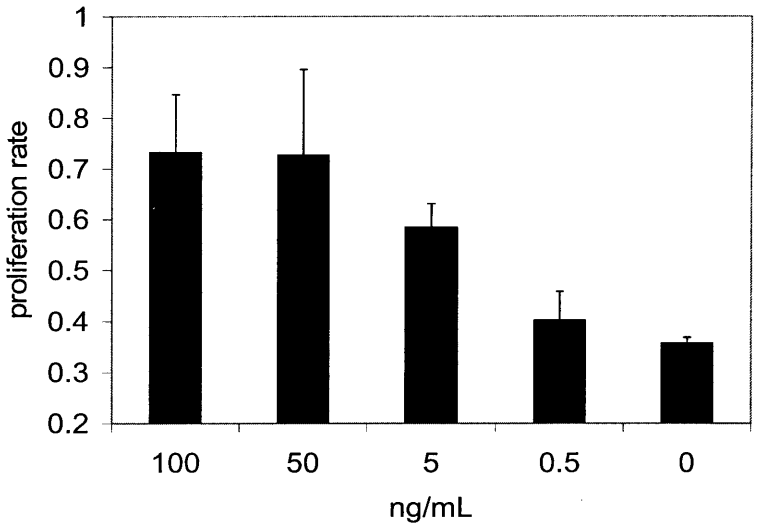

Figure 3-8: Proliferative response of MC3T3 preosteoblast cells to varying concentrations of FGF-2 added to 1% serum cocurrently with film sample exposure to the cells. Dose response can be seen to varying concentrations of FGF-2. Error bars are standard deviation on 3 sample measurements per condition.

and tested on cells. All other film components (Poly1, Poly2, chondroitin, and heparin) alone or in combination, showed no proliferative effect on the MC3T3 cells (Fig 3-7D). Thus, the mitogenic activity of FGF-2 encapsulated within these LbL films is preserved and enhanced by co-delivery with heparin or chondroitin.

3.4 Conclusions

Although growth factors have an acknowledged ability to aid in the formation of new bone tissue, which is still critically needed in many clinical applications, its delivery for clinical applications thus far has been flawed or limited due to loss of activity and inability to control release in a sustained fashion. FGF-2 is one of a family of growth factors that, if released in combination or sequence with other growth factors, could lead to an enhanced bone formation response that would be clinically relevant. LbL is an ideal candidate drug delivery system for such co- and sequential release schemes due to the possibility of sequestering different growth factors in different layers of a constructed film[45] that can be used to coat a bone implant or an engineered scaffold for wound healing. In this work, we demonstrate the first successful incorporation and sustained controlled release of FGF-2 from a synthetic, biodegradable polymer LbL drug delivery system intended to work locally at the site of new bone formation. FGF-2 release is tunable through the polycation, polyanion, and number of tetralayers used to construct the film; FGF-2 released from the film exhibits enhanced ability to promote proliferation in pre-osteoblast cells compared with FGF-2 medium supplementation due to co-release of heparin or chondroitin sulfate. We show the ability to release 100 ng/cm^2 of growth factor with retained bioactivity over 12 days. While other LbL methods that rely on post-manufacture surface adsorption of growth factor onto LbL films [51, 53] can deliver similar amounts of growth factor, because the growth factor is surface-bound rather than sequestered with a degradable synthetic polymer, no control can be exerted over its release profile, nor is sequential release accessible. In other cases [44, 67], the amounts released are modest, rendering autologous in vivo cell response difficult to achieve. Thus here, we show a unique system

which retains LbL's true potential in biomedical surface modification by combining both a high degree of loading of growth factor in multilayer films while preserving the possibility of sequential release of multiple growth factors or other therapeutic agents. These results significantly enhance our understanding of growth factor delivery from LbL films in a way that will enable *in vivo* bone regeneration models in future work, and represent a necessary step in understanding how LbL can be used to treat clinically relevant problems in growth factor delivery.

Chapter 4 Automated misting process for the rapid, conformal deposition of thin films delivering active biomolecules

4.1 Introduction

In the field of regenerative medicine, it has recently become clear that both chemical and mechanical cues from an external scaffold are necessary to coax cell growth into replacement tissues. Traditional porous scaffold designs are limited in this respect, as the same polymer is responsible for both biomolecule release and the mechanical properties of the scaffold; to tune one behavior often comes at the other's expense. Therefore, decoupling chemical and mechanical properties of a scaffold and allowing for independent adjustment, is desirable. In this work, we describe a novel technique for creating highly conformal, functional drug delivery thin films which can conveniently surface modify porous polymer networks and thus add biologically active chemical cues to a scaffold with optimal mechanical properties.

Layer-by-layer (LbL) thin films[21] utilizing synthetic degradable polymers[62] are emerging as an important and versatile tool in drug delivery applications due to flexibility of substrate choice, copious and tunable loading capacity and release, and excellent preservation of biomolecule activity (protein, DNA, polysaccharides, and antibiotics) during incorporation and release[63]. As illustrated in Scheme 1, an innately charged surface, such

glass, plastic, or titanium, is sequentially dipped into a series of polycationic and polyanionic solutions, causing nano-scale layers of polymer to be electrostatically bound to the surface in each step.

LbL films are traditionally deposited by a dipping process in which the substrate of interest is submerged in a polyelectrolyte dipping solution, where adsorption takes place. However, significant advantages are possible using a spray-assisted modification of the technique. Spray-LbL assembly[121-123], in which atomized mists of polymer solution is sprayed onto the substrate, is a relatively new field. There are five advantages especially relevant to therapeutic protein LbL: (1) Spray LbL allows for substantially faster fabrication times (50x reduction in time, from 2-3 days to under 1 hour), potentially preserving fragile protein activity, (2) Spray LbL allows the ability to selectively functionalize different surface portions so that different growth factors could be sprayed on two sides of a scaffold, for example, (3) this rapid construction is highly amenable to commercial applications where continuous roll-through processes are advantageous compared with batch processes, (4) such rapidity also allows the use of polymers at a wider range of pH and aqueous conditions, since the time allowed for degradation to occur is reduced, and (5) spray construction has been shown to conformally coat loose fiber networks of the type that would be attractive for tissue engineering scaffold materials[124]. Spraying conformal drug eluting coatings on scaffold materials, it is possible to successfully decouple the mechanical and chemical cues presented to cells, so that each can be individually optimized.

In Figure 4-1, the protein of interest is layered into polyelectrolyte films utilizing a hydrolytically degradable poly(β-aminoester), Poly1 capable of slow surface erosion[62, 125] and a biological polyanion, heparin, which allows for the surface charge reversal needed, and, in the case of FGF-2, enhances activity[100, 101, 102, 104]. Although here Poly1 was used, many members of the family of poly(β-amino ester)s and indeed multiple other polymer systems are amenable to this process, allowing a wide range of tunability[61, 64].

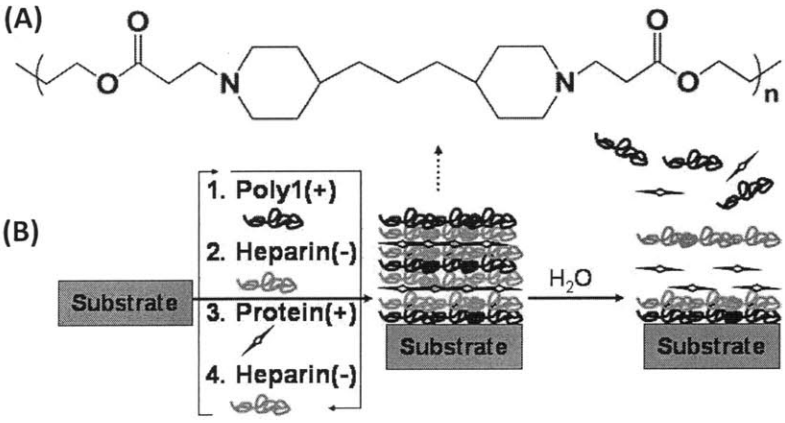

Figure 4-1: (A) Structure of Poly1, a poly(β-amino ester). (B) Construction of degradable layered thin films by the Layer-by-layer process, incorporating (1) a hydrolytically degradable polymer, Poly1, (2) a counterbalancing polyanion, and (3) a protein of interest. . Multiple tetralayer repeat units are added, and the protein is released through surface erosion of the degradable polymer.

To realize the potential of LbL in this domain, it is necessary to explore the incorporation and release of different classes of proteins such as enzymes and growth factors. In this work, we incorporate a representative enzyme, lysozyme, and a representative growth factor, Fibroblast Growth Factor-2 (FGF-2) in the first demonstration to our knowledge of biomolecule incorporation and release from spray LbL films.

4.2 Results and Discussion

Utilizing the LbL spray construction process with 50 tetralayers of the architecture [P1/heparin/protein/heparin] yields 1.2 to 1.5 μm thick films for FGF-2 and lysozyme containing films respectively, which can easily coat a scaffold without drastically changing the pore size. Films were constructed on glass by utilizing commercially available airbrushes from Badger to direct a sequence of atomized charged polymer sprays at pH 5.1, concentrations of 2 mg/mL for Poly1 and heparin, 0.5 mg/mL for lysozyme and 1 μg/mL for FGF-2, and a constant flowrate of 0.31 mL/s, sprayed for a 2 second spray time. The glass in all cases was pre-coated with 10 bilayers of linear poly(ethylene imine) and poly(styrene sulfonate). The film buildup curves, shown in Figure 4-2, have a similar shape to those of LbL dipped films (see Chapter 2, 3) in which there is an exponential and superlinear region of film growth; however, the films are an order of magnitude thinner.

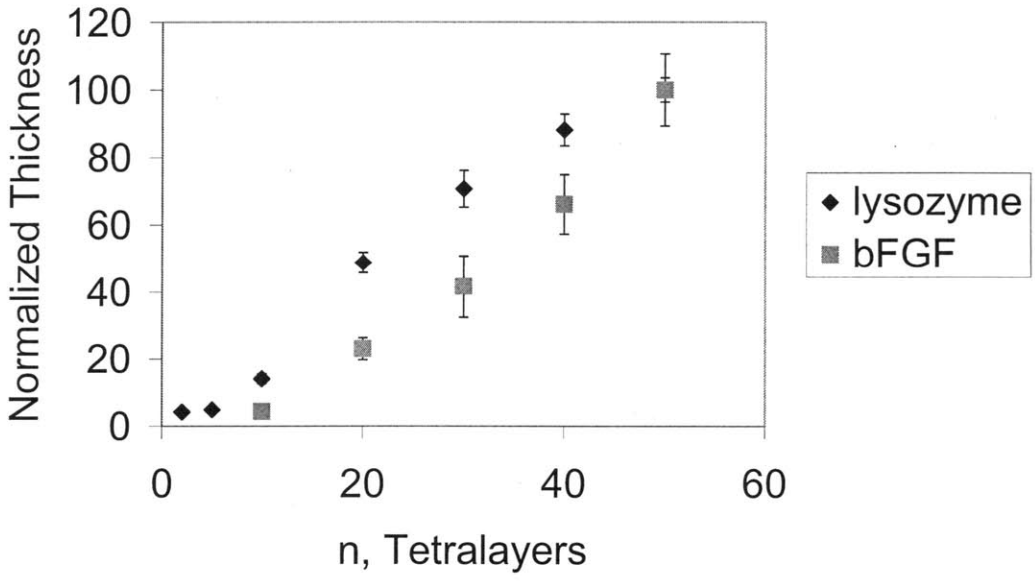

Figure 4-2: Film growth exhibits superlinear characteristics which suggest interdiffusion in Spray LbL. Three films were analyzed with 3-6 profilometry measurements each; error bar is the standard deviation.

Because the deposition in spray LbL actually relies on both convective *and* diffusive forces to adsorb polymer (rather than diffusion alone in dip LbL), while also working in a much tighter time span that could kinetically trap substances and therefore disallow the film diffusion and rearrangement that leads to the superlinear regime seen in dip LbL, it was possible that a linear film building curve would be possible. A linear building curve would imply that diffusion of molecules and film rearrangement were not occurring and only surface adsorption was contributing to increasing film thickness. However, as seen in Figure 4-2, the similarity in the shape of the film building curves between sprayed and dipped LbL films suggests that even during the very short times used to fabricate these spray LbL films, film rearrangement is occurring, leading to superlinear growth.

Figure 4-3 shows lysozyme release from $[Poly1/heparin/lysozyme/heparin]_{50}$ films, where the brackets indicate the sequence of layers deposited and the subscript indicates the number of repeat units (tetralayers). Films were analyzed both with a bicinchonic acid (BCA) assay for total protein release, and an enzymatic assay[63] to determine functional protein content. Release of 60 $\mu g/cm^2$ is observed over a period of 2 days and functionality of 100% within statistical error is observed (error bars represent one standard deviation in all figures).

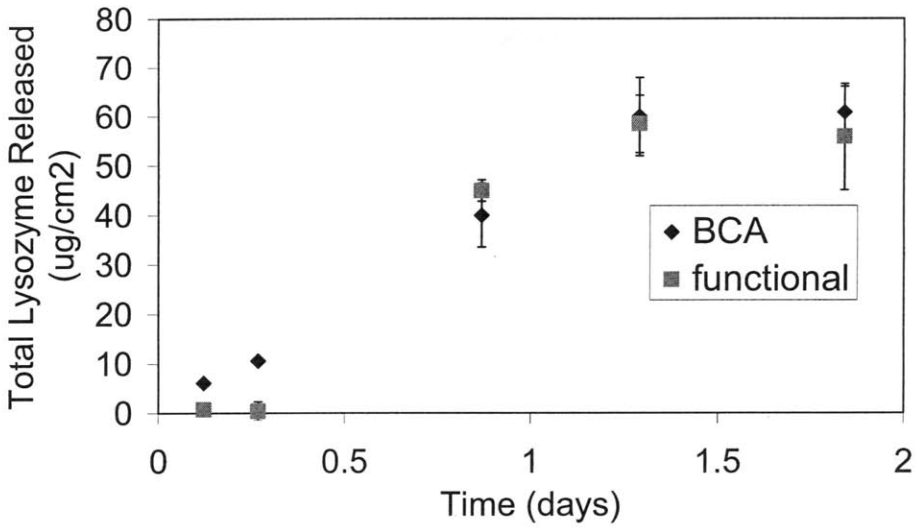

Figure 4-3: Lysozyme released from [P1/heparin/lysozyme/heparin]$_{50}$ Spray LbL films shows 100% retention of activity. Error bars demarcate 95% confidence interval.

It was unclear whether the atomization of the spray would shear the lysozyme during incorporation, affecting its functionality; here we see that 100% of protein functionality is preserved, which is necessary for therapeutic protein spray LbL applications. Dipped LbL films with the same architecture incorporate an order of magnitude more protein and release, and release on the order of 10-20 days (Chapter 2). The linear character of the release profile is retained, suggesting surface erosion of the created film. These results are not surprising given the order of magnitude drop in thickness of the sprayed films; on a per thickness basis, the spray LbL films function on-par with their dipped counterparts. However, it was of interest to see if a similar phenomenon would happen with growth factor films, as therapeutic load must be maintained above a minimum level to see therapeutic effect.

The great anticipated role growth factors are expected to play in regenerative medicine makes them attractive for an LbL growth factor release strategy. These proteins play a pivotal

role in manipulating cell behavior from migration to proliferation to differentiation. Implantable scaffolds required to recruit host cell types must be charged with pre-programmed growth factor delivery. Here, it is particularly important to be able to independently tune mechanical and chemical cues. FGF-2 is a potent mitogen for a diverse array of cell types with particular value in vasculogenesis and bone healing applications. To explore the therapeutic release potential of spray LbL films, [Poly1/heparin/FGF-2/heparin]$_{50}$ films were constructed on [LPEI/PSS]$_{10}$ coated glass and released in alpha MEM supplemented with 10% FBS and 1% penicillin/streptomycin in Figure 4-4. These films successfully incorporate and release FGF-2,

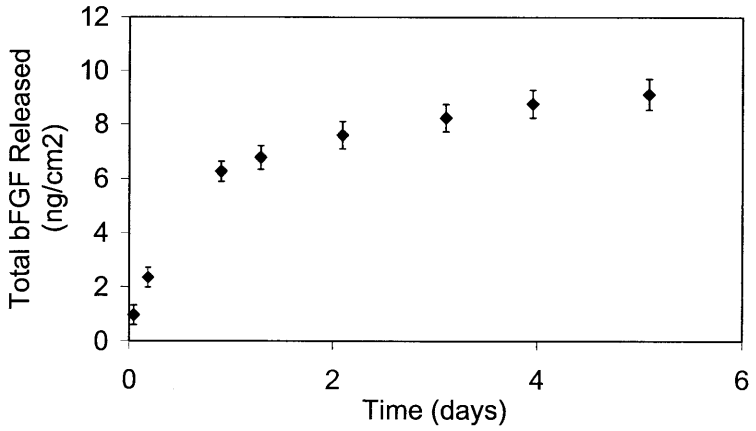

Figure 4-4: ELISA release profile of FGF-2 release from spray LbL films of the architecture [P1/heparin/FGF-2/heparin]$_{50}$ from planar glass substrates (n = 3, error bar is 95% confidence interval).

and protein structure is maintained (allowing for detection by ELISA). Because FGF-2 has potent activity at low concentrations, but inhibits proliferation at high concentrations (above 500 ng/mL), the concentration range observed here is desirable. It is anticipated that application of these FGF-2 releasing spray LbL films to a scaffold surface would yield an

increased incorporation scaling with the available surface area for spraying afforded by the 3D scaffold; to keep concentrations in a mitogenic regime, it is desirable to keep release modest. In the case of other growth factors where larger doses are desirable, adding more tetralayers is predicted to lead to an increase in the drug loading and also release time.

To test the incorporation properties of spray LbL films on 3D scaffolds, electrospun PCL mats were employed as a test substrate. Spray LbL of the architectures $[P1/heparin/FGF\text{-}2/heparin]_{25}$ and $[P1/heparin/FGF\text{-}2/heparin]_{50}$ deposited on PCL electrospun mats were examined with scanning electron microscopy (SEM). The film deposited shows a bridging effect as seen in Figure 4-5. Early in the spray deposition process, the LbL film is able to bridge the pores of the PCL electrospun mat. Past this bridging step, only the first few layers of the electrospun mat experience any deposition. This result is interesting; in such a film, as the LbL film dissolves away, it would therefore expose the underlying three dimensional tissue engineering scaffold to allow ingrowth and penetration by a network of cells. Because the film deposits unevenly throughout the thickness of the scaffold, it is possible that the mat could be turned over and sprayed with a different growth factor on the other side, allowing for growth factor gradients and varied cell reactions to the scaffold depending on location.

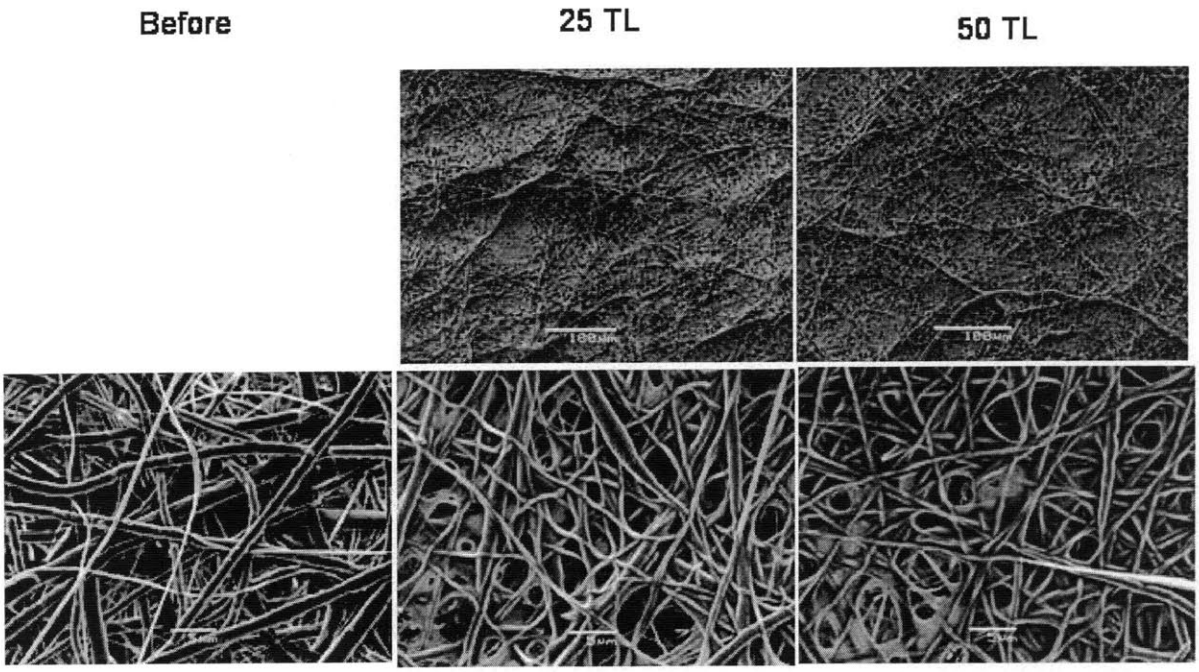

Figure 4-5: SEM images before spray process and after 25 and 50 tetralayers of deposition show a bridging process between fibers that allows for multi-step deposition on different sides of the 3 dimensional scaffold

With only 25 tetralayers of spray on a ¼" by ¼' piece of scaffold, an order of magnitude increase in growth factor incorporation was observed, bringing the total scaffold release into a reasonable range to see cellular response while staying below the threshold to see anti-proliferative effects (Figure 4-6). The total time span of release is similar to that of the planar films while simply increasing the total available load of FGF-2.

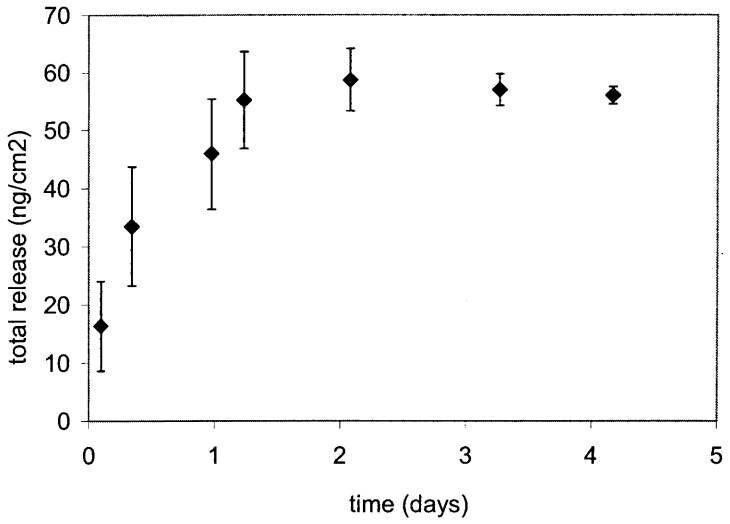

Figure 4-6: Electrospun PCL mats sprayed with [P1/heparin/FGF-2/heaprin]$_{25}$ show an increase in drug load with increased surface area. Duplicate mats were assayed in triplicate each; error bars represent 95% confidence interval.

MC3T3 cells seeded on FGF-2 spray LbL film/PCL electrospun mat combination devices were assayed with MTT to determine cell count on each scaffold. The cells demonstrated increased proliferation rates compared to cells seeded on vehicle only control LbL films containing only Poly1/heparin bilayers (Figure 4-7, left panel). The bioactivity of the FGF-2 released from the films is confirmed here through the continued ability to enhance proliferation of a responsive cell line. This increase in cell count is confirmed with fluorescent imaging of live cells stained with calcein and cell nuclei with Hoescht 33342 within the PCL mat (Figure 4-7, right panel), visualized with an inverted Olympus X71 fluorescent microscope with Applied Precision DeltaVision deconvolution software. Although autofluorescence of the PCL mat in the green channel leads to a blur on the green

channel of the overlaid images, the increase in cellularity of FGF-2 positive mats compared to vehicle control mats is unmistakable.

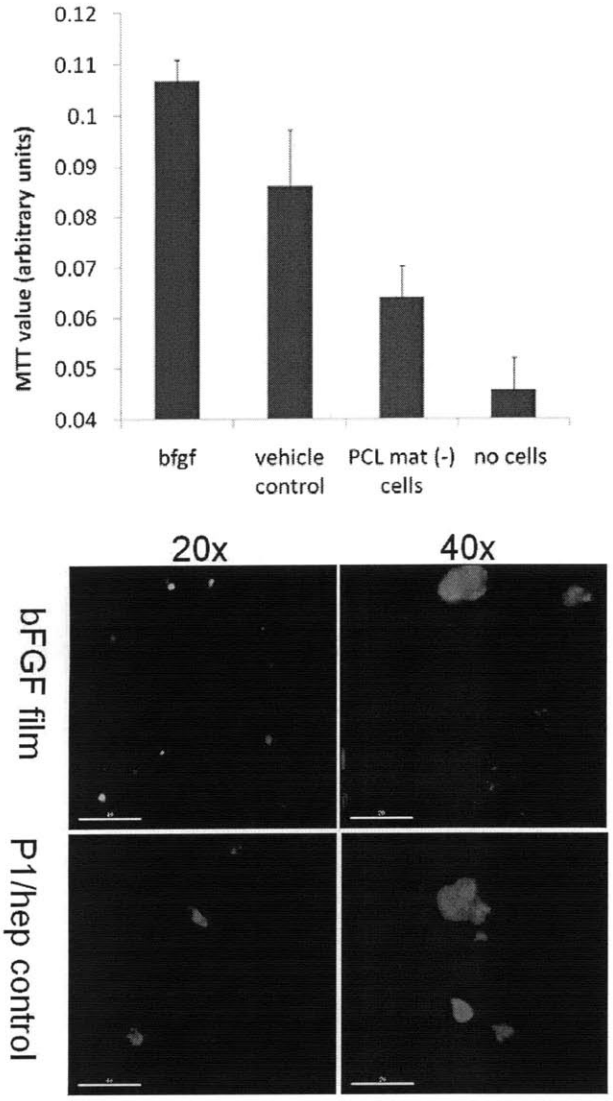

Figure 4-7: MTT assay and DeltaVision confirmation of increased cell populations on FGF-2 releasing LbL films [P1/heparin/FGF-2/heparin]50 compared with vehicle only [P1/heparin]100 films (n = 3 for MTT, 2 for deltavision; error bars are standard deviation). PCL mat (-) cells is the MTT signal attributable to the mat while no cells represents the MTT signal from an empty well.

In this work we have laid a foundation for the incorporation of biologics in spray LbL films, exploring for the first time the incorporation and release behavior of these films for comparison with dipped LbL films of the same composition. We demonstrate the successful functional incorporation and release of two classes of proteins using LbL spray construction, as well as retained functionality for both types of molecules. Although FGF-2 and lysozyme were selected for this work, a wide variety of enzymes and growth factors can be incorporated in complex 3-dimensional matrices using this technique. Our lab continues to investigate the use of bone promoting growth factors, such as FGF-2 and Bone Morphogenetic Protein-2 in LbL films as chemical modifications both to implantable medical devices such as hip implants (the same technology is ideal for stent coatings and other applications) and to tissue engineering scaffolds for bone regrowth in a matrix with independently tunable biological signals and mechanical strength.

Chapter 5 Thin Films for Antibody Release

5.1 Introduction

The approach taken in Chapters 3 and 4 shows a mechanism through which the desired cell behavior of progenitor cell proliferation can be augmented to enhance tissue formation and cement interactions between the implanted medical device and the surrounding host tissue. However, in many cases the goal of therapy may be to reduce, rather than enhance, cellular responses near the implanted surface. In the case of implantable glucose sensors, for example, the natural foreign body immune response surrounding the device with even the thinnest fibrous capsule interferes with its ability to detect glucose. In the case of drug eluting stents, the ability to reduce smooth muscle cell proliferation in response to stent placement has shown profound effects on restenosis times. Another class of therapeutic proteins, the class of neutralizing antibodies, is discussed in this chapter. In this case, the ability to neutralize Vasucular Endothelial Growth Factor (VEGF) with an antibody has proven effective in a variety of human diseases, and provides an engaging model exploring how cellular response can be reduced to implantable medical devices.

The advent of anti-angiogenesis therapy[126] has had wide ranging implications across a spectrum of human diseases. Adding bevacizumab, a VEGF specific antibody, to standard chemotherapy has lead to increased duration of overall survival in colorectal and lung cancer patients[127, 128] and progression-free survival in breast cancer patients.[129] Abnormalities in VEGF regulation amenable to anti-angiogenesis therapy have also been implicated in ocular conditions such as diabetic retinopathy and macular degeneration.[130-132] However, systemic side effects of treatment with anti-VEGF antibodies such as increased mortality from bowel perforation, thromboembolic events, and hemorrhage[133] suggest a possible role for localized delivery. Furthermore, sustained release of anti-VEGF may allow for less frequent

applications, which are invasive and time consuming, particularly in ocular applications where intravitreal injections are standard [132, 134].

One technique with advantageous characteristics for such protein delivery is that of Layer-by-Layer(LbL) deposition.[21] In this technique, oppositely charged polyelectrolytes are deposited on a charged surface, allowing for the buildup of a nano-scale layers of polymer in a tightly controlled film architecture. High retention of protein function within the created films[31, 44, 54, 135][reference growth factor paper and JCR paper], precise tuning of drug release rate and dosage[Reference JCR paper][34], and the ability to uniformly and conformally coat a wide variety of surface chemistries (such as polymer nanoparticles for drug delivery, or titanium for implantable medical devices) make LbL an attractive candidate for localized and sustained drug delivery.

By utilizing LbL deposition with synthetic degradable polyelectrolytes such as poly(β-aminoesters)[29, 60, 63], it is possible to achieve tunable surface erosion[45, 50, 125] in which polymer layers are hydrolyzed, releasing drug trapped in the layer below. Poly(β-aminoesters) have the advantage of being easily synthesized from commercially available monomers allowing facile creation of a library of polymers with different characteristics, stability at construction conditions and degradability at physiological pH, and a charged backbone which allows the polymer to be incorporated in LbL films. Furthermore, *in vitro* and *in vivo* biocompatibility has been explored in a number of different applications, such as those discussed in Chapter 3 and [34, 49]. Surface erosion most importantly allows the possibility of sequential release in which different drugs are captured in different layers of the film and are therefore released at different times[45, 74].

Thus, here we present the first LbL film capable of angiogenesis inhibition, and the first polymeric LbL delivery method for anti-VEGF antibodies that we are aware of. Film buildup and release data from $[Poly1/heparin/anti\text{-}VEGF/heparin]_{80}$ films were examined both *in vitro* on Human Umbilical Vein Endothelial Cells (HUVEC). We found that film

building was super-linear which allows for predictable scaling for different dosage. Release was achieved over the time span of 11 days. *In vitro*, sustained protein activity was observed, making these films attractive for localized anti-angiogenesis control over sustained periods of time.

5.2 Materials and Methods

5.2.1 Materials

Linear poly(ethylenimine) (LPEI, Mn = 25000) was purchased from Polysciences, Inc (Warrington, PA). Poly (sodium 4-styrenesulfonate) (PSS, Mn = 1000000), high molecular weight polyethylene (HMWPE) and Anti Vascular Endothelial Growth Factor antibody (anti-VEGF) were purchased from Sigma-Aldrich (St. Louis, MO). Heparin sodium salt was obtained from Celsus Laboratories (Cincinnati, OH). Poly2 was synthesized as previously described[60]. All commercial polyelectrolytes were used as received without further purification. A micro-BCA assay was obtained from Pierce (Rockford, IL) and a Bromodeoxyuridine (BrdU) Cell Proliferation Colorimetric Assay kit was obtained from Roche Applied Science (Indianapolis, IN). Both were used according to manufacturer instructions. Glass slides (substrates) were obtained from VWR Scientific (Edison NJ). Deionized water (18.2 MΩ) was used for all washing steps. Dulbecco's PBS buffer was prepared from 10x concentrate available from Invitrogen (Frederick, MD). Endothelial Cell medium (EGM-2) was obtained from Lonza.

5.2.2 Preparation of Polyelectrolyte Solutions.

LPEI and PSS were dissolved in deionized water to a concentration of 10mM with respect to repeat unit and pH adjusted to 4.25 and 4.75 respectively. Heparin and Poly2 were prepared at 2 mg/mL and anti-VEGF prepared at 0.25 mg/mL, all in sodium acetate buffer (pH 5.1, 100mM).

5.2.3 Degradable Polyelectrolyte Thin Film Preparation and Characterization

Glass substrates (1" x ¼") were plasma etched in oxygen using a Harrick PDC-32G plasma cleaner on high RF power for 5 minutes. Ten base layers of (LPEI/PSS) were deposited upon plasma etched substrates with a Carl Ziess HSM series programmable slide stainer according to the following protocol: 5 minutes of dipping in LPEI, followed by three washes (10, 20, 30 s respectively) in deionized water, followed by 5 minutes in PSS and three similar washes for 10 repetitions. On top of the base layers, 80 tetralayers incorporating anti-VEGF were built with the following architecture: (Poly 2/Heparin/anti-VEGF/Heparin). A typical dipping protocol would be 10 minutes in Poly 2, 3 washes (10, 20, 30 s), 7.5 minutes in Heparin with 3 washes (10, 20, 30s), 10 minutes in anti-VEGF with 2 washes (20, 30s) and 7.5 minutes Heparin with 3 washes.

5.2.4 Release and Protein Quantification

Samples were released at 37ºC in a microcentrifuge tube containing 1 mL of either phosphate buffered saline for the BCA protein quantification assay or endothelial cell medium for the proliferation activity BrdU assay. At a series of different time points, 0.5 mL of sample was removed and 0.5 mL of fresh PBS or fresh medium, respectively, was introduced to the sample container. Samples were frozen at –20ºC until analyzed. To detect release of anti-VEGF into the PBS solution, a micro-BCA Protein Assay Kit (Pierce Biotechnology, Rockford IL) was used to detect the total amount of protein released. Triplicate 100 uL aliquots of standards and samples were run in 96 well plates according to the manufacturer's protocol.

5.2.5 HUVEC Cell Culture and Proliferation Detection

A BrdU assay was run on the samples released in medium to detect cell proliferation. Briefly, BrdU is an analog of thymidine and the colorimetric assay simply quantifies the BrdU

incorporation into newly synthesized DNA of actively proliferating cells. Human Umbilical Vein Endothelial Cells (HUVEC) were seeded in a 96 well plate at a concentration of 750 cells per well. Anti-VEGF was diluted in medium to concentrations ranging from 35.71x to 0.28x. Dilutions were incubated for one hour at room temperature before being placed on the cells. The cells were incubated at 37 degrees Celsius for 72 hours. The rest of the BrdU assay was performed according to manufacturer's protocol with an incubation period of 6-8 hours after the addition of labeling solution. The plate was read at 370 nm with a reference wavelength of 492 nm every 10 minutes for one hour. Error bars for all figures in this paper represent a 95% confidence interval calculated from triplicate repeat samples.

5.3 Results and Discussion

Although protein incorporation and release have been examined within the field of LbL films both in terms of enzymes[63], and with growth factors[51, 53, 63], only one instance of antibody incorporation into LbL films was found in the literature. It was therefore not immediately apparent that buildup and release of anti-VEGF antibodies from LbL films would possible. To this end, one poly(β-aminoester), Poly2, shown in Figure 5-1A, which had performed very well in preliminary experiments was selected to create films of a tetralayer architecture $[Poly1/heparin/\alpha\text{-}VEGF/heparin]_{80}$.

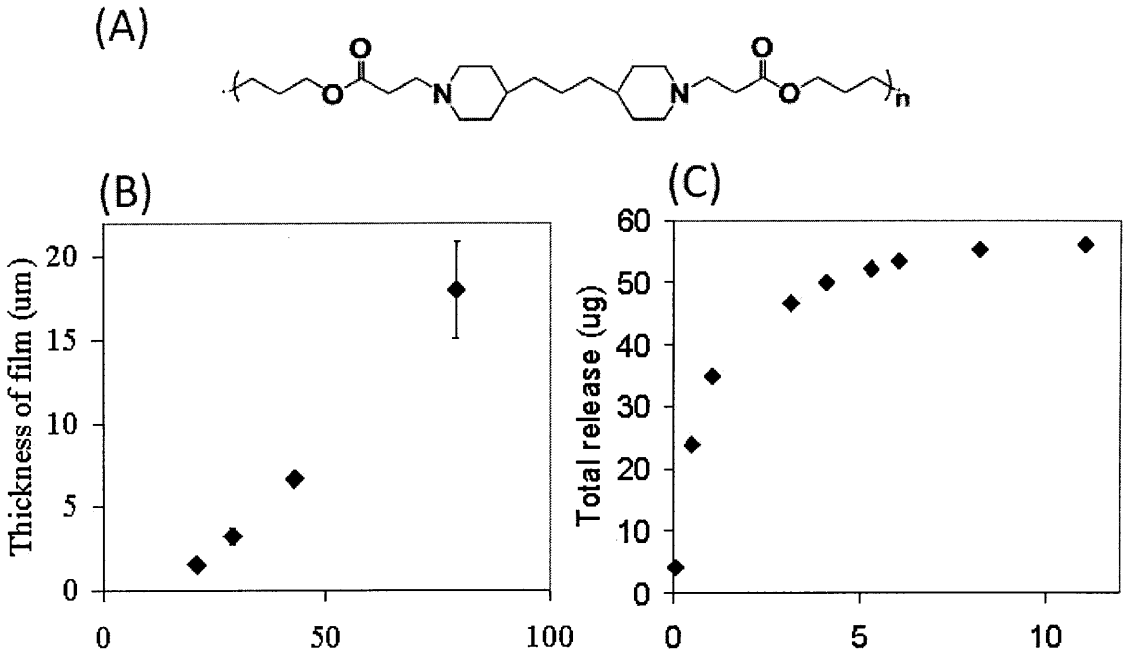

Figure 5-1: Film Characterization. (A) Hydrolytically degradable polymer structure; polymer is cleaved by ester hydrolysis. (V) Film growth with number of tetralayers, showing superlinear growth. (C) Release curve shows high levels of release over 11 days

In Figure 5-1B, the thickness of films built with this architecture is tracked using profilometry, and shows a typical 2 regime behavior similar to work done with other classes of proteins that suggests superlinear growth. In the first 10 tetralayers, very little material is incorporated, as the surface is continually improved to create complete polymer coverage. After 10 tetralayers, the films incorporate large amounts of material in a linear fashion. This buildup behavior is desirable, as it is easy to tune the drug delivery from such a film; additional layers of film add a linear amount of material, making predictions of drug loading and release time relatively easy to calculate, compared with less linear systems. In Figure 5-1C, the *in vitro* release of α-VEGF from the films is tracked, showing a power law release profile spanning 11 days with incorporation of over 50 ug of α-VEGF.

Our primary interest with these constructs was to release therapeutic proteins that had retained a high degree of biological activity. Vascular Endothelial Growth Factor is well

known to enhance endothelial cell proliferation, leading to the leaky types of vasculature that are the hallmark findings within tumors[136-138]. In culture, HUVEC cells similarly require culture medium containing VEGF to be able to proliferate, allowing for a model system in which proliferation in response to VEGF can be tested. α-VEGF released from LbL constructs was applied to HUVEC culture medium and allowed to bind for 1 hour before exposure to cells in the proliferative state. During this hour, α-VEGF binds VEGF, inactivating it. Therefore, culture medium with α-VEGF present will have a decreased ability to enhance endothelial cell proliferation, leading to decreased BRDU incorporation. In Figure 5-2A, the proliferation of HUVEC is monitored in response to α-VEGF from film constructs, compared with the proliferation of HUVEC in regular growth medium. HUVEC exposed to α-VEGF display decreased proliferation rates at all time points compared with control cells in normal medium, indicating that the films maintain *in vitro* therapeutic activity of blocking endothelial cell proliferation. This system models the response of endothelial networks which form the first leaky blood vessel networks most typically associated with tumors to therapy. α-VEGF decreases proliferation of such networks, cutting off the supply of nutrients and oxygen to the tumor and normalizing the permeability of existing blood vessel networks, which has been hypothesized to enhance the delivery of chemotherapeutic agents[139-141].

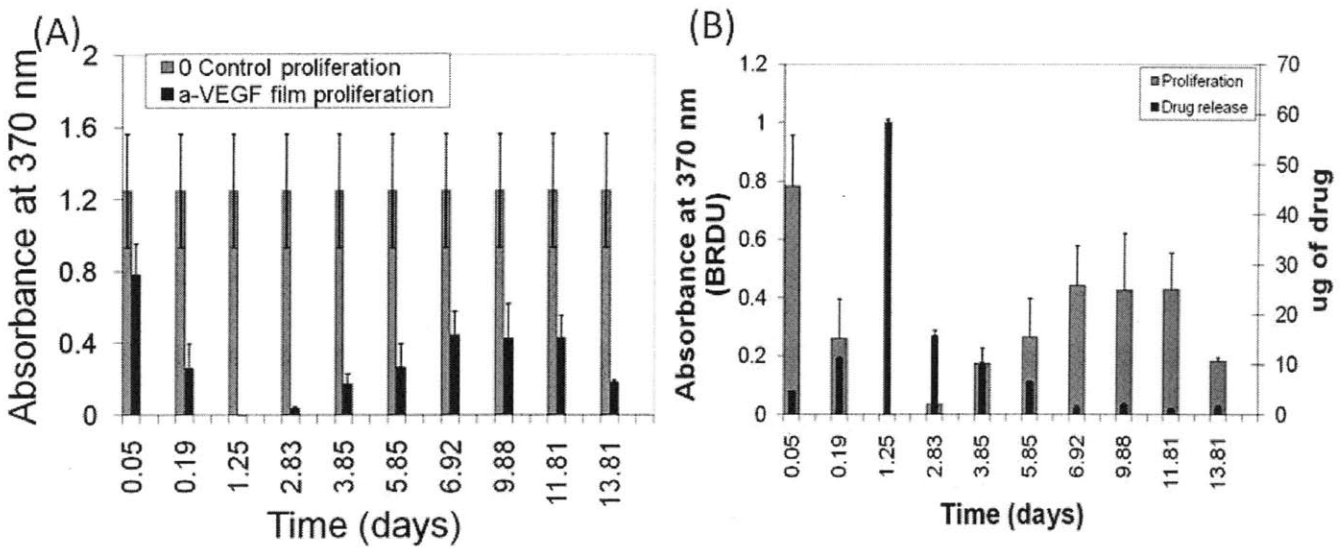

Figure 5-2: (A) HUVEC display decreased proliferation rates in cultures responding to anti-VEGF released from LbL films compared with control cells which have regular growth medium. (B) Proliferation is inversely related to anti-VEGF concentration, showing dose dependence of the effect.

In Figure 5-2B, a precise correlation is found between the amount of α-VEGF delivered and the proliferation response rate of the cells. The highest drug loads of α-VEGF correspond to very low proliferation rates (as all of the VEGF is bound and cannot affect proliferation), and the α-VEGF released is active in the medium for many days.

5.4 Conclusions

Antibody delivery techniques are likely to become more common as the breadth of FDA approved antibodies increases and the applications of this new class of drugs are better understood. Ultimately, controlling unwanted cellular responses is likely to be applicable to a broad range of therapies, and thus exploring the local controlled delivery of these proteins is important. Here, LbL's ability to conformally coat any surface, including a nanoparticle for injectable delivery, allows it to be utilized in a one-two punch against cancer cells, in which

existing nanoparticle technologies can be modified to sequentially release anti-VEGF to normalize tumor vasculature and then release a payload of chemotherapy. Here we have shown that anti-VEGF, a forerunner in the class of therapeutic antibodies, can be successfully incorporated in and released from LbL films with retention of activity in neutralizing VEGF-induced endothelial cell proliferation. This work represents an important step forward in the delivery of such antibodies to discrete local targets for maximal therapeutic effect and synergism with other cancer fighting strategies on the nano-scale.

Chapter 6 Using Bioactive Surfaces to Direct Native Stem Cell Differentiation: Polyelectrolyte Multilayer rhBMP-2 Delivery Films

6.1 Introduction

Biologic-eluting implant technologies represent a paradigm shift, from bare implants or those eluting small molecules, that is likely to become more necessary as the value and variety of therapeutic biologics is recognized across many fields. In the orthopedic space, for example, it has long been predicted that being able to control the release of Bone Morphogenetic Protein 2 (BMP-2) from the surface of a biologically fixated implant would have a tremendous effect on bone in-growth, one of the key parameters in the field [20, 142]. Over $1 billion are spent yearly on revision surgeries in the United States alone due to infection and loosening[19] which could in part be avoided by better integration of the implant with surrounding bone tissue[19, 143]. Although multiple polymer bulk-degrading BMP-2 release systems have been created for critical defect applications[144-147], these systems suffer design issues when applied in the case of an implant surface. Simple surface adsorption releases the growth factor in a burst too short to induce biologic activity[148]. Covalent surface attachment studies offer an alternative method for introducing BMP-2, but inherently cannot access the additional attractive modality of sequential release[149, 150]. Thus, ultrathin, conformal coatings that can load therapeutic doses on implant surfaces through a gentle

aqueous process that preserves fragile biologic activity represent a powerful platform technology.

Furthermore, as the unique and complementary contributions of mechanical and chemical properties to cell microenvironment are explored in cell-interfacing biomaterials, decoupling the chemical and mechanical properties of the scaffold become crucial. The ability to surface modify a cell scaffold of ideal mechanical properties to release chemical cues of interest (rather than the intrinsically linked mechanical/chemical properties of most bulk releasing polymer drug delivery systems) offers a flexible approach to achieving next-generation regenerative medicine scaffold design.

Layer-by-Layer (LbL)[21] deposition is a technology that is well poised to have significant impact in this rapidly developing area of controlled surface release of growth factors. In electrostatic LbL, a charged surface of interest, such as polymer, titanium, ceramic, or glass, is alternately dipped in positively and negatively charged polyelectrolyte solutions; during each dip step a nano-layer of polymer adsorbs to the surface. Because there is nanometer control over the architecture of the resulting film, sequestering different drugs in different domains becomes possible [44, 45], allowing the powerful potential of sequential release of multiple therapeutics. Within the realm of growth factor delivery, LbL simultaneously has the advantages of being able to conformally coat difficult but medically relevant geometries (such as tissue engineering scaffolds, stents or hip implants)[151], and utilizing gentle aqueous baths that preserve fragile protein activity[63], which yields a flexible

and powerful platform technology for directing cell interactions from a nano- to micro- scale film.

By utilizing a synthetically tunable, hydrolytically degradable polymer from the family of poly (β-aminoester)s (PBAEs)[152] as one of the charged polymers employed in LbL, it is possible to obtain controlled surface erosion of the constructed film to release drugs from the surface of interest[29, 35, 36, 49, 50]. The use of synthetic polymers here allows a significant increase in tunable control of drug release characteristics in LbL compared with traditional biopolymers, which have inherent and difficult-to-tune loading and release characteristics. A wide variety of PBAE structures can be easily created through the combinatorial Michael addition of two commercially available classes of starting materials to yield a library of polymers with different characteristics[61]. This approach affords far more tunability of polymer structure and thus drug loading and release. Past studies with PBAEs have found them to be well suited to LbL construction[62].

Here, we use BMP-2, a well known stem cell differentiation factor which can induce bone formation from native, adult stem cells present naturally in implant site. The positively charged BMP-2 protein is incorporated in an LbL film with a positively charged PBAE and negatively charged chondroitin sulfate to create a film capable of sustained release and increased interaction time between resident stem cells and BMP-2 compared with injections, which are cleared too quickly, and with little resulting effect[6]. This micron-scale LbL surface modification would capitalize on the strength of the titanium implant for load

bearing while enhancing integration with surrounding bone tissue through surface released cues. The focus on BMP-2 controlled osseointegration in hip implants is made more attractive by recent advances in anti-inflammatory[36] and antibiotic[34, 35] LbL delivery which would allow for multi-agent release to combat several relevant hip implant source problems simultaneously or in sequence.

However, it is important to realize that such an LbL growth factor delivery film would find many applications across both tissue engineering and implant delivery device areas, and could be broadly applied to the direction of cell fate of any cell known to respond to growth factors in the body. Here, for example, the test substrate employed is a three dimensionally printed, polycaprolactone/β-tricalcium phosphate copolymer blended scaffold that would be equally well suited for enhanced bone formation in critical sized defects, while also serving here as a test-substrate for future hip implant applications.

In this work, we describe the material and release characteristics of our synthetic polymer, LbL BMP-2 films. We show that BMP-2 released from these films retains the ability to accelerate the differentiation of MC3T3-E1 pre-osteoblasts to a bone lineage and enhance bone nodule formation in culture. In vivo, we recruit native host stem cells to differentiate into bone in a rat intramuscular implantation model, precipitated by the BMP-2 released from the implanted surface. Micro-computed tomography studies confirm radiologically visible bone deposits and suggest continuing bone mineralization from one to two month time points. Histology reveals additional markers of bone maturation, including fronts of

osteoblasts on the leading edge of formed bone in the process of matrix deposition, a woven to lamellar bone morphology, as well as the formation of bone marrow cavities associated with the bony structures.

Various LbL growth factor delivery systems, including BMP-2, have been demonstrated in the past[51, 53, 67], however only one in vivo growth factor LbL studies have been previously reported. The current study is the first to use clinically relevant doses of BMP-2 to direct entirely autologous, native stem cells *in vivo* to induce bone formation, rather than exogenous source cells with the concomitant problems of graft-host immunogenicity, feeder layer contamination, and pathogen transfer. As such, this work represents an important step forward for the LbL growth factor delivery technology, which we expect to find diverse applications in tissue engineering and surface drug delivery.

6.2 Materials and Methods

6.2.1 Materials

Chondroitin sulfate sodium salt (Mn = 60000) was obtained from VWR Scientific (Edison NJ). Poly (β-aminoester) 2, hereafter called Poly 2, was synthesized as described[60]. Recombinant human BMP-2 (rhBMP-2) was obtained from Insight Genomics (Falls Church, VA). BMP-2 ELISA kits were obtained from Peprotech (Rocky Hill, NJ). Sodium acetate buffer, 3M was obtained from Sigma Aldrich (St. Louis, MO).

6.2.2 *Preparation of polyelectrolyte solutions*

Poly 2 dipping solutions were 2 mg/mL in 25 mM sodium acetate buffer, pH 5.1. Chondroitin dipping solution consisted of 2 mg/mL chondroitin in deionized water (18.2 MΩ, Milli-Q Ultrapure Water System, Millipore). rhBMP-2 dipping solutions were 50 ug/mL in 100 mM sodium acetate buffer, pH 5.1. Poly 2 and chondroitin dipping solutions were replaced and an additional 50 ug/mL of BMP-2 was added to the pre-existing bath, every 24 hours. All wash baths were deionized water.

6.2.3 *Film construction and characterization*

Therics™ polycaprolactone/β-tricalcium phosphate (PCL/BTCP) co-polymer blend 3D printed scaffolds were plasma etched with room air using a Harrick PDC-32G plasma cleaner on high RF power for 1 minute and immediately immersed in Poly2 solution. A nanolayerd film was fabricated on this scaffold with a Carl Zeiss HMS programmable slide stainer with the following dipping protocol: 5 minutes in Poly 2 solution, 3 washes (10, 20, 30 s), 5 minutes in chondroitin solution, 3 washes (10, 20, 30 s), 10 minutes in BMP-2 solution, 1 wash (10s) and 5 minutes in chondroitin solution with 3 washes (10, 20, 30 s).

6.2.4 *Release characterization*

BMP-2 film coated scaffolds were released at 37ºC into 1 mL of growth medium, consisting of αMEM supplemented with 10% fetal bovine serum and 1% penicillin streptomycin (Invitrogen, Carlsbad CA). At a series of different time points, 0.5 mL of medium and eluted material was removed and 0.5 mL of fresh release medium was replaced. Samples were

analyzed using ELISA development kits according to manufacturer instructions and cell differentiation assays (see below).

6.2.5 Cell culture

MC3T3-E1 Subclone 4 (ATCC, Manassas, VA) were maintained in growth medium and split when subconfluent. MC3T3-E1 cells were seeded at 1 x 10^4 cells/cm^2 and allowed to grow to confluence in 96 well plates (quantification) and in 8 well chamber slides (visualization) in 100 uL of growth medium. MC3T3-E1 cells were cultured under four experimental conditions: (1) growth medium, (2) differentiation medium (growth medium supplemented with 50 μg/ml L-ascorbic acid and 10 mM β-glycerol phosphate), (3) differentiation medium supplemented with 90 ng/mL of BMP-2, and (4) differentiation medium supplemented with 90 ng/mL of PEM-released BMP-2. Cell culture media were changed every two days until analysis for alkaline phosphatase, alizarin red, or Von Kossa as described below.

6.2.6 Alkaline phosphatase activity assay

Alkaline phosphatase (ALP) activity was determined on day 6 after the initiation of MC3T3-E1 osteogenic differentation by visual staining techniques and quantitation of the enzyme activity. Cells were rinsed with PBS without Ca^{2+} and Mg+ and incubated in a stain solution consisting of 50 mM Tris HCL pH 8.0 with 1 mg/mL fast red and 1% napthol AS-MS dissolved in DMSO for 30 minutes at 37ºC. An equal volume of 8% paraformaldehyde was added for 10 minutes at room temperature to fix cells. After rinsing 2x with distilled water, cells were imaged using a Zeiss inverted microscope with a 10X objective lens and Imaging software.

The stain was solublized by adding 0.1% triton in PBS and then freezing to -80 ºC for one freeze-thaw cycle. The cell lysates were transferred to an eppendorf tube, centrifuged at 15,000g for 3 min at 4 ºC, and the supernatant was collected. Fifty µL of lysate was incubated with 150 µL of pNPP solution for 30 min at 37 ºC. The reaction was terminated with 0.1 M NaOH and ALP activity read on a plate reader at 405nm. The ALP activity measurements were normalized to total protein determined by BCA assay.

6.2.7 Alizarin red S differentiation assays

After 28 days of exposure to differentiation medium, MC3T3-E1 cells were assayed for calcium deposition using Alizarin red S (ARS). Cells were washed with PBS and fixed with 4% paraformaldehyde for 10 minutes. After three rinses of 5 min in distilled water, ARS stain solution (2% ARS in distilled water pH balanced to 4.1 with 10% ammonium hydroxide) was incubated with cells for 20 min at room temperature. Cells were then washed in distilled water 4 times for 5 minutes each. The ARS stained cultures were imaging with phase contrast microscopy.

The ARS stain was quantified using a previously published protocol[153]. The ARS stained cultures were incubated in 10% acetic acid for 30 minutes at room temperature and then the cell layers were disrupted by the use a pipette tip. The cell suspensions were transferred to a microcentrifuge tube, vortexed for 30s, paraffin wrapped and heated at 85ºC for 10 min. After transferring to ice for 5 min, the tubes were centrifuged at 16,000 g

for 15 minutes and pH balanced with 10% ammonium hydroxide to 4.1-4.5 pH units. Duplicates were read on a 96-well plate with black sides and a clear bottom at 405 nm.

6.2.8 Von Kossa differentiation assay

Von Kossa staining was performed to determine the presence of mineralization nodules within the MC3T3-E1 cell cultures. Cultures were rinsed with PBS, fixed with 4% PFA for 10 minutes, and then washed in distilled water. The cultures were then incubated in a 3% aqueous silver nitrate solution for 30 minutes at 37 °C. The silver nitrate stained cultures were then treated in a UV Stratalinker under UV light at 254 nm. The cultures were washed with distilled water and then neutralized with 5% sodium thiosulfate for 5 minutes at room temperature. A final wash with distilled water was performed and the cultures were imaged by phase contrast microscopy.

6.2.9 Protein Conformation and Total Protein Analysis

Several studies were performed to understand the protein conformation and the total amount of protein present in release samples. These studies included:

6.2.9.1 Circular Dichroism

Stock BMP-2 solutions were reconstituted to a concentration of 3.33 ug/mL in 1x PBS supplemented with 1% penicillin/streptomycin(P/S). An Aviv Model 202 Circular Dichroism Spectrometer was used to take measurements of 200 µL of blank (consisting of 1x PBS with 1% P/S) or sample over 190-300 nm wavelengths. The blank was subtracted from the BMP-2 measurement to yield a plot.

6.2.9.2 Fluorimetry

Typical BMP-2 LbL films consisting of [P2/chondroitin/BMP-2/chondroitin]$_{100}$ architecture deposited on plasma etched Therics™ scaffolds were released in 1x PBS with 1% P/S for one day to allow enough sample for detection. Fluorescence measurements from 300-600 nm were made using a Jobin Yvon Fluorolog-3 spectrofluorimeter (HORIBA Scientific) and a Spectrosil quartz cuvette (315 µL volume, 3 mm path length; Starna Cells, Atascadero, CA). A calibration curve of BMP-2 emission at 350 nm constructed using known quantities of BMP-2 dissolved in 1x PBS with 1% P/S was found to be linear over the range of 0.1-1 ug of BMP-2. Measurements of up to 0.5 mg/mL of chondroitin were found to have insignificant effect on protein measurements, while Poly2 is known not to interfere with fluorimetry measurements (data not shown). Release samples from 1 day of release were also measured.

6.2.9.3 High Performance Liquid Chromatography-Mass Spectrometry

Seven mg of scaffold with typical BMP-2 architecture films deposited on top were released in 150 µL alpha-MEM cell culture medium supplemented with 1% P/S for one day and were taken for analysis by the Koch Biopolymers lab on the combined High Performance Liquid Chromatrography/Mass Spectrometry (HPLC-Mass Spec) setup. Briefly, the sample was dissolved in 8 M urea, and disulfide bonds were reduced with 10 mM DTT at 60 °C for 1 hour. Cysteine residues were alkylated with 30 mM iodoacetamide for 45 minutes; salts were removed and protein was concentrated with a 3,000 MWCO Micrcrocon centrifugal device

(Millipore) to a 20 µL volume. The sample was dissolved in 100 µL of ammonium bicarbonate, pH 8.5, and divided. Each half was digested with an enzyme treatments, either trypsin and AspN, carried out at room temperature overnight. Each sample was reduced to 5 µL in a vacuum centrifuge, and the digestion was stopped with 15 µL of 0.1% formic acid. Five µL samples were injected for analysis with on line sample desalting and peptide trap. Peptides were separated using a Tempo nanoflow HPLC on a capillary (75µm I.D.) reversed phase C18 column with a water-acetonitrile-0.1% formic acid gradient at a flow rate of 300 nL/min. The HPLC-MS analysis was carried out with a QSTAR Elite quadruple time-of-flight mass spectrometer. The remaining 15 µL of each sample was spun on a column for removing SDS and other detergents from Pierce, eluted following manufacturer protocol, and re-analyzed under similar conditions to remove any polymer contaminants from the system.

6.2.10 Intramuscular bone formation model

All animal work was performed in accordance with protocols approved by the Committee on Animal Care at the Massachusetts Institute of Technology. Sixteen 350-400 g male Sprague Dawley rats were given preoperative analgesics (meloxicam and buprenex), and intraoperative anesthesia via 1-3% isoflurane in oxygen. The right hindlimb of each animal was shaved, cleaned with alcohol and povidone iodine solutions, and sterile drapes were placed around the surgical area. A 2 cm longitudinal incision, centered at the midshaft of the femur, was made laterally along the hindlimb. A pocket made in the quadriceps

muscle mass by blunt dissection anterior to the iliotibial band. One LbL-coated PCL/BTCP scaffold was inserted into the intramuscular pocket, and wounds were closed progressively with three layers of sutures (muscle, subcutaneous, and dermal layers). Each hindlimb was implanted with either a control scaffold, $[P2/chondroitin\ sulfate]_{200}$, or a BMP-2 scaffold, $[P2/chondroitin\ sulfate/rhBMP\text{-}2/chondroitin\ sulfate]_{100}$. Postoperatively, rats were treated with buprenex and meloxicam until signs of distress dissipated. Rats were housed in separate cages with free access to food and water. At four and eight week time points, four rats implanted with the control scaffold and four rats implanted with the BMP-2 scaffold were sacrificed and the implants retrieved for analysis as described below.

6.2.11Micro-computed tomography (MicroCT) analysis

Excised samples were immediately placed in 10% neutral buffered formalin and imaged with MicroCT (eXplore Locus, GE Medical Systems, London, Ontario) at a resolution of 27 μm with proprietary software included with the system (EVS Evolver, GE Medical Systems, Fairfield, CT). The scanning protocol was performed with a 2000 ms shutter speed, 1x1 bin size, at X-ray tube parameters 80kV and 450 μA. Four hundred images were taken at incremental angles, and rendered 3D images were reconstructed with the Reconstruction Utility and analyzed using MicroView (GE Healthcare, Fairfield, CT). Threshold values were chosen by visual inspection and kept constant across 1 month or 2 month data sets. Three independent regions of interest (ROIs) were chosen per sample, and the bone analysis tool was used to measure bone mineral density and stereology measurements of each sample.

Three dimensional representations of bone formation and two dimensional digital slices through the samples were also taken for qualitative comparison.

6.2.12 Histological analysis

After 24 hours in 10% formalin, tissues were transferred to solutions of 70% ethanol prior to decalcification. Tissues were decalcified for 5 days in a solution of 15% EDTA and 10% sodium citrate buffer, pH 7.2 at 4ºC under continuous stirring. Tissues were then serially sectioned, routinely processed, and embedded in paraffin. Microscope sections (4 μm) were stained with hematoxylin and eosin (H&E), Alcian Blue, and Masson's trichrome stains.

6.3 Results and Discussion

6.3.1 Employed LbL System

BMP-2 has an isoelectric point of 8.5 and a molecular weight of 32 kDa and is a positively charged protein under our LbL dipping conditions (pH 5.1). The poly(β-aminoester)s also exhibit positive charge due to the amine groups along the backbone[62]. Hence,a tetralayer architecture was required to incorporate both cationic molecules into a elctrostatically driven LbL multilayer thin film. We used a natural polyanion, chondroitin sulfate, to create tetralayers with the following architecture: [Poly2/chondroitin sulfate/BMP-2/chondroitin sulfate]$_n$, where the term in brackets represents the architecture of one tetralayer repeat unit and n denotes the number of tetralayer units deposited. In previous work with the model protein lysozyme, which has similar molecular weight and isoelectric point to BMP-

2[63], chondroitin sulfate containing films have been shown to have excellent electrostatic binding properties, as well as desirable protein loading and release characteristics and retention of bioactivity.

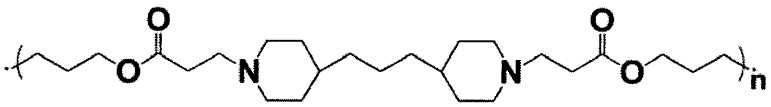

Figure 6-1: Structure of Poly2, the selected poly(-aminoester) used in this work.

Of the family of poly(β-aminoester)s available, Poly2 (Figure 6-1, structure) was chosen because it affords all of the positive characteristics of this class of polymers, including biocompatibility, ease of manufacture, hydrolytic degradation, and positive charge, while additionally providing a more sustained release profile compared to other tested polymers in the class [63]. The prolonged half-life of Poly2 is due to the presence of a hydrophobic region near the ester bond and the consequent decrease water attack, hence slower degradation rate of the polymer. In our previous work, we demonstrated that the advantageous characteristics of an increased hydrophobic region on delaying degradation were found to balance with a point in which the polymer no longer had sufficient ionic cross-links to avoid bulk release[64]; Poly2 therefore balances increased release time with a continued ability to allow for electrostatic construction.

6.3.2 Film Characterization

In Figure 6-2, the film growth of [P2/chondroitin/BMP-2/chondroitin] films deposited on planar substrates is confirmed using profilometry thickness measurements. This formulation

exhibits a classic multilayer exponential buildup behavior (R^2 = 0.96), with each tetralayer incorporating more material than the last. An exponential building behavior indicates that an interdiffusive process is taking place in which polymers adsorb both to the top of the film and also have an ability to penetrate into the bulk of the built film [76-79]. This type of building behavior is most frequently seen in biological systems where the charge density along the polymer backbone is lower, leading to less ionic crosslink density and a loopier polymer architecture[63], or in the case of small molecules which have fewer electrostatic interactions to break and therefore diffuse more readily[34, 35]. It is hypothesized that the dip time and the diffusivity of the polymer interplay to allow one region at the top of the film accessible to polymer; underneath is a reorganized region that is inaccessible to polymer diffusion due to the short periods of dipping.

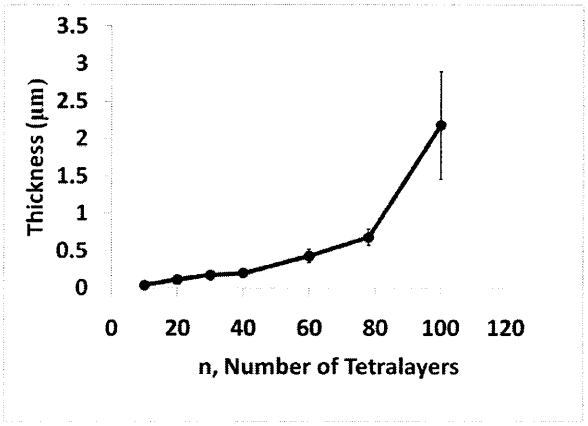

Figure 6-2: Profilometry measurements of film thickness with increasing numbers of tetralayers in a [P2/Chondroitin/BMP-2/Chondroitin]n film. Duplicate films were assayed with 4-6 measurements taken per film; error bars represent the standard deviation of measurements.

At 2-3 microns for a 100 tetralayer film (200-300 nm per tetralayer repeat unit), this formulation is much thicker (an order of magnitude greater) than the typical LbL film, and thus represents a promising candidate for creating a large enough reservoir to be significant in the arena of drug delivery. However, this 2-3 microns thick LbL coating is orders of magnitude smaller than traditional bulk degradation polymer delivery models, hence allowing its applicability to a wide variety of existing implant technologies.

Although the planar substrate utilized above was ideal for profilometry measurements, a three dimensional, porous scaffold was used for in vitro and in vivo testing to enhance the substrate surface area and thus growth factor loading. A macroporous scaffold made of osteoconductive, biocompatible elements was chosen for the following three reasons: (1) total drug load scales with film surface area, allowing for a greater load per volume in a macroporous three dimensional substrate compared with a flat film; (2) such a functionalized, combination osteoconductive/osteoconductive scaffold is of interest in and of itself if biologic molecules can be applied to it in a way that increases bone formation for critical sized defects or when not enough autografted bone can be harvested; (3) typically both an osteoinductive agent, such as BMP-2, and an osteoconductive microenvironment are necessary for ectopic bone formation. In 3D-printed β-tricalcium phosphate/polycaprolactone scaffolds, a precisely defined architecture can be employed, while taking advantage of the biocompatibility and bioactivity of the polymer material blend; they thus were utilized here as a test substrate.

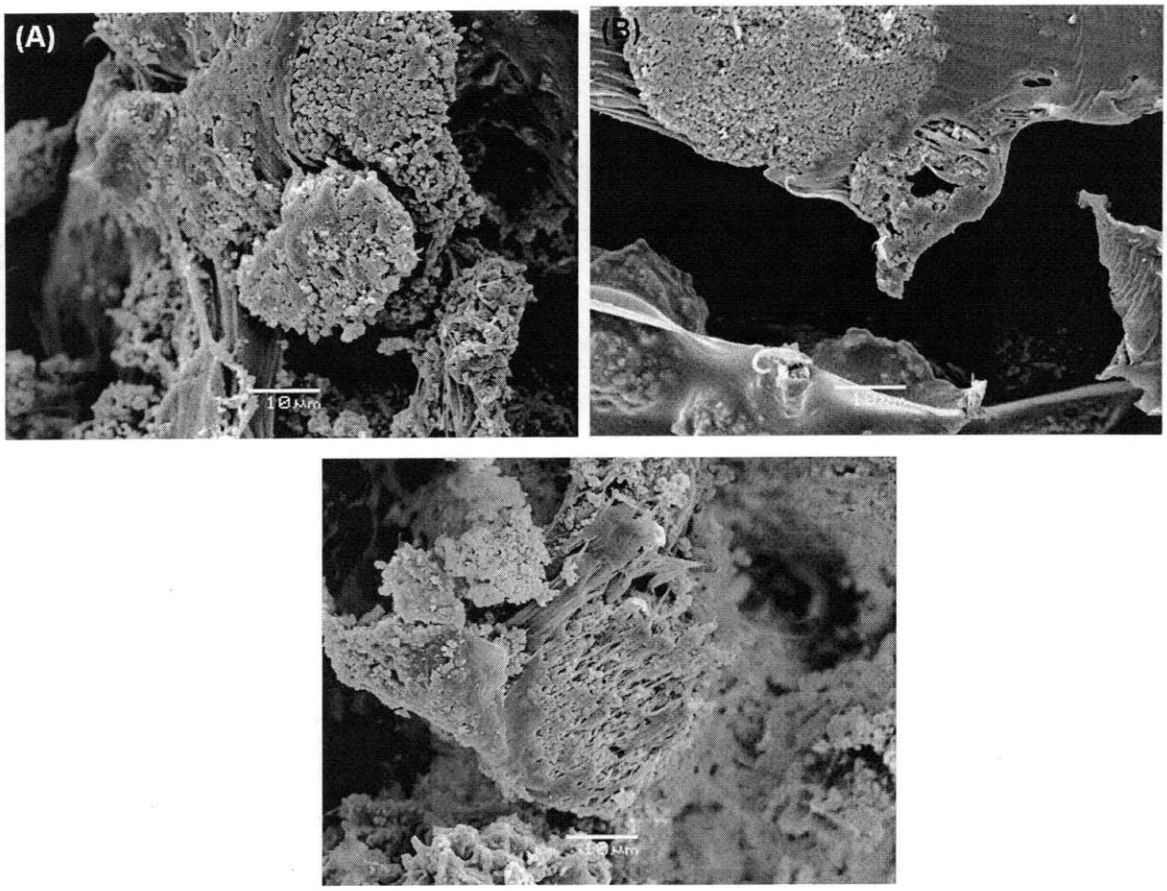

Figure 6-3: SEM cross sectional images (A) before LbL deposition (B) after LbL deposition and (C) after release of LBL film A key strength of LbL is its ability to be applied conformally to a wide variety of medically relevant substrates.

In Figure 6-3, SEM cross sectional images of 3DP scaffolds taken before LBL deposition, after LBL deposition, and after completing drug release show a clear change in morphology due to the dipping process, and a return to the original morphology upon complete release of the films. The surface of the scaffold naturally has a "popcorn',

roughened morphology due to the β-TCP (red arrow), which is embedded in PCL fibers (white lines)[154]. After dipping, the surrounding polymer film is glassy and conformal to the surface of the scaffold; however, it is difficult to conclude much about the surface coverage because the LbL film and the PCL have a similar appearance on SEM. The original architecture is again revealed after release, with the PCL matrix being less smooth. PCL is known to flake and degrade in the presence of cell culture medium over the time periods of interest in this study[154].

Scaffold film coverage was probed using a fluorescent model protein, lysozyme (a model protein with similar isoelectric point and molecular weight to BMP-2) labeled with Alexa Fluor 488. When lysozyme was incorporated in an LbL film, the resulting film demonstrated a smooth coating of the surface, rather than a patchy morphology (Figure 6-4). Three dimensional renderings comparing the scaffold surface to the fluorescent protein layer show close correlation of the fluorescent LbL film (Figure 6-4A) with the scaffold surface (Figure 6-4B) which can be well visualized by the overlay of the two images (Figure 6-4C); however, the three dimensional roughened surface limits the plane of focus, which makes visualizing the surface coverage difficult. Three dimensional reconstruction (Figure 6-4D) assimilating all of the planes of focus shows a smooth coating in which the LbL film takes the shape of the underlying popcorn-like scaffold.

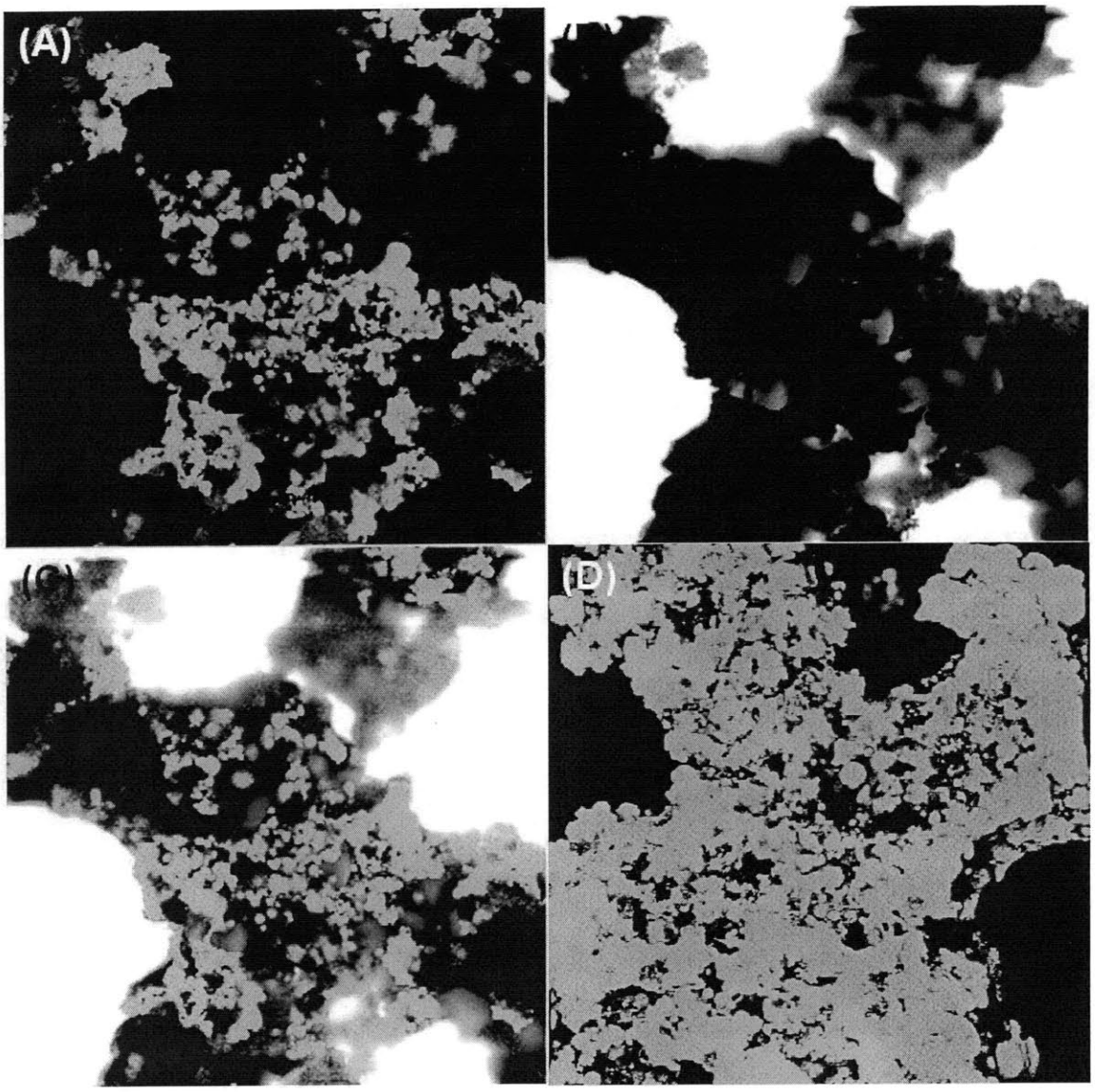

Figure 6-4: LbL deposition with Alexa Fluor 488-labeled lysozyme (a model protein of similar pI to BMP-2) at 10x magnification. (A) LbL fluorescent film (B) Brightfield image of scaffold (C) Overlay of (A) and (B) shows co-localization with the scaffold surface and LbL film. (D) A three dimensional reconstruction of all fluorescent planes shows smooth 3d coverage of the scaffold with LbL film.

6.3.3 Film Release

[P2/chondroitin/BMP-2/chondroitin]$_{100}$ films constructed on the 3DP scaffolds show a distinct two-regime release profile (Figure 6-5). Very little burst release is seen from the film; a sustained linear release profile is observed for the first two days (R^2 = 0.9848) in which 80% of the film contents are released. Here, the release profile shifts to a second regime which is well fit to both linear (R^2 = 0.96) and power law (R^2 =0.997) equations, in which the additional 20% of film release is sustained over an additional 2 weeks. A typical scaffold used for in vitro and in vivo tests weighed 14 mg (both before and after dipping; the LbL film adds a negligible amount of weight), thus releasing 10.6 +/- 0.3 ug of total BMP-2 from the scaffold surface.

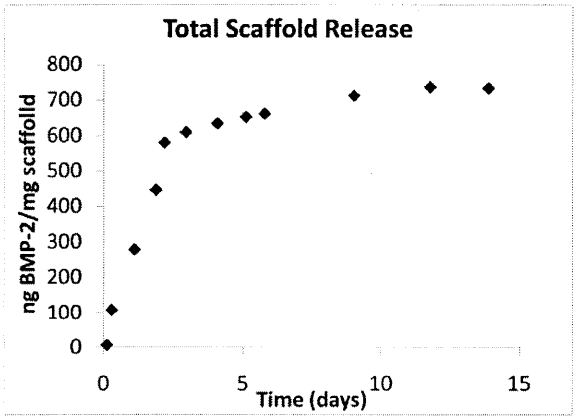

Figure 6-5: Cumulative release from dipped 3DP PCL/β-tricalcium phosphate copolymer blend scaffolds (weight matched to implant samples, equal to 15 mg of implanted scaffold and film). A burst release of 80% over 2 days is followed by sustained release of an additional 20@ of total released BMP-2 over the following two weeks. Fourteen mg of scaffold was implanted in vivo leading to a total release of 10.6 +/- 0.3 ug BMP-2 in vivo.

This release can be compared to three types of literature values: those for other preclinical BMP-2 delivery systems, those for Infuse (the only clinical BMP-2 delivery method using a collagen carrier delivery device), and those for typical BMP-2 implant surface treatments. Typical literature values to see ectopic bone formation *in vivo* from preclinical, bulk carrier systems run from 1-100 ug of BMP-2 incorporated in volumes on the millimeter scale [144-147], indicating that our BMP-2 LbL system is in the correct range to see in vivo results. However, our system can deliver these similar amounts of BMP-2 from a 2-3 micron thick film deposited on any surface of interest. Infuse incorporates impressive doses of BMP-2 (12 mg), but well known issues with the collagen carrier lead to a 40-60% burst release over the first 3 hours[5, 15], which is posited to be the reason such supraphysiologic, costly doses of BMP-2 are required. Here, we exert strong control over release from our ultrathin film to yield two weeks of release, and only 1% of the BMP-2 released in 3 hours. Similarly, while it is predicted that BMP-2 should improve osseointegration in the implant setting, simple surface adsorption is known to be ineffective due to the uncontrolled release of growth factor[148], as it is understood that fleeting doses, even of large concentrations of BMP-2, are ineffective[6]. Thus, here again, this LbL system shows unique advantages in being able to control the release profile. Finally, three other BMP-2 LbL systems have been attempted[44, 53, 155]; however, these systems cannot release microgram or milligram scale quantities of BMP-2, which are certainly necessary for ectopic bone formation. This LbL

system is thus unique in its ability to deliver potent microgram quantities of growth factor from an ultrathin film with control over the release profile.

6.3.4 In Vitro *Studies: Alkaline Phosphatase, Alizarin Red and Von Kossa*

BMP-2 is known to be a potent inductor of bone-lineage differentiation for progenitor cells, both in cell lines [156-158] and in vivo [67, 159]. Pre-osteoblast MC3T3 cells were used *in vitro* to test the differentiation potential of BMP-2 released from LbL films. When cultured in regular growth medium, only a negligible number of a conflent monolayer of MC3T3 cells can be induced to the bone lineage. In contrast, when the regular growth medium is supplemented with β-glycerol phosphate and L-ascorbic acid, a moderate level of bone differentiation occurs, while supplementing this differentiation medium with BMP-2 leads to high levels of bone induction.

Alkaline phosphatase upregulation is an early indicator that the bone differentiation gene expression pathway has been activated in progenitor cells[160]. In Figure 6-6, qualitative stains and a quantitative assay at six days measure the alkaline phosphatase induction of MC3T3 cells cultured with growth medium (M), differentiation medium (D), release medium, consisting of differentiation medium and 90 ng/mL of BMP-2 released from a LbL film (R), and a positive control of differentiation medium supplemented with 90 ng/mL of BMP-2 (B). Qualitatively, the red alkaline phosphatase stain is sparsely visible in the growth medium (M), and moderate staining is observed for cells in differentiation medium (D). The robust red staining in both the positive controls (B) and the test samples (R) indicate an enhanced

induction of the bone differentiation pathway, confirming the bioactivity of BMP-2 released from films.

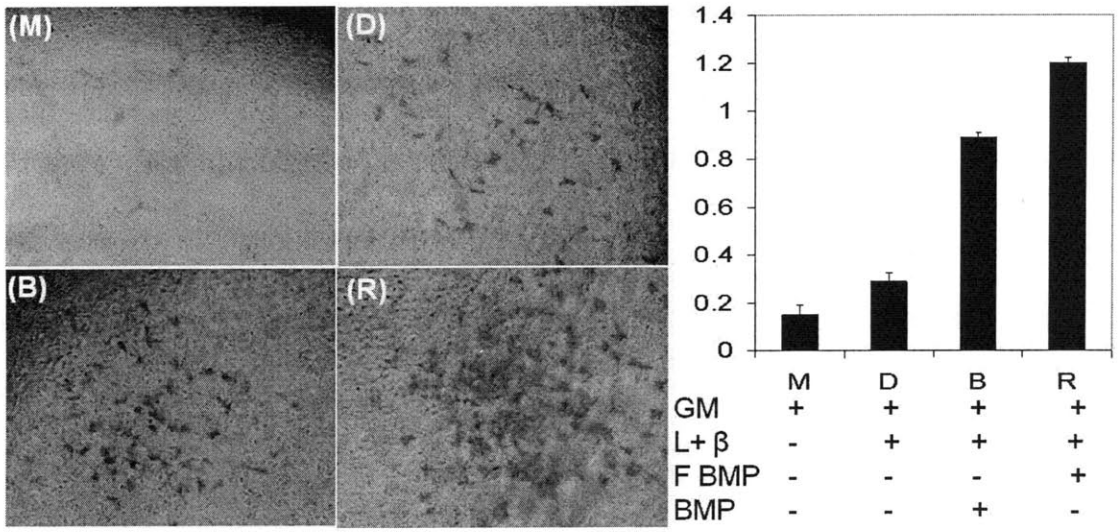

Figure 6-6: Alkaline phosphatase staining and quantification of MC3T3 cells, performed after 6 days of BMP-2 induction. Compared to growth medium alone (M) and differentiation medium (D) consisting of growth medium supplemented with β–glycerol phosphate and L-ascorbic acid, both the positive control (B), consisting of differentiation medium supplemented with 90 ng/mL of BMP-2 and release solution (R), consisting of differentiation medium with 90 ng/mL of BMP-2 released from LbL films show a marked increase in alkaline phosphatase activity visual both by staining and quantification, indicating an enhanced induction of the bone differentiation pathway in these pre-osteoblasts. (GM = growth medium, L+β = L-ascorbic acid and β-glycerol phosphate, F BMP = film released BMP, BMP = BMP added to medium). Each condition was sampled 3-4 times, with triplicate measurements performed per sample; error bars represent standard deviation of the samples. A single factor ANOVA test of all four conditions was performed with resulting p value of 4.5E-9, through which the null hypothesis was rejected. A Tukey-Kramer test indicated that all groups were different from each other with a p-value less than 0.01, with the exception of the comparison between M and D, which were found to have a p value of greater than 0.05 and are therefore considered to be insignificant.

This qualitative comparison is borne out in quantitative readings of alkaline phosphatase levels in the right hand panel of Figure 6-6; in fact, interestingly, the quantification suggests that the BMP-2 released from the films is more active than BMP-2 simply added to the medium. It is possible that BMP-2 released from the film is not freed on the molecular level but is rather still partially electrostatically engaged with carrier polymer and chondroitin. In this case, it is possible that the carrier poly(β-aminoester) may electrostatically interact with the cell membrane, helping to concentrate and present complexed BMP-2 at the surface of the cell and therefore increase the local surface concentration of BMP-2 recognized by the cell.

To confirm the commitment of MC3T3 cells to a mature bone fate, two stains of mature bone cell activity were employed. At 28 days, MC3T3 which have differentiated into osteoblasts will fix calcium from the medium into deposits which stain bright red with Alizarin red staining. In the left hand panel of Figure 6-7, in vitro stains show that cells cultured in growth medium (M) show nearly no calcium deposition, correlating with the lack of bone differentiation induction shown in alkaline phosphatase staining. Those in differentiation medium (D) show intermediate calcium fixation compared with BMP-2 containing samples (R and B) which show copious red deposits of calcium deposition. Here also the quantitative assay matches the stain results, indicating that BMP-2 released from our film induces a similar or greater amount of differentiation and subsequent calcium deposition compared to BMP-2 added in liquid form to the culture. This assay confirms the

presence of osteoblast-like cells in culture, indicating that BMP-2 differentiation was successful.

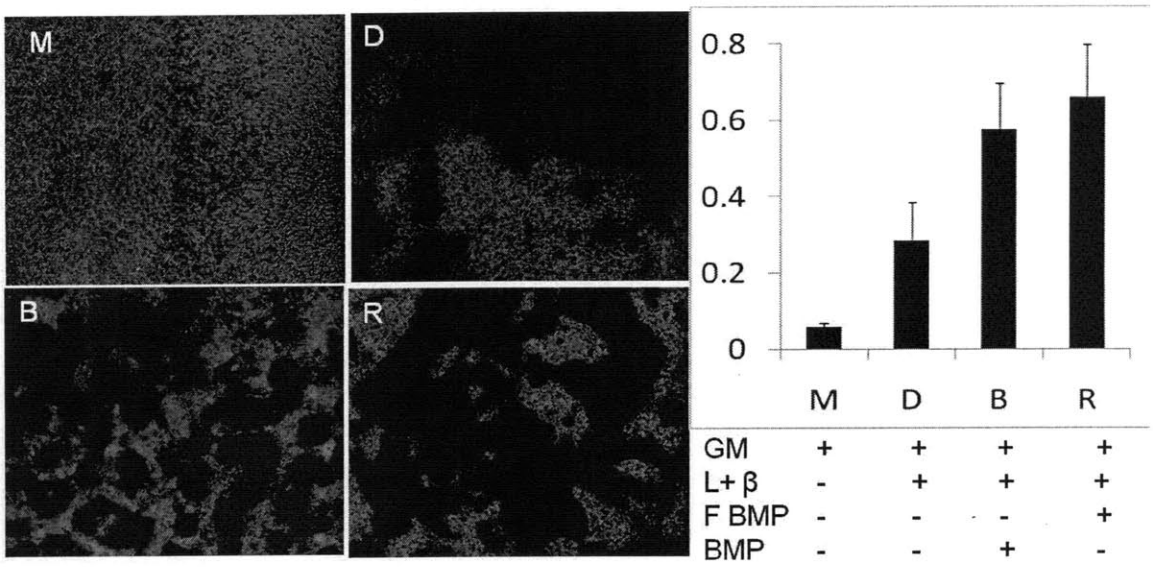

Figure 6-7: Alizarin red staining done at 28 days reveals that the positive control (B) and LbL film released BMP-2 (R) show more calcium staining (red) than do those cultured in growth medium (M) and differentiation medium (D). Figure legend: GM = growth medium, L+β = L-ascorbic acid and β glycerol phosphate, F BMP = BMP-2 released from film, and BMP = BMP-2 supplemented in medium. MC3T3 that have matured into bone cells are able to fix calcium from the medium into the deposits stained here. Each condition was sampled 3-4 times, with triplicate readings per sample; the error bars here represent standard deviation of the samples. A single factor ANOVA test of all four conditions was performed with resulting p value of 5.6E-5, through which the null hypothesis was rejected. A Tukey-Kramer test indicated that both B and R (BMP-2 containing samples) were statistically different from M and B (BMP-2 negative samples) in any permutation with $p < 0.05$; both M-D and B-R differences were found to be insignificant.

Von Kossa staining for calcium phosphate confirms that the calcium deposited is in a mineralized, bone-like form. Its presence suggests a higher level of maturity of the calcium

deposits. In Figure 6-8, the large quanity of black silver nitrate staining confirms that the calcium deposited by the positive control (B) and the test sample (R) are extensively mineralized into a calcium phosphate, bone-like material. In a pattern similar to other in vitro results, growth medium (M) is insufficient to precipitate bone matrix formation, and differentiation medium (D) is able to precipitate some matrix, but less so than the cells that were specifically directed to the bone differentiation lineage by BMP-2.

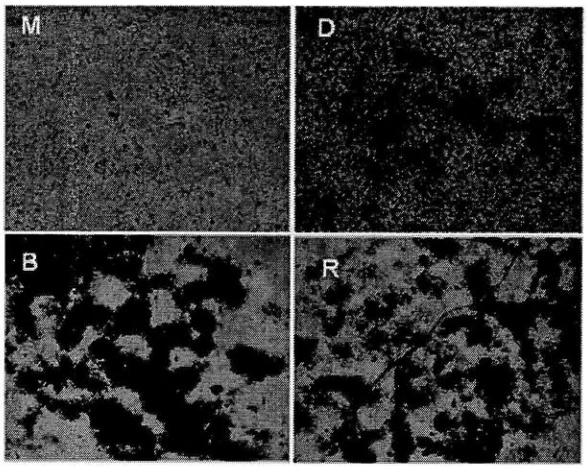

Figure 6-8: Von Kossa staining at 28 days suggests high levels of differentiation in (B) and (R) samples compared with (M) and (B)

6.3.5 Probing Fractional Functionality of Released Protein

One potential complication that has recently been highlighted in *in vivo* protein delivery devices being developed for commercial applications is the possibility for a raised immune reaction to the therapeutic protein of interest. Denatured protein can lead to a heighted immune response, which in its most extreme form could lead to neutralizing antibodies to conformationally intact therapeutic proteins within the device and even the natural, host

produced forms of the therapeutic protein, diffusing both the therapeutic function of the device and the host's ability to naturally interact with the cellular process of interest. It is thus of high interest to understand the fraction of the protein that remains functional within the device to understand the risk of forming neutralizing antibodies. We thus pursued this question through multiple avenues of analysis.

The most definitive measurement to answer this question would be to measure the total amount of active protein and compare it to the amount of total protein, in a manner analogous to the approach used for lysozyme in Chapter2. The only test for true protein functionality with growth factors is a bioactivity assay, such as those run in the previous section for alkaline phosphatase, Alizarin Red, or Von Kossa. If a dose response to known concentrations of BMP-2 supplement could be used as a standard curve, and the response rate of an "unknown" concentration BMP-2 release sample interpolated, it would be possible to get a measurement of the functional protein in the assay. However, in our systems, the presence of a confounding factor (in this case, the proposed surface concentration effect that makes an equivalent amount of BMP-2 released from LbL appear to be more active than BMP-2 supplemented in the medium) suggests that the BMP-2 release cannot be reliably plotted back to the dose response curve to get a meaningful measurement of functional protein. This surface concentration effect would lead to an overestimate of the functional protein present in the film, confounding any efforts to quantify fractional release. Thus, the only true measurement of functionality is not available

for quantification in our LbL system. Complexation, as it turns out, is problematic for many of the detection techniques we would like to employ.

In the absence of this best alternative, a second approach is to use ELISA as a reasonable surrogate for total conformationally active protein (which is not necessarily a given, as the ELISA detection technique recognizes only a small binding recognition site rather than the whole conformationally intact protein), and to use a second measurement technique that could report the total amount of protein, conformationally active or not, in the sample. For this method, we chose to measure total protein of a sample enzymatically digested with either trypsin or AspN. High Performance Liquid Chromatography (HPLC) separated peptide sequences detected by Mass Spectrometry (MS) for detection could be compared with a database to first confirm the identity of the protein but also to calculate total protein through the height of the peak signals. To this end, samples were prepared for analysis by HPLC-MS, which were run by the Koch Biopolymers lab.

The results from the column run show very high background contamination levels by relatively hydrophobic contaminants which confound measurement efforts in spite of protein concentrations detected by ELISA that should be readable. Protein digest peaks show characteristic doublet or triplet peaks of proscribed proportions relative to each other, while here, single peaks attributable to a contaminant are the majority of the signal. The trypsin digest showed no peaks that could be identified through the database as being from

BMP-2, while AspN found only one fragment from BMP-2. A representative portion of these results can be seen in Figure 6-9.

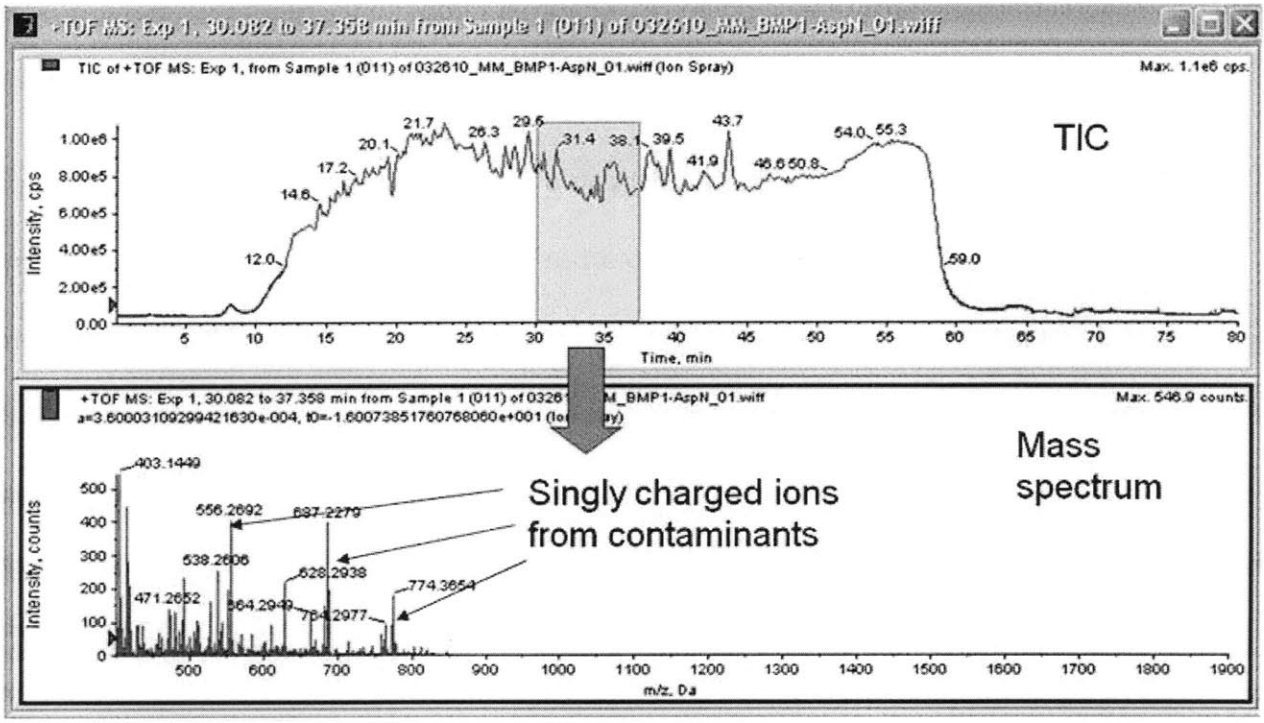

Figure 6-9: Sample data from HPLC – MS run on an AspN digested BMP-2 release sample reveals no detectable protein signal peaks, which show signature doublet and triplet peaks, and contaminating singly charged ion peaks suspected to be contributed by remaining polymer degradation products. Figure courtesy of Dr. Ioannis Papayannopoulos.

Spinning remaining sample with a column intended to remove detergents improved the signal, but not to the level where BMP-2 could be successfully identified, let alone allowing for quantification. These results suggest that the strong signal from hydrophobic contaminants, likely Poly2 degradation products, are masking the weaker BMP-2 signal, rendering detection impossible, even in light of ample protein concentrations. While it is

possible to first run an SDS PAGE gel to separate out these contaminants based on weight, and then cut out the gel band of interest for detection with HPLC-MS, this method has several transfer steps that could be reasonably assumed to decrease the total protein signal, leading to a measurement with no practical meaning for the purposes at hand.

A third and final approach of using conformational intactness as a surrogate for protein function was also explored. Here, two attempts were made: using circular dichroism (CD), and using fluorimetry, which both shed light on protein conformation. With CD, one can detect the presence of random coil, alpha helix, or beta pleated sheet architecture. BMP-2 has significant beta pleated sheet architecture when in its native folded state; thus if this could be measured compared with BMP-2 standards (both denatured and in native conformation), it might be possible to show conformational same-ness to intact protein as has been shown in the literature with BMP-2 previously [161]. However, in literature accounts, a much higher concentration of BMP-2 was used for measurements, and it was seen that the signal faded with the transition from beta pleated sheets to random coil configuration. Measurements of a standard solution of 3.33 μg/mL (a difficult-to-achieve concentration in our LbL release), shown in Figure 6-10, show a lot of scatter in the region below 235 nm, but follow the general trend of reported BMP-2 CD data; the scatter is likely due to the dilute protein solution used here. It would be difficult to observe a fade attributable to denaturing protein from this data since the concentration is already very low.

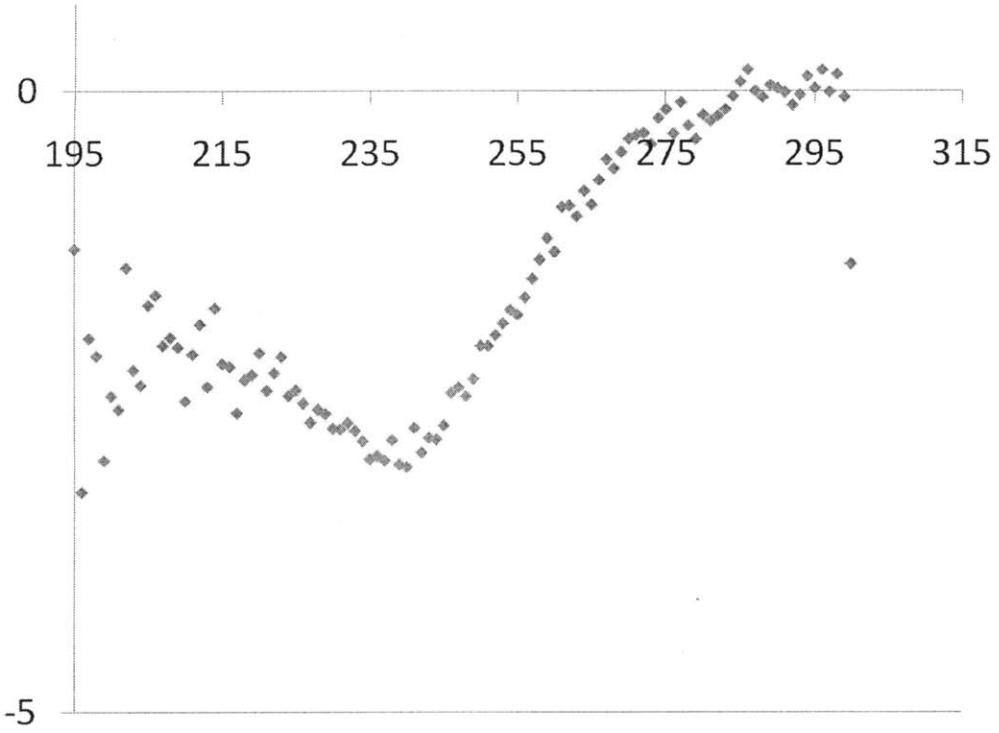

Figure 6-10: Circular dichroism plot of BMP-2 in solution shows the general trend expected; the scatter in the lower wavelength readings is likely due to the low concentrations of protein used in this system compared with literature concentrations for detection.

A second approach to probe the conformation used was fluorimetry. It can be shown that the amplitude of the peak correlates with concentration of the sample[35], and that a shift in wavelength of the peak maximum can indicate protein denaturation[161] (increasing wavelength corresponding with more denatured protein), allowing important information about both needed parameters. Unfortunately, upon testing release samples, the "peak" for the reaction sample was very broad with no distinct maximum, exhibiting classic signs of an interacting system as seen in Figure 6-11. Such data is not interpretable.

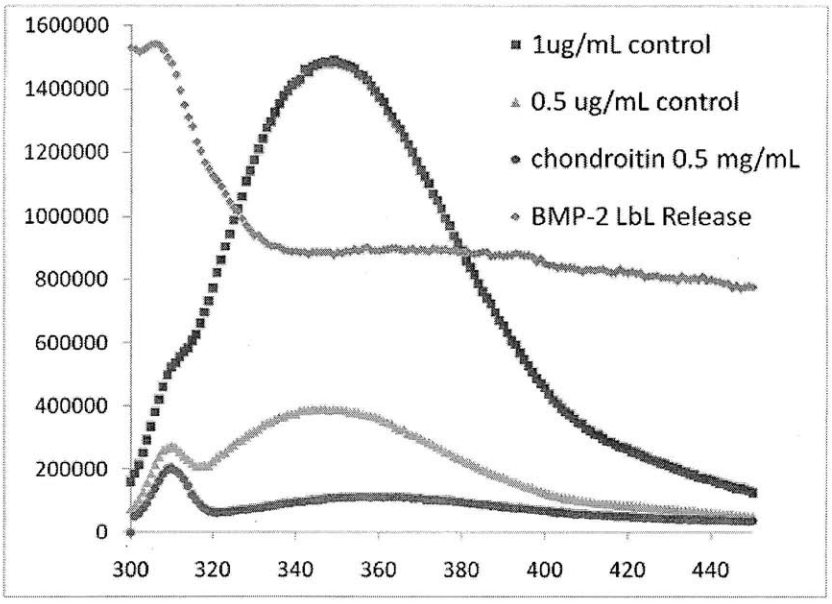

Figure 6-11 Fluorimetry data of release data (blue) showing a broad peak with no distinct maximum at 350 nm, compared with 1 and 0.5 ug.mL controls of BMP-2 (red and green, respectively) which show increasing amplitude of signal with increasing BMP-2 concentration and a 0.5 mg/mL sample of chondroitin, which shows that chondroitin is not contributing significantly to the fluorescent signal at 350 nm.

Thus, with all of the methods described, there are technical issues which prevent the assembly of strong data to understand the fractional functionality of protein released from our LbL films.

One proposal for future work that may be able to shed light on the question of protein intactness is based on the successes seen with *in vivo* studies that will be addressed in the next section. By taking animals and serially implanting LbL BMP-2 releasing films every 1-2 months, we can look for the diminished in vivo response over time that could be caused by

the production of the neutralizing antibodies of concern; if bone creation was as robust in the nth implant compared with the first implant, it would bode well for this highly important question. However, while this approach has promise, more needs to be done to understand the frequency of this complication across many protein therapeutic devices in order to understand the number of animals needed to capture this effect. For example, if protein denaturation leads to neutralizing antibodies in 5% of the population that take it (which could still be catastrophic), one would need twenty animals for every one that would show the effect, leading to a large number of animals needed to feel confident that we would catch this phenomenon if it was occurring, with concurrent high animal trial costs and increased analysis time periods. It is clear, however, that this question is of high importance to the success of protein therapeutic delivery schemes.

6.3.6 In Vivo *Studies: MicroCT and Histological Findings*

In vivo ectopic bone formation depends on the differentiation of host progenitor cells to the bone lineage. To test in vivo activity, we implanted 3DP scaffolds coated with either [P2/chondroitin/BMP-2/chondroitin]100 films releasing 10.6 ug of BMP-2 or [P2/chondroitin]200 films vehicle controls intramuscularly in a rat quadriceps model and took timepoints at 1 and 2 months.

Upon explantation, micro-computed tomography (microCT) images show macroscopically visible bone in 3 of 4 one month BMP-2 releasing samples, and 4 of 4 two month BMP-2 releasing samples as shown by the semi-quantitative scoring of Table 1; no

bone was detected in any of the control film scaffolds lacking BMP-2. The fourth sample at one month did not show macroscopic bone, although microCT showed increased opacity compared with controls (data not shown); microscopic signs of differentiation in this sample are discussed below. In the left hand images of Figure 6-12, two dimensional slices through one and two month BMP-2 active implants show that the bone forms in plate-like trabeculi, and that the thickness of the trabeculi increases from one month to two month samples. Three dimensional

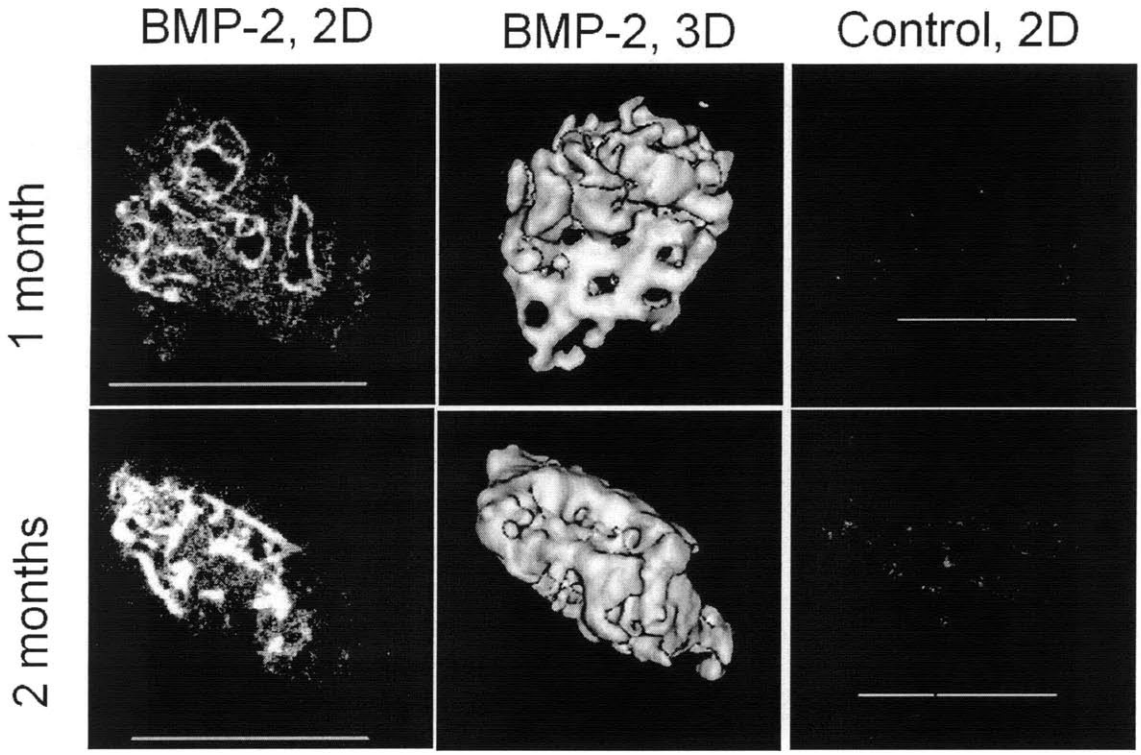

Figure 6-12: Micro computed tomography images of explanted in vivo samples at one and two months. Two dimensional slices through BMP-2 active samples show bone thickening and more intense signal suggesting higher bone mineral density with increasing time. Three dimensional images show the concentric positioning of the bone around the 3DP struts. Controls thresholded to the same values show very little

opacity to x-rays and therefore scarce osteoblast differentiation within these scaffolds. 3D isosurfaces could not be generated off of this scarce signal.

reconstructions (Figure 6-12, central panels) show that the bone forms with pattern fidelity to the 3DP scaffold underlying the film, strongly suggesting an outward-radiating pattern of bone formation from exposure to BMP-2 at the scaffold surface. At two months, the thickness of the bone trabeculi begins to obscure the original pattern. The controls lacking BMP-2 release exhibited very little opacity (Figure 6-12, right panels), indicating no bone was formed without the BMP-2 induction signal; three dimensional reconstructions were not possible. Thus osteoinductive BMP-2 released from LbL films is required for host progenitor cell differentiation to the bone lineage, and these initial deposits appear to continue to grow and remodel from one to two months.

Quantification of several bone parameters is possible using the bone analysis software. Bone mineral density increases with time in the bone formed by BMP-2 active films and remains unchanged in control films (Figure 6-13). The progressive increase in BMD strongly suggests that bone induced by BMP-2 release continues to mature, reorganize, and become mineral-dense up to the two month's timepoint. Similar trends in the stereology (which describe the shape and thickness of bone) measurements support the conclusion of progressive

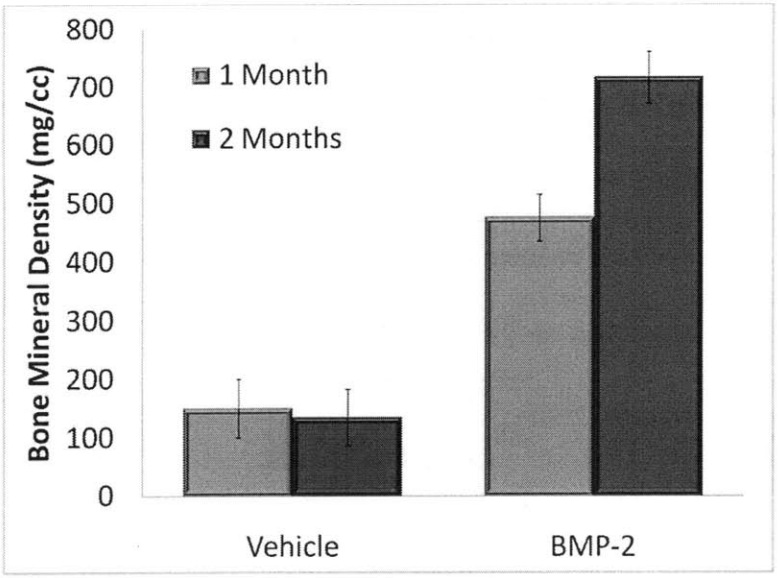

Figure 6-13: Quantitative microCT output of bone mineral density within bone segments suggests increased maturity of bone matrix. Each sample (n = 4) was measured in three locations; error bars are standard deviation on the mean of the 4 samples.

maturation on the de novo bone. In particular, the total bone volume is increasing as a fraction of the total tissue volume, the bone surface to bone volume parameter is shrinking, and the trabecular thickness is increasing (Figure 6-14).

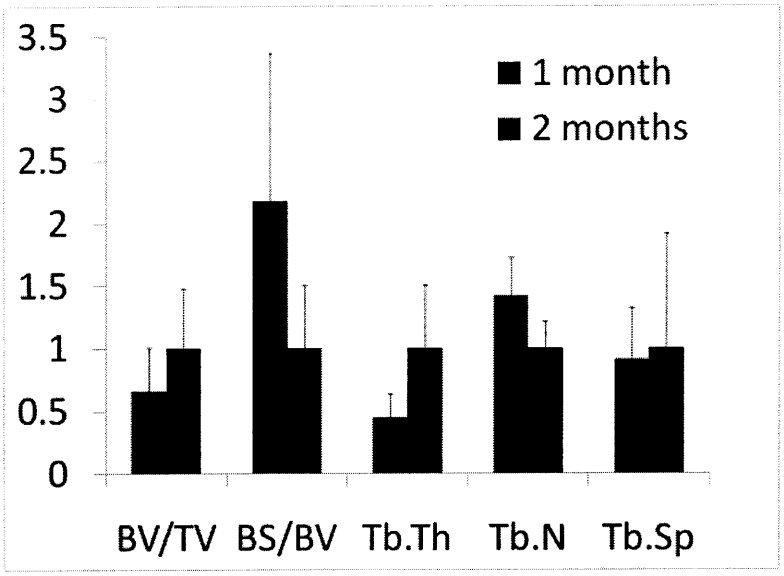

Figure 6-14: Quantitative stereology measurements of BMP-2 active LbL scaffolds in vivo at one and two months show a trend of increasing bone volume. BV/TV = bone volume/total volume; BS/BV = bone surface area/bone volume; Tb.Th = trabecular thickness; Tb.N = trabecular number; Tb.Sp = trabecular spacing. Error bars represent standard deviation of 4 in vivo samples measured three times each per timepoint.

These parameters suggest that original bone nodules induced by BMP-2 are expanding over time to make larger deposits of bone and correlate well with the 2D images (Figure 6-12) showing thickened plates. Taken together, these results suggest that bone deposits initially formed by BMP-2 stem cell induction continue to mature and increase in size. MicroCT imaging thus confirms that host progenitor cells coming into contact with the surface-released BMP-2 were able to recapitulate the bone differentiation process resulting in production of macrsopically visible calcified tissue.

By optical microscopy of Masson's Trichrome stained histology slides, in which collagen bone deposits stain blue, it is possible to clearly visualize the formed bone in BMP-2

active LbL samples compared with control films (Figure 6-15). Both at one and two months, vibrant, glassy blue bone can be visualized in full thickness views through the scaffold, while in all control samples, no blue staining can be found.

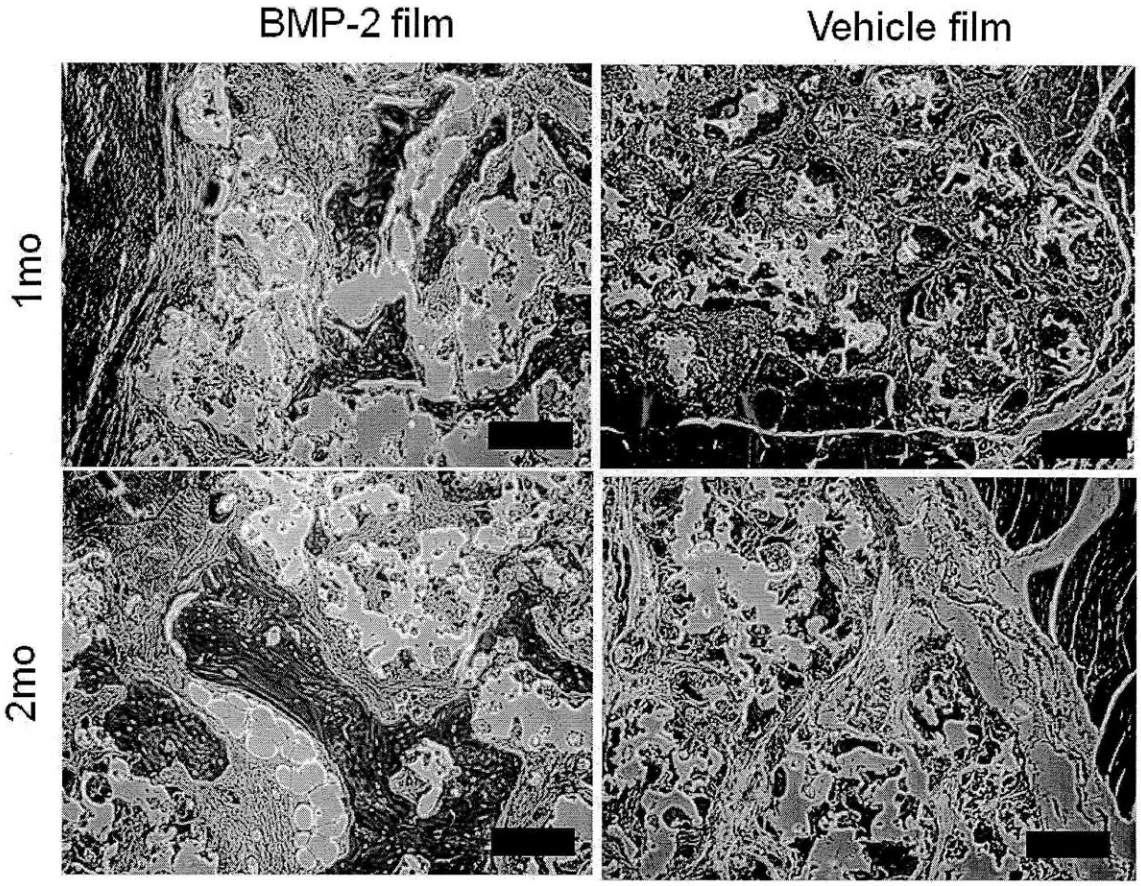

Figure 6-15: Trichrome stains of in vivo samples at one and two months highlight decalcified bone (collagen) in blue. No bone was detected in vehicle scaffold controls; within the BMP-2 active samples, an increase in plate thickness correlates with microCT bone surface to volume measurements. Skeletal muscle from the site surrounding the implant is visible at the edges of the images.

Two markers of maturing bone are progressively apparent at both one and two month time points. In the healing process, bone is initially deposited as woven bone, characterized by unaligned collagen fibers, which gives it a fluffy appearance on histology sections. However, as the osteocytes and osteoblasts remodel their microenvironment, they deposit a more mature, lamellar architecture of bone which is characterized by smooth, aligned fibers. The remodeling front typically takes a triangular shape, in which woven bone is replaced by the lamellar counterpart. In one month samples, several remodeling fronts are visible, while at the two month time point very smooth lamellae are visible (Figure 6-16 A, B). This woven-to-lamellar process is highly visible under a polarizing filter, in which the aligned collagen fibrils are birefringent under polarized light (Figure 6-16F, with 6-16E as a matched view with normal light) while less mature/aligned fibers remain dark.

A second indication of maturing bone present most predominantly at the 2-month time point is the accompaniment of fat deposits, which suggest the recruitment and development of bone marrow populations to the bone microenvironment. At one month, fat deposits visualized as white foamy spaces (see black asterisk) associate with areas where many contacts with bone surfaces are possible; however, the bone encasement is not complete, and the associated fat is relatively sparse. At two months, well defined geometries of bone encircling marrow cavities with fat deposits are visible (Figure 6-16 C, D). Even at two months, however, the marrow associated with this cavity is immature; although

fat deposits are visible, the concomitant immature hematopoietic cells that would be present in true marrow are still not

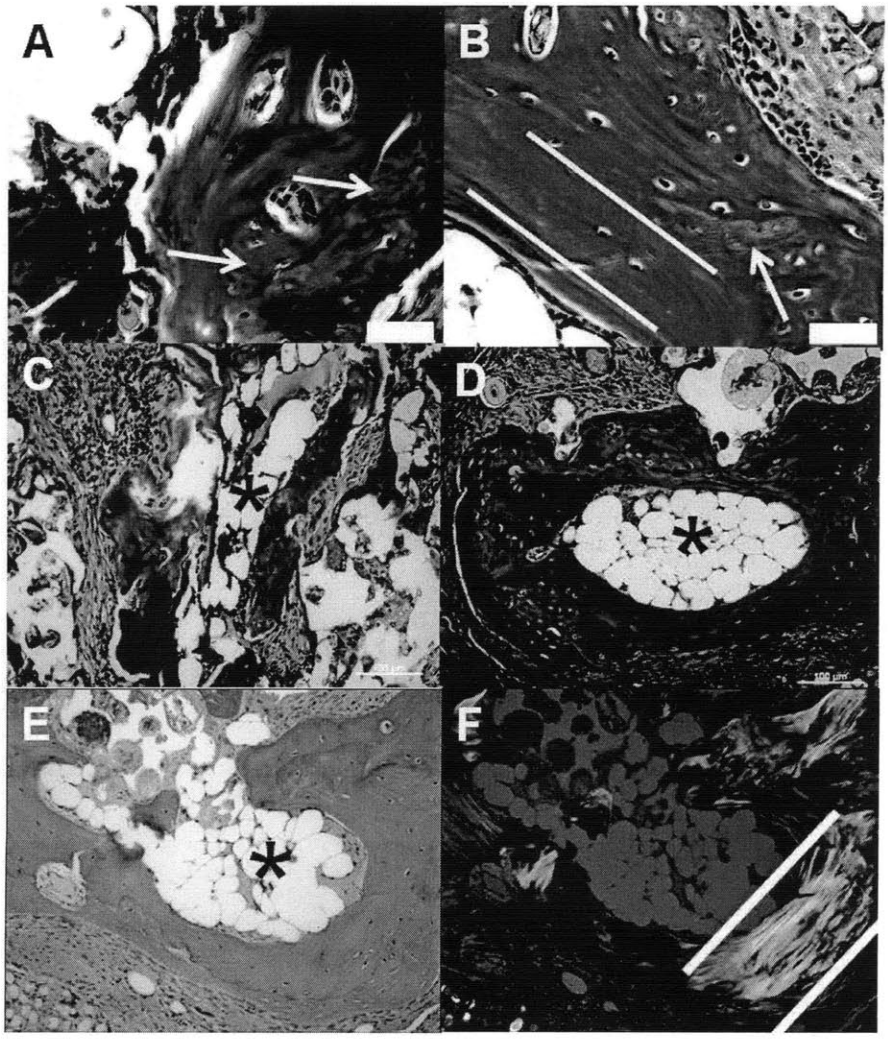

Figure 6-16: Bone tissue remodels and forms marrow cavities. In trichrome staining, at one month (A), woven bone which has a wavy architecture (white arrows) is being replaced by lamellar bone. At two months (B), much more lamellar bone is present (white lines). Marrow cavities characterized by foamy appearance (asterisk) are present by one month (C) in an unclosed region with many bone contacts. At two months (D), a bone marrow cavity is surrounded by bone with more developed fat deposits. Aligned, more

mature collagen fibers in lamellar bone, reflect polarized light, highlighted by white lines (F) with matched H&E photo (E). (A) and (B) at 20x with 2.5 magnification; (C) through (F) at 10x. White scale bars are 40 μm.

developed. It is nonetheless encouraging that many of the steps of maturation and indications of healthy remodeling of tissue are present in this designed microenvironment; by simply presenting an early cue, the rest of the biologic processes to create healthy tissue are precipitated.

At higher magnification, it is possible to clearly visualize osteocytes in their lacuna, and osteoblasts at the leading edge of bone formation (Figure 6-17A). In Figure 6-17A it is also possible to see a cement line (white arrow), where previous osteoblasts produced newer bone radiating out from a previous bone front. The expected chronic inflammatory reaction to the remaining 3DP scaffold is present but not extraordinary; no necrosis is observed in the surrounding muscle tissue and the fibrous capsule around the implant is quite thin. Interestingly, on trichrome stains lighter areas of blue stains, suggesting immature collagen formation of new, starting foci of bone differentiation also become clear (Figure 6-17B). It is unclear whether these newly differentiating cells are being induced by the original exogenous rhBMP-2 delivered from the LbL layers that subsequently were sequestered in the extracellular matrix and thus have delayed activity, or whether in the presence of a bone microenvironment, there are other cell types secreting endogenous paracrine osteoinductive signals to self-support further bone formation.

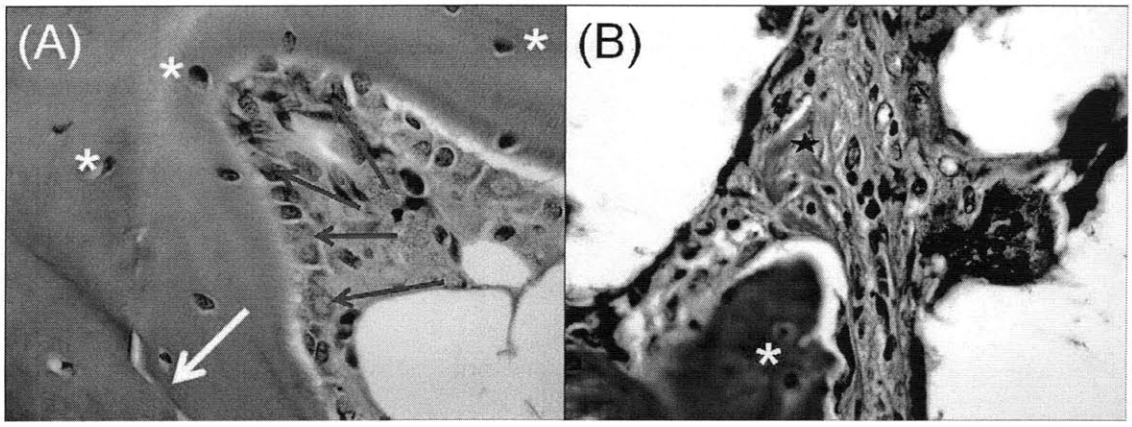

Figure 6-17: Mineralization is due to both continued deposition on existing nodules as well as formation of new bone deposits. In (A), cell types recapitulating activities in healthy bone tissue are observed. Osteocytes (asterisks) are found in their lacunae in the bone matrix. Osteoblasts (blue arrows) are moving the front of bone forward, creating new mineralized matrix. An old cement line from a previous front advancement is shown with a white arrow. In (B), light blue staining of less mature collagen suggests matrix deposition of an immature bone forming region, distinct from the more mature bone at the bottom of the slide.

Bone can be formed through two possible mechanisms. Intramembranous formation occurs when mesenchymal stem cells differentiate directly into bone, and is associated with the formation of plate-like bones such as skull bones. Endochondral bone formation is associated with the formation of long bones, such as the femur, and occurs when mesenchymal stem cells first differentiate into a cartilaginous intermediate form, which is then rearranged to produce bone. To explore which type of ossification process was occurring in the LbL BMP-2 film system, histological sections were stained for glycosaminoglycans (prevalent in cartilage) with Alcian Blue in both *in vivo* BMP-2 positive

and negative LbL coated scaffolds. In Figure 6-18, large areas of turquoise-positive cells indicate that cartilage extracellular matrix is present, and thus an endochondral bone formation process occurred. In the light image of the stain (Figure 6-18A), one can see both lamellar and woven architectures in which the cartilage clearly stains in conjunction with newer woven bone in distinct regions separate from the more mature lamellar bone. Under the polarizing filter (Figure 6-18B) the distinct regions of mature, polarizing bone and the turquoise immature bone are highlighted. Although chondroitin was included in the original LbL film in minute quantities, both the pattern of staining and that all controls (which also had chondroitin in them) were negative for Alcian blue indicate that the

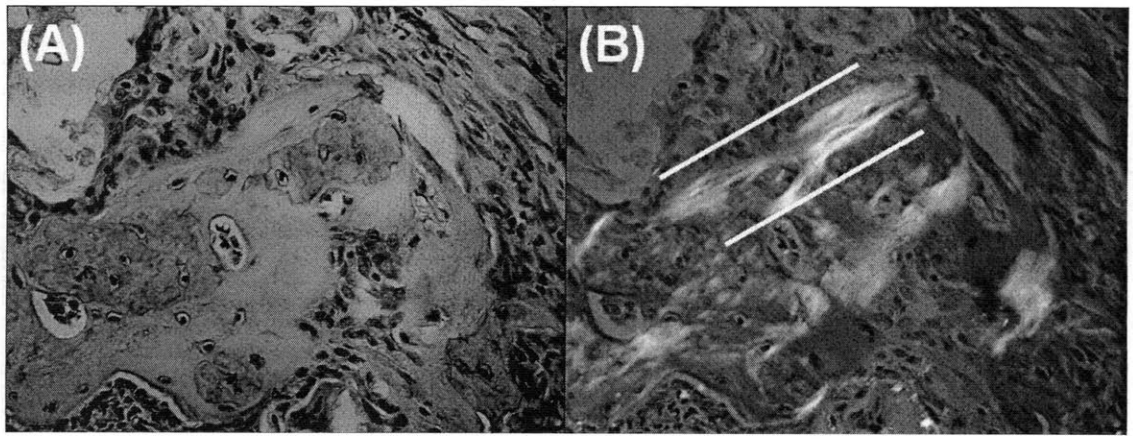

Figure 6-18: Alcian blue staining for glycosaminoglycans (GAGs) typically found in cartilage indicate that an endochondral intermediate stage is accessed before bone formation. In (A), an alcian blue stained slide shows mature lamellar bone (light pink) separated by cement lines from new bone with a more wavy, woven architecture with residual GAG presence stained turquoise by alcian blue. (B) Mature lamellar aligned collagen fibrils can be visualized under polarized light (light area between the two white lines) in areas distinct from the newer, more woven bone which still contains GAGs.

GAGs stained were likely related to the endochondral process rather than LbL introduction. Furthermore, although only 3 of 4 BMP-2 samples at one month showed macroscopic bone deposition, all four stained positive for Alcian Blue. This indicates that BMP-2 induction had occurred in the fourth scaffold and that the differentiation process had been precipitated; however, the bone product forming was still too immature (not calcified enough) to be detected by microCT.

6.4 **Conclusions**

Biologic-eluting LbL coating technologies represent a fertile opportunity to affect both the area of implantable medical devices and tissue engineering/regenerative medicine scaffolds for second generation design. This study shows that LbL technology can be utilized to construct nanolayered thin films which contain a micron-scale reservoir of BMP-2 that exhibits controlled release over a time span of two weeks despite their ultrathin profile. The load is comparable to that of bulk-releasing systems, and is tunable by tuning the number of tetralayers or the synthetic polymer used. BMP-2 released from these films maintains bioactivity both in vitro, where it shows enhanced activity compared to BMP-2 added to culture medium, and in vivo, where it is able to induce differentiation of native host mesenchymal stem cells to the bone lineage. Furthermore, this study shows that an osteoconducive microenvironment is perpetuated within the implanted scaffold in vivo, which is characterized by remodeling, association of marrow-like spaces, and continued

construction of bone, both from previyously induced bony surfaces as well as de-novo population centers. This work represents an important step forward in understanding how biologic coating technologies can improve implant integration with host tissue, an opportunity to approach sequential and co-release modalities, and most importantly, as a paradigm shift in how implants are used in human health care.

Chapter 7 Stamp Templated Co-cultures for Microvascular Tissue Engineering

~Note: This work was done while abroad on a Fulbright Fellowship~

7.1 Introduction

Two of the major challenges confronting the fields of tissue engineering and regenerative medicine today are the need 1) for a vascular supply within engineered tissues to allow construct thicknesses to exceed diffusion barrier thicknesses and the need 2) to organize multiple partner cell types to make a functional and integrated organ. Because most current approaches utilize only one cell type (the parenchymal or functional cell type of an organ), little has been done to pre-pattern implants to promote specific organization or arrangement of different cell types during tissue formation. Furthermore, the lack of developed means for vascularizing three-dimensional (3D) tissues have limited most clinical successes to very thin (skin or bladder) or avascular (cartilage) tissues which do not immediately need the nutrient exchange upon implantation[162]. However, to achieve the formation or regeneration of clinically relevant 3D tissues for many internal organs, both issues of vascularization and of spatial organization of several cell types will need to be addressed to a much greater extent.

In the body, there is rarely a greater distance than 200 um between a cell and the nearest blood vessel[163]. Monoculture-based tissue engineered implants which lack vasculature must therefore depend on diffusion based oxygen and nutrient delivery and waste removal, effectively limiting the size of the tissue engineered construct which can be created. In

constructs thicker than the diffusion limit, nutrient and oxygen limitations combined with waste product buildup lead to toxic gradients that limit cell viability in the core[164, 165] while cell density is typically highest at the periphery of the constructed implant[164-167]. Full thickness, functional implants remain difficult to achieve.

Beyond the difficulties of implant creation, it has been noted that transplanted tissues demonstrate better survival and function when prevascularization is initiated prior to implantation. Pancreatic islet cells transplanted into pre-vascularized chambers were more successful than those seeded into empty chambers at controlling hyperglycemia in mice[168]. Similarly, osteogenesis of bone marrow stromal cells within a ceramic biomaterial is increased by diverting host vasculature to the implant[169]. Prevascularization of skeletal muscle constructs leads to enhanced vascularization, perfusion and construct survival[170]. Thus prevascularization both enables creation of thicker tissues and enhances survival and function upon implantation.

In addition to removing waste and supplying nutrients and oxygen, blood vessels are currently emerging as a source of pattern regulation and support signals which can direct parenchymal cell placement and migration within tissues. Diverse organs including the heart, liver, thyroid, nerves and pancreas are at least partially patterned by interactions with the endothelium[171, 172]. It has furthermore been shown that liver cells which are seeded onto randomly patterned vascular networks will migrate to the vessel network, and, supported by the endothelial cells (ECs), create hepatic sinusoid-like patterns with concomitant increases in liver cell function and survival[173]. Thus, controlling the vascular pattern of an implant not only would allow for better tissue survival upon implantation due to functional waste and

nutrient exchange, but also allows an important handle on the process of enabling more complex patterning and differentiation of cells than is currently possible.

Pioneering work by Darland et al[174] showed that when ECs and mesenchymal stem cells are both seeded in a 3-dimensional extracellular matrix (Matrigel), they co-localize through growth factor signaling to form vessel-like structures within the host matrix. The formation of these vessels occurs after approximately 6 hours, and the vessel forms regress between 24 and 48 hours of initial seeding. Further work by Levenberg et al[170] has shown that engineered tissues which include such vascular forms, when implanted, are able to connect with the host vasculature and carry host blood to the implant thus providing the implanted tissue with nutrient exchange and leading to better implant survival. However, in both of these cases, the vessel forms are created randomly, and no controlled vessel patterning is possible. Thus, while nutrient exchange is improved, the latent potential of generating blood vessel networks to direct differentiation and enhance parenchymal cell patterning has not been tapped.

Until this point, most attempts to study co-culture tissue self assembly have been performed in random co-cultures in which no external organization has been exerted. Matrigel angiogenesis[174] co-culture assays were utilized for these experiments, and, because ECs are known to be able to chemoattract smooth muscle cells (SMCs) through TGF-β and PDGF-BB concentration gradients[162, 174], we hypothesize that by controlling the position of ECs within the Matrigel environment, it is possible to control the final placement and orientation of forming blood vessels in tissue co-cultures. In this work, we propose to direct

the development of such vessel forms with underlying surface chemistry patterns, providing a versatile tool for the vascularization of a wide range of tissue engineered constructs.

Microcontact printing[175, 176] has been easily adapted to the selective patterning of cells upon surfaces[177]. In this technique, a material of interest is transferred from a patterned PDMS stamp onto a surface with micrometer scale precision. A commonly used variant of the technique is to stamp a cell-adhesive pattern to a cell resistant background before seeding cells on top; the cells preferentially adhere to the pattern while those which do not attach are washed away[42]. In this way, two-dimensional patterns of cells can be created to probe micro-scale interactions of cells with their environments. In this work, we use an adaptation of microcontact printing, polymer-on-polymer stamping[178], to transfer a pattern of fibronectin, a 400 kDa protein with adhesion domains, onto a polydimethylsiloxane (PDMS) polymer substrate; we are able to confine ECs to a predetermined and easily manipulated geometry. SMCs which are overlaid in a three dimensional gel matrix atop these patterned ECs migrate through the Matrigel to contact the ECs; in this way we are able to dictate the pattern of the blood vessel network. The pre-vascular forms remain stable in their dictated patterns for thirteen days in culture, and represent a simple, efficient, scalable method for creating a pre-vascularized pattern which can be used to direct differentiation and organization of a wide variety of other cell types such as liver, pancreas, or heart cells within engineered constructs and gain maximal opportunity for successful implantation through pre-vascularization.

7.2 Materials and Methods

7.2.1 Preparation of PDMS stamps and surfaces

A Teflon-coated silicon master mold was created using photolithography and deep reactive ion etching was used to achieve a template for generating PDMS stamps. A branched stamp starting with a 600 um trunk with systematic bifurcations to 300 μm, 150 μm, 75 μm, 36 μm, and 20 μm was utilized. In addition, a diamond pattern of 25 μm lines separated by 250 μm (60 and 120 degree angles) and a perforated straight line pattern with 25 μm lines separated by 300 μm were used. A 10:1 v/v mixture of siloxane elastomer and hardener (Sylgard 184, Dow Corning) was extensively mixed and poured either over the silicon mold of interest to create a stamp or over a flat glass dish to make flat substrate surfaces. After degassing to remove bubbles, the siloxane filled molds were placed in a 65°C oven for 1 hour to attain polymerization. Molds were allowed to cool to room temperature and a coring instrument was used to remove cores of PDMS the diameter of a 24-well tissue culture plate.

7.2.2 Microcontact printing of PDMS surfaces

The technique of Katanosaka et al[179] and the general use of polymer-on-polymer stamping[178] were modified for use here. Briefly, PDMS stamps were plasma etched with oxygen for 45 seconds with a March PX-500 plasma etcher to induce hydrophilicity on the surface, and 100 uL of 0.1 mg/mL fibronectin (Sigma, St. Louis, MO) was applied to each surface (Figure 8-1). The stamps were wet with the fibronectin "ink" solution for 30 minutes

at 37°C. Meanwhile, flat PDMS surfaces were plasma etched with oxygen for 45 seconds. Stamps were spun in an SCS G 3P-8 spincoater for 1 minute at 3000 rpm to remove excess fibronectin solution from the stamp. The surface of the flat PDMS section was placed in contact with the stamp to allow pattern transfer. Fibronectin patterns transferred to the flat PDMS discs were checked with optical microscopy before use in tissue culture experiments. Patterned surfaces were placed in 24 well plates and UV irradiated for 30 minutes for sterilization.

7.2.3 HUVEC and SMC culture

Human Umbilical Vein Endothelial Cells (HUVEC)s (Lonza, Basel, Switzerland) were maintained in Endothelial Growth Cell Medium (Lonza). Cells were passaged before confluence and only used until passage 6. Smooth muscle cells (SMCs) (Lonza) were maintained in SMC medium consisting of DMEM with 1% penicillin/streptomycin and 10% FBS (Invitrogen, Carlsbad, CA) Medium for both cell types was changed every other day.

7.2.4 Preparation of patterned surfaces; HUVEC and SMC attachment

Sterile 1% bovine serum albumin (Sigma Aldrich, St. Louis, MO) in 1x PBS was applied for 30 min at 37°C to UV sterilized patterned surfaces to block non-specific binding. HUVECs were detached from flasks with trypsin (Lonza), and 50,000 cells (25,000 cells/cm^2) were seeded on each 24-well in 1 mL of medium. Cells were monitored for cell attachment

and once cells attached to the pattern (20-30 min after seeding), the wells were rinsed with PBS to remove any unattached cells and cultured with HUVEC medium overnight.

The next day, SMCs were trypsinized, counted, and 50,000 SMCs per 24-well (25,000 cells/cm^2) were placed in an eppendorf tube and spun at 2,000 rpm in a microcentrifuge for 4 minutes. The medium was aspirated leaving the cell pellet, and 15 uL of mixed medium (50% HUVEC medium, 50% SMC medium) per 24 well was added to the pellet. The cell suspension was cooled on ice. The HUVEC medium was removed from the patterned HUVEC surfaces, and the bottoms and sides of the PDMS discs dried using sterile absorbent material with sterile forceps. These discs were placed in new 24 wells immediately before seeding SMC on top. An equal volume of matrigel (15 uL per 24 well) was added to the ice-cold cell suspension and mixed well, and quickly 30 uL of the cell and matrigel suspension was added to each disc. Matrigel was allowed to harden for 30 min at 37°C, after which 1mL of mixed medium was gently added for incubation. The medium was changed every other day until analysis.

7.2.5 Immunocytochemical Analysis

PDMS discs were fixed with 4% paraformaldehyde for 30 min at room temperature and permeabilized with 0.5% Triton-X 100. Mouse anti-smooth muscle α-actin and goat anti-Von Willebrand Factor (Sigma) were applied overnight at 4°C. After washing with PBS, Alexa 633 labeled anti-goat IGG (Invitrogen) and FITC labeled anti-mouse IGG (Sigma)

were applied for 2 hours. Cells were examined using an LSM510 meta confocal microscope (Carl Zeiss Germany).

7.3 Results and Discussion

The process used to generate patterned co-cultures is summarized in the schematic in Figure 8-1. To control EC placement, a PDMS stamping method was employed, utilizing an adaptation of microcontact printing to transfer patterns of charged protein onto a substrate[178, 179]. PDMS stamps were created by pouring unpolymerized PDMS onto a silicon mold with chosen patterns etched upon it, followed by PDMS thermosetting. The stamps were peeled from the mold for use in stamping experiments. For microcontact printing, stamps were plasma etched to induce a surface charge with a radio frequency plasma etcher. A fibronectin solution was deposited on the stamps and allowed to wet the stamps completely for 30 minutes at 37°C and then excess solution was removed by spinning the stamp in a spincaster as described in the experimental section.

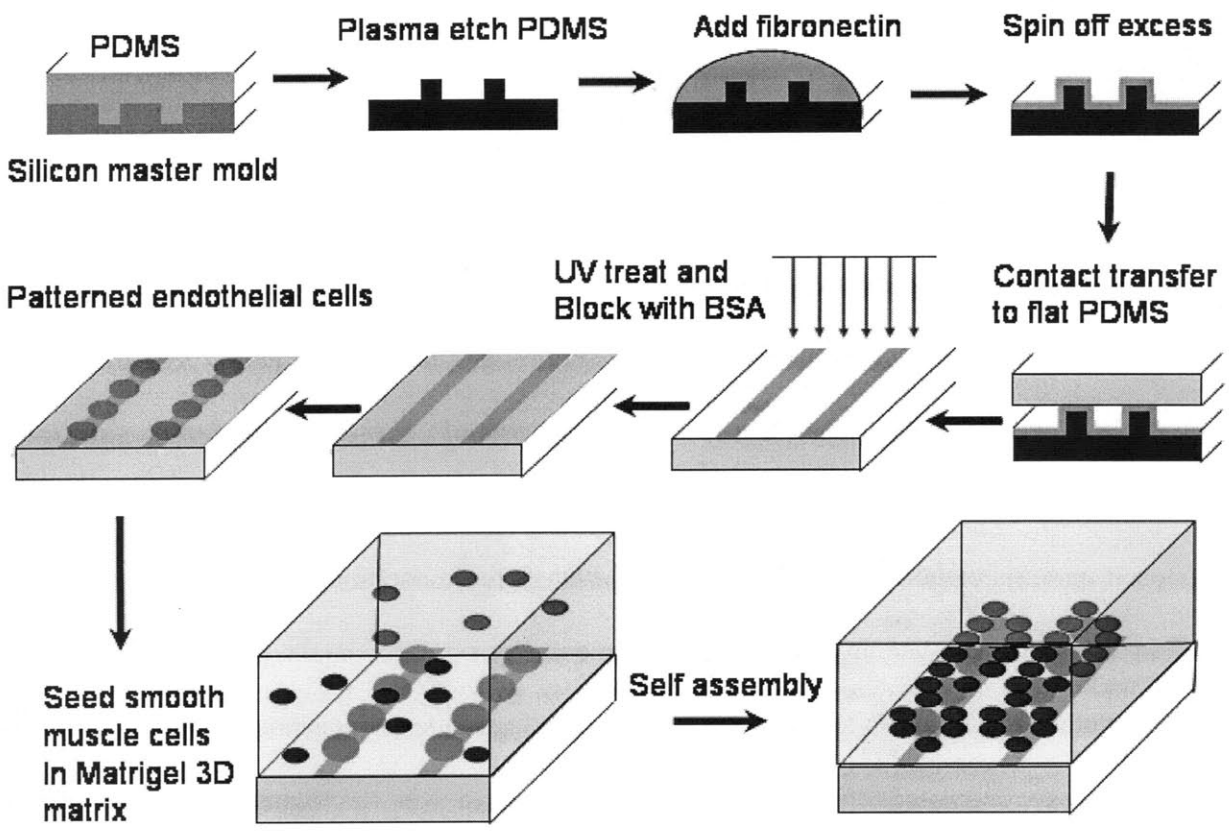

Figure 7-1: Schematic representation of micropatterning protocol. The pattern is controlled through photolithography of the silicon master template. Stamps are plasma etched to induce a temporary surface charge and fibronectin applied to the stamp is transferred to flat PDMS through microcontact printing. After blocking with BSA, ECs selectively adhere to the fibronectin, shunning the hydrophobic PDMS. SMCs seeded in matrigel migrate through the extracellular matrix to contact ECs, creating dense concentrations of pre vascular forms along desired experimental patterns

The flat PDMS sheets prepared for the cellular substrate were plasma etched to yield a negative charge just prior to stamping. The fibronectin coated stamp was then placed directly onto the PDMS substrate to enable transfer of fibronectin to the surface, leaving a pattern of cell adhesive regions on a relatively cell resistant PDMS background. Fibronectin was chosen because it presents specific peptide sequences that bind the integrin receptors

associated with cell adhesion[180]. In Figure 8-2, the PDMS stamp patterns chosen for this study have been imaged with optical microscopy in the top three panels. The second row of panels in Figure 8-2 shows the transferred stamp pattern of fibronectin on flat discs of PDMS. It should be noted that the first column in Figure 8-2 represents a small portion (that which could be captured under 5x microscopy) of an extensively branched network pattern ranging from 600 to 20 μm as noted in the Experimental Methods section; this pattern was designed so that the larger end could be surgically grafted to host vasculature, while the thinner ends would be the correct spacing and width for capillaries. This pattern could be used to make functional tissues approximately 2 cm long, and because prevascularization would lend a nutritional source to newly transplanted cells, grafts much thicker than the current diffusion thickness limit could be transferred with increased cell survival.

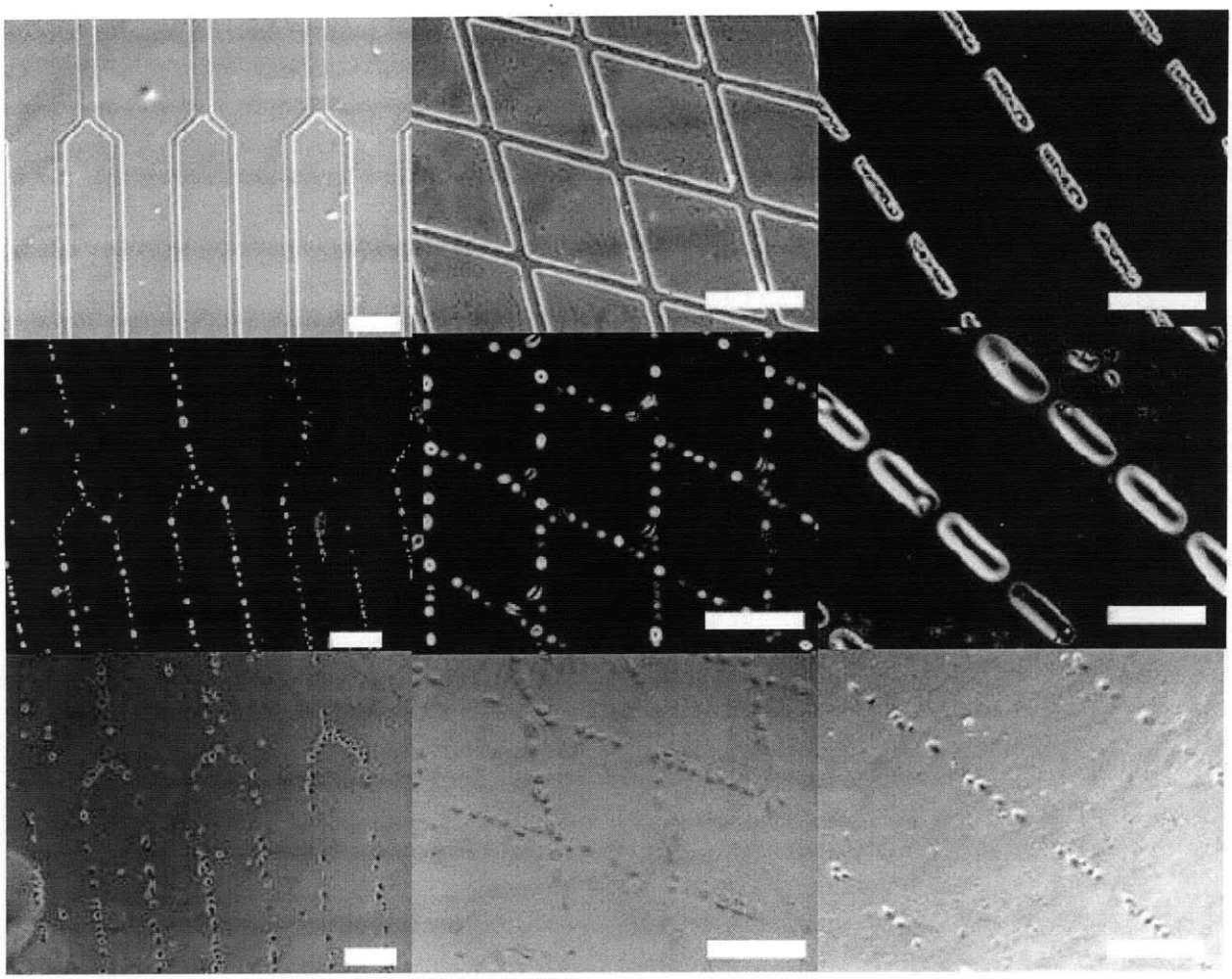

Figure 7-2: Stamp, fibronectin transfer, and EC adherence for three patterns. The top panel of each column depicts the PDMS stamp used. The second panel shows the pattern of fibronectin that is transferred to flat PDMS discs, and the third panel shows EC attachment preferentially to the fibronectin stamped areas. Scale bar 200 μm.

After UV sterilization the patterned substrate was exposed to a 1% bovine serum albumin (BSA) solution to further block nonspecific interactions between cells and the cell resist (non-coated) regions on the PDMS substrate. ECs were seeded onto the fibronectin patterns via direct culturing of the cells atop the stamped PDMS surface and were allowed to contact the surface for only 30 minutes to limit non-specific attachment. In the bottom three

panels of Figure 8-2, the resulting endothelial pattern is observed. ECs are well confined to the desired pattern geometry, and tend to attach to all available fibronectin surfaces while easily being washed from cell resist pattern portions. The cells in these panels (Fig. 7-2 bottom) are shown immediately post-seeding and thus exhibit a rounded morphology typical of a cell which is not yet well-attached to a surface. Endothelial cells observed after 12 hours of culture exhibit a healthy and typical cobblestone EC morphology confined to the fibronectin pattern.

In Figure 8-3, cocultures are created by seeding SMCs embedded in a 3D matrigel matrix on top of the EC patterns. Both of the cell lines used here are human primary cell lines rather than immortalized cell lines, which have the advantage of potentially being harvested from the host without immunocompatibility donor issues. ECs (green) were stained with Von Willebrand Factor, a marker specific for endothelial cell differentiation while SMCs (red) were stained with anti- smooth muscle α-actin, specific for SMC differentiation. The SMCs and ECs are tracked individually through the gel in the first two columns, and merged image is shown in the third column, where yellow color indicates strong overlap of the two cell types. The matrigel was allowed to harden for 30 min at 37°C to create a three dimensional matrix on top of the endothelial patterns. In the first row, after 30 minutes, SMCs have not yet attached to the extracellular matrix (ECM) proteins in the matrigel and retain a rounded morphology. By 3.5 hours, the characteristic spread morphology of the SMCs suggest that they have attached to the matrigel, but have not yet been able to migrate to their EC targets. In good agreement with previous studies, by 9 hours, the SMCs have migrated to the EC patterns. SMC α-actin staining at 9 hours reveals the spatial conformity of

the SMCs to the EC patterned cells; the ECs are able to draw the SMCs into precise and tightly located bands of cells at regular intervals. In previous

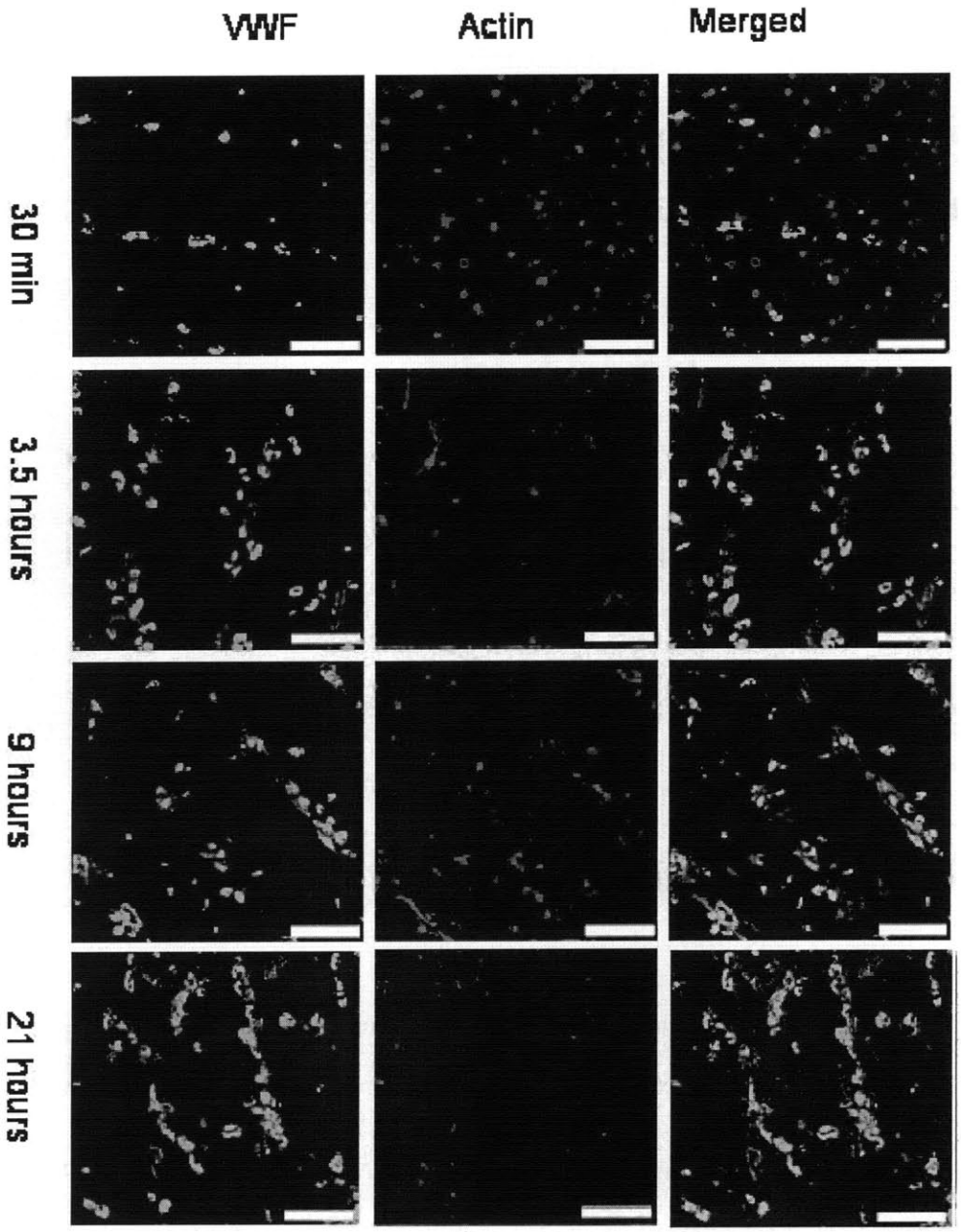

Figure 7-3: Merged images of the time course showing the migration of SMCs to EC patterns. Cocultures of ECs and SMCs were stained with Von Willebrand Factor (green) and smooth muscle α-actin (red) and imaged with confocal microscopy. By 3.5 hours, SMCs have attached to the surrounding gel, but have not yet

migrated to EC patterns. By 9 hours, SMCs migrate and form a distinct pattern in conjunction with underlying ECs. By 21 hours, SMCs proliferate, overrunning these precisely located bands of SMCs. Scale bar 200 μm.

work, due to the random arrangement of both cell types in the culture, it has been unclear if the ECs attracted support cells, vice versa, or both cell types migrate to create the vascular networks within the matrigel matrix. In this work the pre-patterning of the EC show that they remain well-adhered to the underlying substrate, and attract the SMCs to their position, rather than SMCs influencing EC placement. After 21 hours, the underlying ECs remain, but the SMCs have proliferated to such a degree that this close conformity to the original pattern is obscured. However, even at this late timepoint, both EC and SMC cells remain recognizably aligned along an original fibronectin pattern. It has been shown that alignment[181] cues are important in directing SMC phenotype to a more functional and less synthetic form, and that three dimensional cultures of aligned SMC show increased F- and α-actin alignment, which could increase tensile strength of resulting vessel forms[182].

Co-localization of support cells and ECs within Matrigel has been established in the literature; typically randomly seeded cells take 6 hours to co-localize, and well-formed vessels appear by 9 hours[174]. This cell formation appears to be unstable, and regresses by 21 hours[174], which is posited to be due to an unknown signal deficient in their system. More recent work suggests that the presence of mature SMCs, and potentially mechanical stimuli presented by a stiffer scaffold, may provide the necessary signals to allow for differentiated structures in 3D culture present up to a month after culture initiation[170, 173], avoiding dissolution of the nascent blood vessels.

To see if the SMCs were able to prevent vessel dissolution, experiments were extended to a two week period. After this time period, the cells were fixed and stained with Von Willebrand Factor to visualize the ECs within the three dimensional co-culture. In Figure 8-4, non patterned surfaces show small clumps of unorganized ECs after 6 days (panel B). After 13 days (panel D), unpatterned surfaces display developed blood vessel networks, randomly arranged across the surface, indicating that the SMCs present are able to stabilize the forming blood vessels for long-term culture. Encouragingly, ECs initially patterned with our microcontact patterning approach maintain their patterns at six and thirteen days (Figure 8-4A, C), indicating that a chosen fibronectin/PDMS pattern can persist through the duration of two weeks in culture. SMCs continue to permeate the culture. Typically, SMCs exhibit strong preference for alignment with the long axis of EC patterns. Previous studies[170] have suggested that blood vessels present in matrigel at two weeks' time, when implanted, are able to connect with host vasculature and carry host blood, enabling nutrient exchange within the transplanted material.

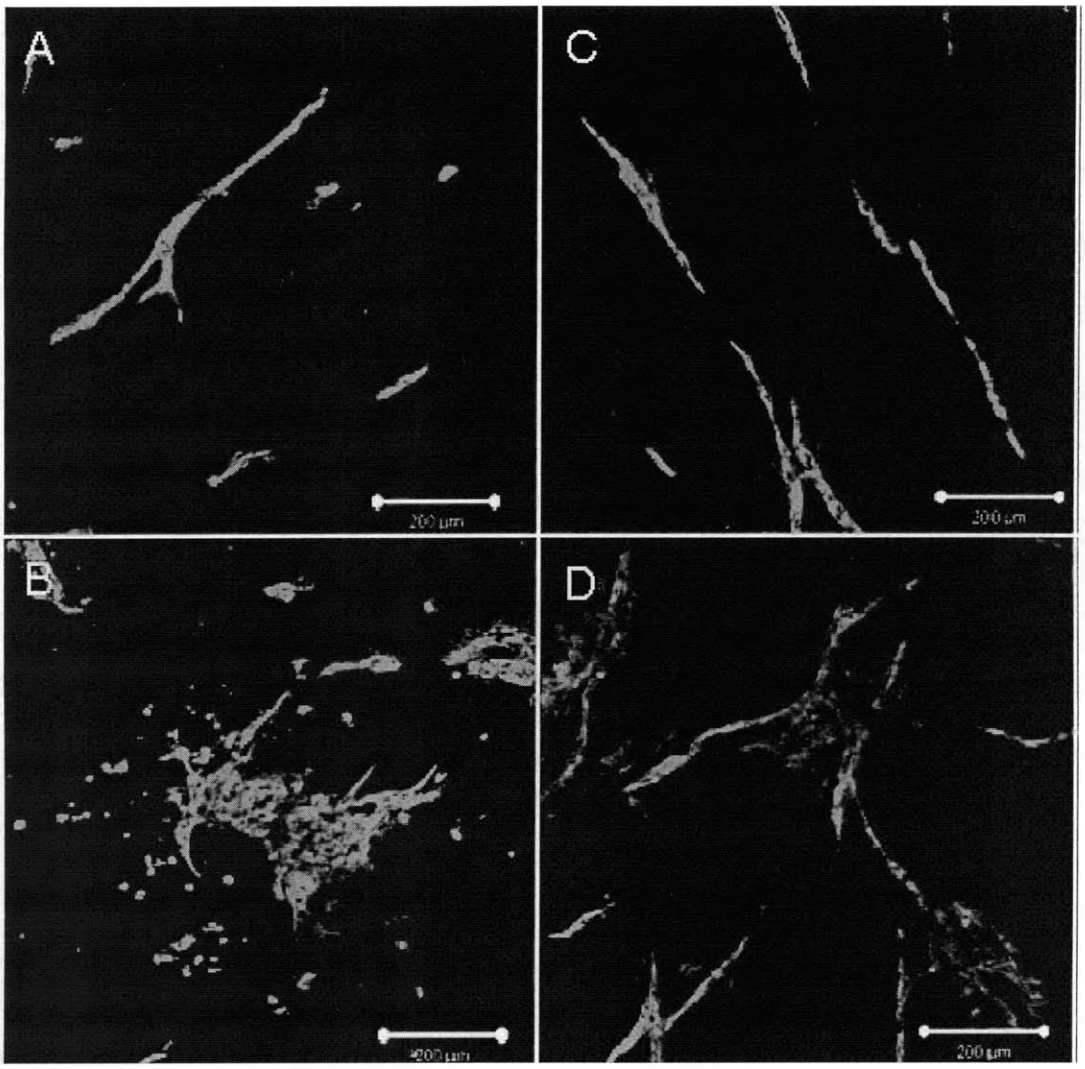

Figure 7-4: Long term pattern stability is achieved. Co-cultures of ECs and SMCs were allowed to reorganize for up to two weeks' time, and then were stained with Von Willebrand Factor. Compared to non patterned controls (B, 6 days, D, 13 days), pattern at six (panel A) and thirteen (panel C) days. Scale bar 200 µm.

Such blood vessels have been shown to be crucial for functional behavior of parenchymal cells. Nahmias et al[173] were able to show that, compared with monocultures of hepatocytes, which never formed cell islets within matrigel, and lost typical cell functions such as albumin

production over time, those hepatocytes co-cultured with endothelial networks both migrated to be in contact with ECs in a pattern reminiscent of the liver sinusoid's architecture, and sustained albumin production for more than twice the time of the hepatocytes deprived of co-stimulatory cells. Tissue engineered implants with blood vessel support and improvement of parenchymal cell function are likely to show better results compared to monoculture implants vascularized after implantation.

7.4 Conclusion

Here we describe a novel system for patterning blood vessel networks for tissue engineering. Preformed vascular networks are crucial for advancing the field of tissue engineering, both to surpass the diffusion thickness barrier currently confronting attempts at clinically relevant volumes of implantable tissues, and also as a powerful tool for organizing complex tissues involving multiple cooperative cell types. The random self-assembly commonly seen in co-culture experiments is here directed by the simple use of a fibronectin pattern. By patterning ECs through the cell adhesive/resistant pattern displayed by the fibronectin/PDMS stamp, it is possible to direct complementary, migratory cells such as SMCs to the spatial positions desired within the three dimensional matrix to create vessel-like entities that could further be used to pattern parenchymal cells such as liver, heart, and pancreas. Not only can interesting questions about the cell microenvironment be posed by altering the EC pattern and thus the chemoattractant gradients and support that parenchymal cells receive, but this method allows attachment of a microvascularized, engineered tissue to the host vasculature through the branching pattern which at its widest point is 600 um across and therefore of a size that can be

surgically sutured to host vasculature, allowing for immediate perfusion of nutrients and waste removal of implantable tissues. This method is simple and can be generalized to a wide variety of systems; the pattern can be chosen at will, the materials needed are inexpensive, and the technical difficulties associated with this technique are minimal. In the future, our laboratories anticipate studying the effects that such blood vessel networks have in supporting parenchymal cell function and directing cellular organization.

Chapter 8 Summary and Future Work

8.1 Summary

The push to incorporate fragile biologic therapeutics in drug/medical device combinations represents a paradigm shift that will become increasingly crucial with the concurrent shift in research and development towards biologic compounds. Therapeutic protein delivery requires new delivery strategies that both maintain intimate, conformal coating between the implant and the drug delivery system while preserving fragile protein activity and allowing the possibility of sequential or co-eluted release of therapeutics from the coating. LbL is a promising technique that uniquely addresses the criteria above. In this thesis, the first demonstrations of controlled LbL release of protein therapeutics using a synthetic (and therefore tunable) PBAE system have indicated a high likelihood of success for this technology in directing host cell behavior *in vivo*.

Such biologic therapeutic coatings have a large potential to impact human health. As discussed in Chapter 1, local controlled delivery is necessary to deliver fragile protein therapeutics that are inactivated by traditional means of delivery such as injections or pill formulations. In the specific case of drug/medical device combinations, the combination of localized delivery of the therapeutic from the implant surface can outperform the bare implant performance, even with co-administration of the therapeutic using traditional delivery methods. In the area of orthopedic hip implants, even a small reduction in the number of complications from an implant coating can drastically reduce both the morbidity and mortality and the associated costs of complications. The technique of LbL was introduced as a tool to address this opportunity, and previous LbL strategies, successes, and shortcomings were reviewed.

Work with a model protein allows rapid, inexpensive coverage of a wide variety of experimental conditions. In Chapter 2, lysozyme was shown to easily incorporate in many different formulations of synthetic LbL films. Protein release can be controlled through choice of the synthetic polymer used in an important improvement from previous difficult to tune profiles from biopolymer based films. The release profile is also tunable through the number of layers deposited and the polyanion used. The release of over a milligram of protein over periods of weeks to months from a surface eroding film shows that these LbL films had copious capability to load relevant amounts and timings of growth factor release. High retention of enzymatic activity is preserved throughout the fabrication, release, and analysis period.

The growth factors selected for LbL testing were chosen to first induce proliferation of bone progenitor cells and then differentiation to a committed bone lineage of osteoblasts and osteocytes. Fibroblast Growth Factor 2 (FGF-2) is known to be a potent mitogen of preosteoblast cell types, while Bone Morphogenetic Protein 2 (BMP-2) has the ability to induce progenitor cell commitment to the bone cell lineage. Thus, in Chapter 3, *in vitro* FGF-2 delivery from LbL films was explored. This work confirmed many of the conclusions of the lysozyme work; delivery is tunable with choice of synthetic polymer and polyanion employed, and the bioactivity of the FGF-2 was confirmed. One important question that could not be addressed in lysozyme work is the role of polyanion choice in enhancing growth factor function, as lysozyme has no known interactions with the polyanions used. Both of the polyanions employed in our model system, chondroitin and heparin, enhance the activity of FGF-2. MC3T3 E1 Subclone 4 cells, a preosteoblast cell line, responded to FGF-2 released from LbL films with proliferation rates up to eight times that of the control cells, while interestingly free FGF-2 not associated with other LbL release products such as the enhancing polyanions could only enhance proliferation rates by two fold. This work suggests that the enhancement of growth factor activity possible with non-tunable biopolyions can

still be accessed in synthetic LbL films by inclusion in a tetralayer architecture, allowing the best of both worlds.

Although most of the body of literature on LbL refers to dipped LbL films, an alternative fabrication strategy employing atomized sprays of polymer solution to create LbL films also exists. Spray LbL has many advantages over dip LbL, including faster fabrication time (hours vs. several days), the potential to kinetically trap molecules and affect their release behavior, and spatial specificity that could allow different growth factor incorporation in different portions of the sprayed substrate. In Chapter 4, the utility of spray LbL in growth factor releasing films was explored. It was found that in the case of the system utilized here (lysozyme and FGF-2 releasing films similar to those explored in Chapters 2-3), similar characteristics emerged; the films still grew superlinearly, maintained protein activity, and released for multiple days. The first work with three dimensional scaffolds is explored in this chapter using an electrospun polycaprolactone mat, indicating the success of LbL films to modify cell behavior within a three dimensional architecture.

Chapter 5 explores another application of the LbL protein release platform technology. Here, we discovered that antibodies, another class of therapeutic proteins, are easily incorporated in LbL films, and allow a mechanism for decreasing cellular response (rather than enhancing cellular response, as is the case with FGF-2) by inactivating growth factors present in the microenvironment. Anti-Vascular Endothelial Growth Factor was found to release over a time span of approximately two weeks, and retain its ability to bind and inactivate VEGF in a HUVEC proliferation assay.

In vivo growth factor delivery from LbL films is still in its infancy, with only one reported literature case with a substantially different strategy involving exogenous stem cell transfer. The work in Chapter 6 represents the only known example of LbL growth factor delivery of sufficient concentration of a growth factor to induce native host stem cell tissue response. The concentrations of growth factor delivered in this work is necessary to affect implant

surface/tissue interactions and is unprecedented in the literature. BMP-2 LbL films are shown to have potent ability to induce progenitor cell differentiation *in vitro* through three biological assays. *In vivo*, we show the capability of recruiting and differentiating *host* progenitor cells to induce bone formation visible on the macroscopic and microscopic level in a porous test implant similar to the woven mesh geometries of hip implant surfaces.

8.2 Future Work

The work outlined in this thesis provides many insights into the feasibility of using LbL films for protein therapeutic coatings for implantable medical devices, while simultaneously opening many interesting avenues of inquiry for future studies. Four areas of future exploration are proposed below.

8.2.1 Sequential or Co-Delivery of Growth Factors and Antibiotic Agents

One of the most unique and attractive characteristics of LbL films is the nano-scale control of film architecture and the resultant possibility of sequential (or co-) release strategies to address implant complications. In the specific application of orthopedic hip implants, a host of growth factors, including FGF-2 and BMP-2, discussed in this thesis, in addition to VEGF for enhanced angiogenesis and stem cell recruitment are known to contribute synergistically to tissue formation. The release of different combinations of growth factors over complex time scales of release are highly likely to enhance tissue growth; that it can be accomplished from a thin film applicable to any mechanical substrate is doubly appealing. This concept is powerful not only in implant technologies but also in the arena of tissue engineering and drug delivery across a wide variety of fields and applications. Furthermore, the application of multiple therapeutic classes, such as antibiotic release to remediate infection followed by BMP-2 release to enhance tissue ingrowth allow for sophisticated control of the tissue/implant microenvironment which could dramatically reduce complication rates with this common surgery. Co-current work done in the Hammond lab has shown that both

antibiotic (Moskowitz and Hammond, results accepted for publication in Biomaterials);[34, 35] and anti-inflammatory[36] synthetic LbL drug delivery systems show efficacy as well, making this an accessible strategy.

However, despite the simplicity of the concept of LbL sequential release, such release has been difficult to realize experimentally. A few factors are known to complicate the situation. Interlayer diffusion, in which polymer chains can diffuse through the bulk of the LbL film as it is constructed lead to film rearrangements during fabrication that confound the precise nanolayer architecture desired. The ejection of polymers due to a pH shift in the film, frequently seen when construction pH and release pH are different leading to a charge imbalance in the film, is known to destroy nanolayer architecture upon release[118]. These mechanisms are treated more fully in Section 3.3.3. These effects do not totally dominate release, and sequential release is still possible[44, 45], but it is anticipated that finer control could be exerted on these systems with control of these phenomena. Thus, work should simultaneously be done to (1) explore the biological implications of co- and sequentially releasing films in their current state, as well as (2) delve into the fundamental mechanisms of film buildup and release to understand this area in far greater detail than is currently possible, allowing for stronger control to be exerted.

8.2.2 Investigation of More Clinically Viable In Vivo *Models*

The gold standard ectopic bone formation model was used in this thesis to irrefutably prove that bioactive BMP-2 itself, released from LbL films, was responsible for stem cell induction to the bone lineage. Placing a similar construct in a bone cavity would have potentially confounded there results, as bone formation could also then be attributed partially or in full to the osteoconductivty of the test matrix, rather than the osteoinduction of BMP-2.

However, with this work in hand, it is now possible to move to more clinically relevant model systems. Clinical markers of improvement include decreased infection rates, for antibiotic treatment, and increased bone tissue penetration of the implant surface, as

well as increased pull-out strength (testing the integration of the implant and the bone tissue) due to BMP-2 bone induction. More relevant clinical information can be accessed for both of these questions by utilizing a variety of clinical models, including calvarial defect models, critical defect models, and screw models, as well as in animal hip implant models.

8.2.3 Exploration of New Synthetic Polymer Classes

The work done in this thesis suggests that PBAE synthetic LbL films have a bright future in drug/medical device coatings. Although the ability to synthetically tune release from PBAEs makes them extremely flexible compared to their bio-polyion alternatives, with co-release of bio-polyions further increasing tunability, it is likely that moving forward with investigations into new classes of polymers may afford further attractive characteristics yet. Improvements may allow higher loading, longer release time spans, more control over release due to decreased interdiffusion and an ability to construct films at pH 7.4, and a host of other attractive benefits, further increasing the flexibility of this approach.

8.2.4 Engineering New Functionalities

All of the work discussed herein relies on the passive release mechanism of ester hydrolysis in the presence of water. Synergistic LbL technologies exist which allow for release through application of an electric pulse[183] provide a way to release therapeutic agents at the control of a button. Such control would allow for the post-implantation control of dose release from the implant, allowing another method of control. Furthermore, the ability to stamp LbL films into intricate patterns affords another fertile field for investigation of the cellular microenvironment.

8.3 **Conclusions**

This work has shown that therapeutic proteins capable of enhancing proliferation, preventing proliferation, and inducing differentiation to a specific tissue lineage are all

possible, in thereapeutically relevant quantities, from LbL films, and that these proteins retain their activity and have the *ability to direct host cell response* to the implant *in vivo*. However, these examples are just a few of the potential applications accessible with the LbL platform technology; growth factors and antibodies provide extremely diverse cues to the cellular microenvironment, creating a powerful handle of host tissue response to a given implant (or tissue engineering scaffold). Furthermore, the ability to combine LbL growth factor delivery with LbL delivery of other classes of therapeutic agents including antibiotics and anti-inflammatory agents for co- or sequential delivery gives LbL a unique advantage in mediating the tissue/implant microenvironment to improve the success rates of these life-saving medical devices. Although LbL still has significant hurdles and improvements are still necessary for it to reach its full potential, its future in drug/device combination therapies is bright.

Bibliography

1. Wu, P.; Grainger, D. W., Drug/device combinations for local drug therapies and infection prophylaxis. *Biomaterials* **2006,** *27* (11), 2450-2467.
2. Langer, R., Drug delivery and targeting. *Nature* **1998,** *392* (6679), 5-10.
3. Langer, R., NEW METHODS OF DRUG DELIVERY. *Science* **1990,** *249* (4976), 1527-1533.
4. Uhrich, K. E.; Cannizzaro, S. M.; Langer, R. S.; Shakesheff, K. M., Polymeric systems for controlled drug release. *Chem. Rev.* **1999,** *99* (11), 3181-3198.
5. Balmayor, E. R.; Feichtinger, G. A.; Azevedo, H. S.; van Griensven, M.; Reis, R. L., Starch-poly-N"-caprolactone Microparticles Reduce the Needed Amount of BMP-2. *Clinical Orthopaedics and Related Research* **2009,** *467* (12), 3138-3148.
6. Hsu, H. P.; Zanella, J. M.; Peckham, S. M.; Spector, M., Comparing ectopic bone growth induced by rhBMP-2 on an absorbable collagen sponge in rat and rabbit models. *Journal of Orthopaedic Research* **2006,** *24* (8), 1660-1669.
7. Winn, S. R.; Uludag, H.; Hollinger, J. O., Carrier systems for bone morphogenetic proteins. *Clinical Orthopaedics and Related Research* **1999,** (367), S95-S106.
8. DiMasi, J. A.; Hansen, R. W.; Grabowski, H. G., The price of innovation: new estimates of drug development costs. *Journal of Health Economics* **2003,** *22* (2), 151-185.
9. Davis, M. E.; Brewster, M. E., Cyclodextrin-based pharmaceutics: Past, present and future. *Nature Reviews Drug Discovery* **2004,** *3* (12), 1023-1035.
10. LaVan, D. A.; McGuire, T.; Langer, R., Small-scale systems for in vivo drug delivery. *Nature biotechnology* **2003,** *21* (10), 1184-1191.
11. Pai, M. P.; Pendland, S. L.; Danziger, L. H., Antimicrobial-coated/bonded and -impregnated intravascular catheters. *Annals of Pharmacotherapy* **2001,** *35* (10), 1255-1263.
12. Veenstra, D. L.; Saint, S.; Saha, S.; Lumley, T.; Sullivan, S. D., Efficacy of antiseptic-impregnated central venous catheters in preventing catheter-related bloodstream infection - A meta-analysis. *Jama-Journal of the American Medical Association* **1999,** *281* (3), 261-267.
13. Veenstra, D. L.; Saint, S.; Sullivan, S. D., Cost-effectiveness of antiseptic-impregnated central venous catheters for the prevention of catheter-related bloodstream infection. *Jama-Journal of the American Medical Association* **1999,** *282* (6), 554-560.
14. Alt, V.; Heissel, A., Economic considerations for the use of recombinant human bone morphogenetic protein-2 in open tibial fractures in Europe: The German model. *Curr. Med. Res. Opin.* **2006,** *22*, S19-S22.
15. Uludag, H.; Gao, T. J.; Porter, T. J.; Friess, W.; Wozney, J. M., Delivery systems for BMPs: Factors contributing to protein retention at an application site. *Journal of Bone and Joint Surgery-American Volume* **2001,** *83A*, S128-S135.

16. Fu, K.; Pack, D. W.; Klibanov, A. M.; Langer, R., Visual evidence of acidic environment within degrading poly(lactic-co-glycolic acid) (PLGA) microspheres. *Pharmaceutical Research* **2000,** *17* (1), 100-106.
17. Bernard, L.; Hoffmeyer, P.; Assal, M.; Vaudaux, P.; Schrenzel, J.; Lew, D., Trends in the treatment of orthopaedic prosthetic infections. *Journal of Antimicrobial Chemotherapy* **2004,** *53* (2), 127-129.
18. Bauer, T. W.; Schils, J., The pathology of total joint arthroplasty - II. Mechanisms of implant failure. *Skeletal Radiology* **1999,** *28* (9), 483-497.
19. Lavernia, C. J.; Drakeford, M. K.; Tsao, A. K.; Gittelsohn, A.; Krackow, K. A.; Hungerford, D. S., Revision and Primary Hip and Knee Arthroplasty - a Cost-Analysis. *Clinical Orthopaedics and Related Research* **1995,** (311), 136-141.
20. Bragdon, C. R.; Jasty, M.; Greene, M.; Rubash, H. E.; Harris, W. H., Biologic fixation of total hip implants - Insights gained from a series of canine studies. *Journal of Bone and Joint Surgery-American Volume* **2004,** *86A*, 105-117.
21. Decher, G., Fuzzy nanoassemblies: Toward layered polymeric multicomposites. *Science* **1997,** *277* (5330), 1232-1237.
22. Decher, G.; Hong, J. D.; Schmitt, J., BUILDUP OF ULTRATHIN MULTILAYER FILMS BY A SELF-ASSEMBLY PROCESS .3. CONSECUTIVELY ALTERNATING ADSORPTION OF ANIONIC AND CATIONIC POLYELECTROLYTES ON CHARGED SURFACES. *Thin Solid Films* **1992,** *210* (1-2), 831-835.
23. Kim, B. S.; Park, S. W.; Hammond, P. T., Hydrogen-bonding layer-by-layer assembled biodegradable polymeric micelles as drug delivery vehicles from surfaces. *Acs Nano* **2008,** *2* (2), 386-392.
24. Stockton, W. B.; Rubner, M. F., Molecular-level processing of conjugated polymers .4. Layer-by-layer manipulation of polyaniline via hydrogen-bonding interactions. *Macromolecules* **1997,** *30* (9), 2717-2725.
25. Yang, S. Y.; Rubner, M. F., Micropatterning of polymer thin films with pH-sensitive and cross-linkable hydrogen-bonded polyelectrolyte multilayers. *Journal of the American Chemical Society* **2002,** *124* (10), 2100-2101.
26. Kotov, N. A., Layer-by-layer self-assembly: The contribution of hydrophobic interactions. *Nanostructured Materials* **1999,** *12* (5-8), 789-796.
27. Richert, L.; Lavalle, P.; Payan, E.; Shu, X. Z.; Prestwich, G. D.; Stoltz, J. F.; Schaaf, P.; Voegel, J. C.; Picart, C., Layer by layer buildup of polysaccharide films: Physical chemistry and cellular adhesion aspects. *Langmuir* **2004,** *20* (2), 448-458.
28. Thierry, B.; Winnik, F. M.; Merhi, Y.; Tabrizian, M., Nanocoatings onto arteries via layer-by-layer deposition: Toward the in vivo repair of damaged blood vessels. *Journal of the American Chemical Society* **2003,** *125* (25), 7494-7495.
29. Wood, K. C.; Boedicker, J. Q.; Lynn, D. M.; Hammond, P. T., Tunable drug release from hydrolytically degradable layer-by-layer thin films. *Langmuir* **2005,** *21* (4), 1603-9.

30. Benkirane-Jessel, N.; Lavalle, P.; Hubsch, E.; Holl, V.; Senger, B.; Haikel, Y.; Voegel, J. C.; Ogier, J.; Schaaf, P., Short-time timing of the biological activity of functionalized polyelectrolyte multilayers. *Advanced Functional Materials* **2005,** *15* (4), 648-654.
31. Onda, M.; Lvov, Y.; Ariga, K.; Kunitake, T., Sequential reaction and product separation on molecular films of glucoamylase and glucose oxidase assembled on an ultrafilter. *Journal of Fermentation and Bioengineering* **1996,** *82* (5), 502-506.
32. Lvov, Y.; Ariga, K.; Ichinose, I.; Kunitake, T., Assembly of Multicomponent Protein Films by Means of Electrostatic Layer-by-Layer Adsorption. *Journal of the American Chemical Society* **1995,** *117* (22), 6117-6123.
33. Onda, M.; Lvov, Y.; Ariga, K.; Kunitake, T., Sequential actions of glucose oxidase and peroxidase in molecular films assembled by layer-by-layer alternate adsorption. *Biotechnology and Bioengineering* **1996,** *51* (2), 163-167.
34. Chuang, H. F.; Smith, R. C.; Hammond, P. T., Polyelectrolyte multilayers for tunable release of antibiotics. *Biomacromolecules* **2008,** *9* (6), 1660-1668.
35. Shukla, A.; Fleming, K. E.; Chuang, H. F.; Chau, T. M.; Loose, C. R.; Stephanopoulos, G. N.; Hammond, P. T., Controlling the release of peptide antimicrobial agents from surfaces. *Biomaterials 31* (8), 2348-2357.
36. Smith, R. C.; Riollano, M.; Leung, A.; Hammond, P. T., Layer-by-Layer Platform Technology for Small-Molecule Delivery. *Angewandte Chemie-International Edition* **2009,** *48* (47), 8974-8977.
37. Caruso, F.; Yang, W. J.; Trau, D.; Renneberg, R., Microencapsulation of uncharged low molecular weight organic materials by polyelectrolyte multilayer self-assembly. *Langmuir* **2000,** *16* (23), 8932-8936.
38. Lee, S. W.; Kim, B. S.; Chen, S.; Shao-Horn, Y.; Hammond, P. T., Layer-by-Layer Assembly of All Carbon Nanotube Ultrathin Films for Electrochemical Applications. *Journal of the American Chemical Society* **2009,** *131* (2), 671-679.
39. Tsukruk, V. V.; Rinderspacher, F.; Bliznyuk, V. N., Self-assembled multilayer films from dendrimers. *Langmuir* **1997,** *13* (8), 2171-2176.
40. Bertrand, P.; Jonas, A.; Laschewsky, A.; Legras, R., Ultrathin polymer coatings by complexation of polyelectrolytes at interfaces: suitable materials, structure and properties. *Macromol. Rapid Commun.* **2000,** *21* (7), 319-348.
41. Hammond, P. T., Form and function in multilayer assembly: New applications at the nanoscale. *Advanced Materials* **2004,** *16* (15), 1271-1293.
42. Berg, M. C.; Yang, S. Y.; Hammond, P. T.; Rubner, M. F., Controlling mammalian cell interactions on patterned polyelectrolyte multilayer surfaces. *Langmuir* **2004,** *20* (4), 1362-1368.
43. Caruso, F., Nanoengineering of particle surfaces. *Advanced Materials* **2001,** *13* (1), 11-+.

44. Dierich, A.; Le Guen, E.; Messaddeq, N.; Stoltz, J. F.; Netter, P.; Schaaf, P.; Voegel, J. C.; Benkirane-Jessel, N., Bone formation mediated by synergy-acting growth factors embedded in a polyelectrolyte multilayer film. *Advanced Materials* **2007,** *19* (5), 693-+.
45. Wood, K. C., Chuang, Helen F., Batten, Robert D., Lynn, David M., Hammond, Paula T., Controlling interlayer diffusion to achieve sustained, multiagent delivery from layer-by-layer thin films. *PNAS* **2006,** *103* (27), 10207-10212.
46. Chung, A. J.; Rubner, M. F., Methods of loading and releasing low molecular weight cationic molecules in weak polyelectrolyte multilayer films. *Langmuir* **2002,** *18* (4), 1176-1183.
47. Sukhishvili, S. A.; Granick, S., Layered, erasable polymer multilayers formed by hydrogen-bonded sequential self-assembly. *Macromolecules* **2002,** *35* (1), 301-310.
48. Pargaonkar, N.; Lvov, Y. M.; Li, N.; Steenekamp, J. H.; de Villiers, M. M., Controlled release of dexamethasone from microcapsules produced by polyelectrolyte layer-by-layer nanoassembly. *Pharmaceutical Research* **2005,** *22* (5), 826-835.
49. Jewell, C. M.; Zhang, J.; Fredin, N. J.; Lynn, D. M., Multilayered polyelectrolyte films promote the direct and localized delivery of DNA to cells. *J Control Release* **2005,** *106* (1-2), 214-23.
50. Zhang, J. T.; Montanez, S. I.; Jewell, C. M.; Lynn, D. M., Multilayered films fabricated from plasmid DNA and a side-chain functionalized poly(beta-amino ester): Surface-type erosion and sequential release of multiple plasmid constructs-from surfaces. *Langmuir* **2007,** *23* (22), 11139-11146.
51. Muller, S.; Koenig, G.; Charpiot, A.; Debry, C.; Voegel, J. C.; Lavalle, P.; Vautier, D., VEGF-functionalized polyelectrolyte multilayers as proangiogenic prosthetic coatings. *Advanced Functional Materials* **2008,** *18* (12), 1767-1775.
52. Berg, M. C.; Zhai, L.; Cohen, R. E.; Rubner, M. F., Controlled drug release from porous polyelectrolyte multilayers. *Biomacromolecules* **2006,** *7* (1), 357-364.
53. Crouzier, T.; Ren, K.; Nicolas, C.; Roy, C.; Picart, C., Layer-By-Layer Films as a Biomimetic Reservoir for rhBMP-2 Delivery: Controlled Differentiation of Myoblasts to Osteoblasts. *Small* **2009,** *5* (5), 598-608.
54. Caruso, F.; Trau, D.; Mohwald, H.; Renneberg, R., Enzyme encapsulation in layer-by-layer engineered polymer multilayer capsules. *Langmuir* **2000,** *16* (4), 1485-1488.
55. Schuler, C.; Caruso, F., Decomposable hollow biopolymer-based capsules. *Biomacromolecules* **2001,** *2* (3), 921-926.
56. Tiourina, O. P.; Sukhorukov, G. B., Multilayer alginate/protamine microsized capsules: encapsulation of alpha-chymotrypsin and controlled release study. *International Journal of Pharmaceutics* **2002,** *242* (1-2), 155-161.
57. Khopade, A. J.; Arulsudar, N.; Khopade, S. A.; Hartmann, J., Ultrathin antibiotic walled microcapsules. *Biomacromolecules* **2005,** *6* (1), 229-234.

58. Bhadra, D.; Gupta, G.; Bhadra, S.; Umamaheshwari, R. B.; Jain, N. K., Multicomposite ultrathin capsules for sustained ocular delivery of ciprofloxacin hydrochloride. *J. Pharm. Pharm. Sci.* **2004,** *7* (2), 241-251.
59. Zhu, H. G.; Srivastava, R.; McShane, M. J., Spontaneous loading of positively charged macromolecules into alginate-templated polyelectrolyte multilayer microcapsules. *Biomacromolecules* **2005,** *6* (4), 2221-2228.
60. Lynn, D. M., Langer, R., Degradable poly(beta-amino esters): synthesis, characterization, and self-assembly with plasmid DNA. *Journal of the American Chemical Society* **2000,** *122*, 10761– 10768.
61. Anderson, D. G.; Lynn, D. M.; Langer, R., Semi-automated synthesis and screening of a large library of degradable cationic polymers for gene delivery. *Angewandte Chemie-International Edition* **2003,** *42* (27), 3153-3158.
62. Vazquez, E.; Dewitt, D. M.; Hammond, P. T.; Lynn, D. M., Construction of hydrolytically-degradable thin films via layer-by-layer deposition of degradable polyelectrolytes. *Journal of the American Chemical Society* **2002,** *124* (47), 13992-13993.
63. Macdonald, M.; Rodriguez, N. M.; Smith, R.; Hammond, P. T., Release of a model protein from biodegradable self assembled films for surface delivery applications. *Journal of Controlled Release* **2008,** *131* (3), 228-234.
64. Smith, R. C.; Leung, A.; Kim, B. S.; Hammond, P. T., Hydrophobic Effects in the Critical Destabilization and Release Dynamics of Degradable Multilayer Films. *Chemistry of Materials* **2009,** *21* (6), 1108-1115.
65. Balabushevich, N. G.; Lebedeva, O. V.; Vinogradova, O. I.; Larionova, N. I., Polyelectrolyte assembling for protein microencapsulation. *J. Drug Deliv. Sci. Technol.* **2006,** *16* (4), 315-319.
66. Mehrotra, S.; Lynam, D.; Maloney, R.; Pawelec, K. M.; Tuszynski, M. H.; Lee, I.; Chan, C.; Sakamoto, J., Time Controlled Protein Release from Layer-by-Layer Assembled Multilayer Functionalized Agarose Hydrogels. *Advanced Functional Materials 20* (2), 247-258.
67. Facca, S.; Cortez, C.; Mendoza-Palomares, C.; Messadeq, N.; Dierich, A.; Johnston, A. P. R.; Mainard, D.; Voegel, J.-C.; Caruso, F.; Benkirane-Jessel, N., Active multilayered capsules for in vivo bone formation. *Proceedings of the National Academy of Sciences 107* (8), 3406-3411.
68. Decher, G.; Eckle, M.; Schmitt, J.; Struth, B., Layer-by-layer assembled multicomposite films. *Current Opinion in Colloid & Interface Science* **1998,** *3* (1), 32-39.
69. Etienne, O.; Schneider, A.; Taddei, C.; Richert, L.; Schaaf, P.; Voegel, J. C.; Egles, C.; Picart, C., Degradability of polysaccharides multilayer films in the oral environment: an in vitro and in vivo study. *Biomacromolecules* **2005,** *6* (2), 726-733.
70. Picart, C.; Schneider, A.; Etienne, O.; Mutterer, J.; Schaaf, P.; Egles, C.; Jessel, N.; Voegel, J. C., Controlled degradability of polysaccharide multilayer films in vitro and in vivo. *Advanced Functional Materials* **2005,** *15* (11), 1771-1780.

71. Lynn, D. M.; Langer, R., Degradable poly(beta-amino esters): Synthesis, characterization, and self-assembly with plasmid DNA. *Journal of the American Chemical Society* **2000,** *122* (44), 10761-10768.
72. Akinc, A.; Anderson, D. G.; Lynn, D. M.; Langer, R., Synthesis of poly(beta-amino ester)s optimized for highly effective gene delivery. *Bioconjugate Chemistry* **2003,** *14* (5), 979-988.
73. Little, S. R.; Lynn, D. M.; Ge, Q.; Anderson, D. G.; Puram, S. V.; Chen, J. Z.; Eisen, H. N.; Langer, R., Poly-beta amino ester-containing microparticles enhance the activity of nonviral genetic vaccines. *Proceedings of the National Academy of Sciences of the United States of America* **2004,** *101* (26), 9534-9539.
74. Jessel, N.; Oulad-Abdeighani, M.; Meyer, F.; Lavalle, P.; Haikel, Y.; Schaaf, P.; Voegel, J. C., Multiple and time-scheduled in situ DNA delivery mediated by beta-cyclodextrin embedded in a polyelectrolyte multilayer. *Proceedings of the National Academy of Sciences of the United States of America* **2006,** *103* (23), 8618-8621.
75. Puleo, D. A.; Kissling, R. A.; Sheu, M. S., A technique to immobilize bioactive proteins, including bone morphogenetic protein-4 (BMP-4), on titanium alloy. *Biomaterials* **2002,** *23* (9), 2079-2087.
76. Porcel, C.; Lavalle, P.; Decher, G.; Senger, B.; Voegel, J. C.; Schaaf, P., Influence of the polyelectrolyte molecular weight on exponentially growing multilayer films in the linear regime. *Langmuir* **2007,** *23* (4), 1898-1904.
77. Porcel, C.; Lavalle, P.; Ball, V.; Decher, G.; Senger, B.; Voegel, J. C.; Schaaf, P., From exponential to linear growth in polyelectrolyte multilayers. *Langmuir* **2006,** *22* (9), 4376-4383.
78. Jourdainne, L.; Arntz, Y.; Senger, B.; Debry, C.; Voegel, J. C.; Schaaf, P.; Lavalle, P., Multiple strata of exponentially growing polyelectrolyte multilayer films. *Macromolecules* **2007,** *40* (2), 316-321.
79. Lavalle, P.; Gergely, C.; Cuisinier, F. J. G.; Decher, G.; Schaaf, P.; Voegel, J. C.; Picart, C., Comparison of the structure of polyelectrolyte multilayer films exhibiting a linear and an exponential growth regime: An in situ atomic force microscopy study. *Macromolecules* **2002,** *35* (11), 4458-4465.
80. Schlenoff, J. B.; Dubas, S. T., Mechanism of polyelectrolyte multilayer growth: Charge overcompensation and distribution. *Macromolecules* **2001,** *34* (3), 592-598.
81. Zhang, J. T.; Fredin, N. J.; Lynn, D. M., Erosion of multilayered films fabricated from degradable polyamines: Characterization and evidence in support of a mechanism that involves polymer hydrolysis. *Journal of Polymer Science Part a-Polymer Chemistry* **2006,** *44* (17), 5161-5173.
82. Dubas, S. T.; Schlenoff, J. B., Polyelectrolyte multilayers containing a weak polyacid: Construction and deconstruction. *Macromolecules* **2001,** *34* (11), 3736-3740.
83. Derbal, L.; Lesot, H.; Voegel, J. C.; Ball, V., Incorporation of alkaline phosphatase into layer-by-layer polyelectrolyte films on the surface of Affi-gel heparin beads: Physicochemical

characterization and evaluation of the enzyme stability. *Biomacromolecules* **2003,** *4* (5), 1255-1263.
84. Bonora-Centelles, A.; Jover, R.; Mirabet, V.; Lahoz, A.; Carbonell, F.; Castell, J. V.; Gomez-Lechon, M. J., Sequential Hepatogenic Transdifferentiation of Adipose Tissue-Derived Stem Cells: Relevance of Different Extracellular Signaling Molecules, Transcription Factors Involved, and Expression of New Key Marker Genes. *Cell Transplantation* **2009,** *18* (12), 1319-1340.
85. Touboul, T.; Hannan, N. R. F.; Corbineau, S.; Martinez, A.; Martinet, C.; Branchereau, S.; Mainot, S.; Strick-Marchand, H.; Pedersen, R.; Santo, J. D.; Weber, A.; Vallier, L., Generation of functional hepatocytes from human embryonic stem cells under chemically defined conditions that recapitulate liver development. *Hepatology 9999* (9999), NA.
86. Kasai M, J. T., Fukumitsu H, Furukawa S, FGF-2-responsive and spinal cord-resident cells improve locomotor function after spinal cord injury. *Journal of Neurotrauma* **2009,** *doi:10.1089/neu.2009.1108.*
87. Sanalkumar R, V. S., Lalitha Indulekha C, James J., Neuronal vs. Glial Fate of Embryonic Stem Cell-Derived Neural Progenitors (ES-NPs) is Determined by FGF2/EGF During Proliferation. *Journal of Molecular Neuroscience* **2010**.
88. Solchaga, L. A.; Penick, K.; Goldberg, V. M.; Caplan, A. I.; Welter, J. F., Fibroblast growth factor-2 enhances proliferation and delays loss of chondrogenic potential in human adult bone-marrow-derived mesenchymal stem cells. *Tissue Eng Part A 16* (3), 1009-19.
89. Betz, O. B.; Betz, V. M.; Nazarian, A.; Pilapil, C. G.; Vrahas, M. S.; Bouxsein, M. L.; Gerstenfeld, L. C.; Einhorn, T. A.; Evans, C. H., Direct percutaneous gene delivery to enhance healing of segmental bone defects. *Journal of Bone and Joint Surgery-American Volume* **2006,** *88A* (2), 355-365.
90. Lieberman, J. R.; Daluiski, A.; Einhorn, T. A., The role of growth factors in the repair of bone - Biology and clinical applications. *Journal of Bone and Joint Surgery-American Volume* **2002,** *84A* (6), 1032-1044.
91. Ma, T.; Gutnick, J.; Salazar, B.; Larsen, M. D.; Suenaga, E.; Zilber, S.; Huang, Z.; Huddleston, J.; Smith, R. L.; Goodman, S., Modulation of allograft incorporation by growth factors over a prolonged continuous infusion of duration in vivo. *Bone* **2007,** *41* (3), 386-392.
92. Murakami, S.; Takayama, S.; Ikezawa, K.; Shimabukuro, Y.; Kitamura, M.; Nozaki, T.; Terashima, A.; Asano, T.; Okada, H., Regeneration of periodontal tissues by basic fibroblast growth factor. *J. Periodont. Res.* **1999,** *34* (7), 425-430.
93. Power, R. A.; Iwaniec, U. T.; Wronski, T. J., Changes in gene expression associated with the bone anabolic effects of basic fibroblast growth factor in aged ovariectomized rats. *Bone* **2002,** *31* (1), 143-148.
94. Hanada, K.; Dennis, J. E.; Caplan, A. I., Stimulatory effects of basic fibroblast growth factor and bone morphogenetic protein-2 on osteogenic differentiation of rat bone marrow-derived mesenchymal stem cells. *Journal of Bone and Mineral Research* **1997,** *12* (10), 1606-1614.

95. Cote, M. F.; Laroche, G.; Gagnon, E.; Chevallier, P.; Doillon, C. J., Denatured collagen as support for a FGF-2 delivery system: physicochemical characterizations and in vitro release kinetics and bioactivity. *Biomaterials* **2004,** *25* (17), 3761-3772.
96. Suzuki, A.; Palmer, G.; Bonjour, J. P.; Caverzasio, J., Stimulation of sodium-dependent phosphate transport and signaling mechanisms induced by basic fibroblast growth factor in MC3T3-E1 osteoblast-like cells. *Journal of Bone and Mineral Research* **2000,** *15* (1), 95-102.
97. Tokuda, H.; Kozawa, O.; Uematsu, T., Basic fibroblast growth factor stimulates vascular endothelial growth factor release in osteoblasts: Divergent regulation by p42/p44 mitogen-activated protein kinase and p38 mitogen-activated protein kinase. *Journal of Bone and Mineral Research* **2000,** *15* (12), 2371-2379.
98. Richardson, T. P.; Peters, M. C.; Ennett, A. B.; Mooney, D. J., Polymeric system for dual growth factor delivery. *Nature biotechnology* **2001,** *19* (11), 1029-1034.
99. Kim, B. S.; Smith, R. C.; Poon, Z.; Hammond, P. T., MAD (Multiagent Delivery) Nanolayer: Delivering Multiple Therapeutics from Hierarchically Assembled Surface Coatings. *Langmuir* **2009,** *25* (24), 14086-14092.
100. Rapraeger, A. C.; Krufka, A.; Olwin, B. B., Requirement of Heparan-Sulfate for Bfgf-Mediated Fibroblast Growth and Myoblast Differentiation. *Science* **1991,** *252* (5013), 1705-1708.
101. Yayon, A.; Klagsbrun, M.; Esko, J. D.; Leder, P.; Ornitz, D. M., Cell-Surface, Heparin-Like Molecules Are Required for Binding of Basic Fibroblast Growth-Factor to Its High-Affinity Receptor. *Cell* **1991,** *64* (4), 841-848.
102. Masuoka, K.; Ishihara, M.; Asazuma, T.; Hattori, H.; Matsui, T.; Takase, B.; Kanatami, Y.; Fujita, M.; Saito, Y.; Yura, H.; Fujikawa, K.; Nemoto, K., The interaction of chitosan with fibroblast growth factor-2 and its protection from inactivation. *Biomaterials* **2005,** *26* (16), 3277-3284.
103. Maccarana, M.; Casu, B.; Lindahl, U., Minimal Sequence in Heparin Heparan-Sulfate Required for Binding of Basic Fibroblast Growth-Factor. *Journal of Biological Chemistry* **1993,** *268* (32), 23898-23905.
104. Guimond, S.; Maccarana, M.; Olwin, B. B.; Lindahl, U.; Rapraeger, A. C., Activating and Inhibitory Heparin Sequences for Fgf-2 (Basic Fgf) - Distinct Requirements for Fgf-1, Fgf-2, and Fgf-4. *Journal of Biological Chemistry* **1993,** *268* (32), 23906-23914.
105. Liu, L. S.; Ng, C. K.; Thompson, A. Y.; Poser, J. W.; Spiro, R. C., Hyaluronate-heparin conjugate gels for the delivery of basic fibroblast growth factor (FGF-2). *J. Biomed. Mater. Res.* **2002,** *62* (1), 128-135.
106. Nakamura, S.; Ishihara, M.; Obara, K.; Masuoka, K.; Ishizuka, T.; Kanatani, Y.; Takase, B.; Matsui, T.; Hattori, H.; Sato, T.; Kariya, Y.; Maehara, T., Controlled release of fibroblast growth factor-2 from an injectable 6-O-desulfated heparin hydrogel and subsequent effect on in vivo vascularization. *J. Biomed. Mater. Res. Part A* **2006,** *78A* (2), 364-371.

107. Nie, T.; Baldwin, A.; Yamaguchi, N.; Kiick, K. L., Production of heparin-functionalized hydrogels for the development of responsive and controlled growth factor delivery systems. *Journal of Controlled Release* **2007,** *122* (3), 287-296.
108. Zhang, L.; Furst, E. M.; Kiick, K. L., Manipulation of hydrogel assembly and growth factor delivery via the use of peptide-polysaccharide interactions. *Journal of Controlled Release* **2006,** *114* (2), 130-142.
109. Nikitovic, D.; Assouti, M.; Sifaki, M.; Katonis, P.; Krasagakis, K.; Karamanos, N. K.; Tzanakakis, G. N., Chondroitin sulfate and heparan sulfate-containing proteoglycans are both partners and targets of basic fibroblast growth factor-mediated proliferation in human metastatic melanoma cell lines. *International Journal of Biochemistry & Cell Biology* **2008,** *40* (1), 72-83.
110. Dziewiatkowski, D. D., Isolation of Chondroitin Sulfate-S-35 from Articular Cartilage of Rats. *Journal of Biological Chemistry* **1951,** *189* (1), 187-190.
111. Einbinder, J.; Schubert, M., Separation of Chondroitin Sulfate from Cartilage. *Journal of Biological Chemistry* **1950,** *185* (2), 725-730.
112. Schneiders, W.; Reinstorf, A.; Ruhnow, M.; Rehberg, S.; Heineck, J.; Hinterseher, I.; Biewener, A.; Zwipp, H.; Rammelt, S., Effect of chondroitin sulphate on material properties and bone remodelling around hydroxyapatite/collagen composites. *J. Biomed. Mater. Res. Part A* **2008,** *85A* (3), 638-645.
113. Shukla, A.; Fleming, K. E.; Chuang, H. F.; Chau, T. M.; Loose, C. R.; Stephanopoulos, G. N.; Hammond, P. T., Controlling the release of peptide antimicrobial agents from surfaces. *Biomaterials In Press, Corrected Proof*.
114. Schwartz, J. B.; Simonell.Ap; Higuchi, W. I., DRUG RELEASE FROM WAX MATRICES .I. ANALYSIS OF DATA WITH FIRST-ORDER KINETICS AND WITH DIFFUSION-CONTROLLED MODEL. *Journal of Pharmaceutical Sciences* **1968,** *57* (2), 274-&.
115. Rothstein, S. N.; Federspiel, W. J.; Little, S. R., A unified mathematical model for the prediction of controlled release from surface and bulk eroding polymer matrices. *Biomaterials* **2009,** *30* (8), 1657-1664.
116. von Burkersroda, F.; Schedl, L.; Gopferich, A., Why degradable polymers undergo surface erosion or bulk erosion. *Biomaterials* **2002,** *23* (21), 4221-4231.
117. Zhang, J. T.; Fredin, N. J.; Janz, J. F.; Sun, B.; Lynn, D. M., Structure/property relationships in erodible multilayered films: Influence of polycation structure on erosion profiles and the release of anionic polyelectrolytes. *Langmuir* **2006,** *22* (1), 239-245.
118. Kharlampieva, E.; Ankner, J. F.; Rubinstein, M.; Sukhishvili, S. A., pH-induced release of polyanions from multilayer films. *Phys. Rev. Lett.* **2008,** *100* (12), 4.
119. Chaudhary, L. R.; Avioli, L. V., Identification and activation of mitogen-activated protein (MAP) kinase in normal human osteoblastic and bone marrow stromal cells: Attenuation of MAP kinase activation by cAMP, parathyroid hormone and forskolin. *Mol. Cell. Biochem.* **1998,** *178* (1-2), 59-68.

120. Jackson, R. A.; Murali, S.; Van Wijnen, A. J.; Stein, G. S.; Nurcombe, V.; Cool, S. M., Heparan sulfate regulates the anabolic activity of MC3T3-E1 preosteoblast cells by induction of Runx2. *Journal of Cellular Physiology* **2007,** *210* (1), 38-50.
121. Krogman, K. C.; Zacharia, N. S.; Schroeder, S.; Hammond, P. T., Automated process for improved uniformity and versatility of layer-by-layer deposition. *Langmuir* **2007,** *23* (6), 3137-3141.
122. Schlenoff, J. B.; Dubas, S. T.; Farhat, T., Sprayed polyelectrolyte multilayers. *Langmuir* **2000,** *16* (26), 9968-9969.
123. Izquierdo, A.; Ono, S. S.; Voegel, J. C.; Schaaff, P.; Decher, G., Dipping versus spraying: Exploring the deposition conditions for speeding up layer-by-layer assembly. *Langmuir* **2005,** *21* (16), 7558-7567.
124. Krogman, K. C.; Lowery, J. L.; Zacharia, N. S.; Rutledge, G. C.; Hammond, P. T., Spraying asymmetry into functional membranes layer-by-layer. *Nature Materials* **2009,** *8* (6), 512-518.
125. Fredin, N. J.; Zhang, J. T.; Lynn, D. M., Surface analysis of erodible multilayered polyelectrolyte films: Nanometer-scale structure and erosion profiles. *Langmuir* **2005,** *21* (13), 5803-5811.
126. Folkman, J., Angiogenesis in Cancer, Vascular, Rheumatoid and Other Disease. *Nat. Med.* **1995,** *1* (1), 27-31.
127. Hurwitz, H.; Fehrenbacher, L.; Novotny, W.; Cartwright, T.; Hainsworth, J.; Heim, W.; Berlin, J.; Baron, A.; Griffing, S.; Holmgren, E.; Ferrara, N.; Fyfe, G.; Rogers, B.; Ross, R.; Kabbinavar, F., Bevacizumab plus irinotecan, fluorouracil, and leucovorin for metastatic colorectal cancer. *New England Journal of Medicine* **2004,** *350* (23), 2335-2342.
128. Sandler, A.; Gray, R.; Perry, M. C.; Brahmer, J.; Schiller, J. H.; Dowlati, A.; Lilenbaum, R.; Johnson, D. H., Paclitaxel-carboplatin alone or with bevacizumab for non-small-cell lung cancer. *New England Journal of Medicine* **2006,** *355* (24), 2542-2550.
129. Miller, K.; Wang, M. L.; Gralow, J.; Dickler, M.; Cobleigh, M.; Perez, E. A.; Shenkier, T.; Cella, D.; Davidson, N. E., Paclitaxel plus bevacizumab versus paclitaxel alone for metastatic breast cancer. *New England Journal of Medicine* **2007,** *357* (26), 2666-2676.
130. Aiello, L. P.; Avery, R. L.; Arrigg, P. G.; Keyt, B. A.; Jampel, H. D.; Shah, S. T.; Pasquale, L. R.; Thieme, H.; Iwamoto, M. A.; Park, J. E.; Nguyen, H. V.; Aiello, L. M.; Ferrara, N.; King, G. L., Vascular Endothelial Growth-Factor in Ocular Fluid of Patients with Diabetic-Retinopathy and Other Retinal Disorders. *New England Journal of Medicine* **1994,** *331* (22), 1480-1487.
131. Kvanta, A.; Algvere, P. V.; Berglin, L.; Seregard, S., Subfoveal fibrovascular membranes in age-related macular degeneration express vascular endothelial growth factor (VEGF). *Vision Res.* **1996,** *36*, 1136-1136.
132. Narayanan, R.; Kuppermann, B. D.; Jones, C.; Kirkpatrick, P., Fresh from the pipeline - Ranibizumab. *Nature Reviews Drug Discovery* **2006,** *5* (10), 815-816.
133. Jain, R. K.; Duda, D. G.; Clark, J. W.; Loeffler, J. S., Lessons from phase III clinical trials on anti-VEGF therapy for cancer. *Nat. Clin. Pract. Oncol.* **2006,** *3* (1), 24-40.

134. Bashshur, Z. F.; Schakal, A.; Hamam, R. N.; El Haibi, C. P.; Jaafar, R. F.; Noureddin, B. N., Intravitreal bevacizumab vs verteporfin photodynamic therapy for Neovascular age-related macular degeneration. *Archives of Ophthalmology* **2007,** *125* (10), 1357-1361.
135. Jessel, N.; Atalar, F.; Lavalle, P.; Mutterer, J.; Decher, G.; Schaaf, P.; Voegel, J. C.; Ogier, J., Bioactive coatings based on a polyelectrolyte multilayer architecture functionalized by embedded proteins. *Advanced Materials* **2003,** *15* (9), 692-695.
136. Cao, Y. H.; Liu, Q., Therapeutic targets of multiple angiogenic factors for the treatment of cancer and metastasis. In *Advances in Cancer Research, Vol 97*, Elsevier Academic Press Inc: San Diego, 2007; Vol. 97, pp 203-+.
137. Dvorak, H. F.; Sioussat, T. M.; Brown, L. F.; Berse, B.; Nagy, J. A.; Sotrel, A.; Manseau, E. J.; Vandewater, L.; Senger, D. R., Distribution of Vascular-Permeability Factor (Vascular Endothelial Growth-Factor) in Tumors - Concentration in Tumor Blood-Vessels. *J. Exp. Med.* **1991,** *174* (5), 1275-1278.
138. Ferrara, N., VEGF as a therapeutic target in cancer. *Oncology* **2005,** *69*, 11-16.
139. Fukumura, D.; Jain, R. K., Tumor microenvironment abnormalities: Causes, consequences, and strategies to normalize. *Journal of Cellular Biochemistry* **2007,** *101* (4), 937-949.
140. Hu, L. M.; Hofmann, J.; Holash, J.; Yancopoulos, G. D.; Sood, A. K.; Jaffe, R. B., Vascular endothelial growth factor trap combined with paclitaxel strikingly inhibits tumor and ascites, prolonging survival in a human ovarian cancer model. *Clin. Cancer Res.* **2005,** *11* (19), 6966-6971.
141. Yang, A. D.; Bauer, T. W.; Camp, E. R.; Somcio, R.; Liu, W. B.; Fan, F.; Ellis, L. M., Improving delivery of antineoplastic agents with anti-vascular endothelial growth factor therapy. *Cancer* **2005,** *103* (8), 1561-1570.
142. Wikesjo, U. M. E.; Qahash, M.; Huang, Y. H.; Xiropaidis, A.; Polimeni, G.; Susin, C., Bone morphogenetic proteins for periodontal and alveolar indications; biological observations - clinical implications. *Orthod. Craniofac. Res.* **2009,** *12* (3), 263-270.
143. Shi, Z. L.; Chua, P. H.; Neoh, K. G.; Kang, E. T.; Wang, W., Bioactive titanium implant surfaces with bacterial inhibition and osteoblast function enhancement properties. *Int. J. Artif. Organs* **2008,** *31* (9), 777-785.
144. Bergman, K.; Engstrand, T.; Hilborn, J.; Ossipov, D.; Piskounova, S.; Bowden, T., Injectable cell-free template for bone-tissue formation. *J. Biomed. Mater. Res. Part A* **2009,** *91A* (4), 1111-1118.
145. Degat, M. C.; Dubreucq, G.; Meunier, A.; Dahri-Correia, L.; Sedel, L.; Petite, H.; Logeart-Avramoglou, D., Enhancement of the biological activity of BMP-2 by synthetic dextran derivatives. *J. Biomed. Mater. Res. Part A* **2009,** *88A* (1), 174-183.
146. Jeon, O.; Song, S. J.; Kang, S. W.; Putnam, A. J.; Kim, B. S., Enhancement of ectopic bone formation by bone morphogenetic protein-2 released from a heparin-conjugated poly(L-lactic-co-glycolic acid) scaffold. *Biomaterials* **2007,** *28* (17), 2763-2771.

147. Zhou, H. J.; Qian, J. C.; Wang, J.; Yao, W. T.; Liu, C. S.; Chen, J. G.; Cao, X. H., Enhanced bioactivity of bone morphogenetic protein-2 with low dose of 2-N, 6-O-sulfated chitosan in vitro and in vivo. *Biomaterials* **2009,** *30* (9), 1715-1724.
148. Schliephake, H.; Aref, A.; Scharnweber, D.; Bierbaum, S.; Roessler, S.; Sewing, A., Effect of immobilized bone morphogenic protein 2 coating of titanium implants on peri-implant bone formation. *Clinical Oral Implants Research* **2005,** *16* (5), 563-569.
149. Aebli, N.; Stich, H.; Schawalder, P.; Theis, J. C.; Krebs, J., Effects of bone morphogenetic protein-2 and hyaluronic acid on the osseointegration of hydroxyapatite-coated implants: An experimental study in sheep. *J. Biomed. Mater. Res. Part A* **2005,** *73A* (3), 295-302.
150. Piskounova, S.; Forsgren, J.; Brohede, U.; Engqvist, H.; Stromme, M., In Vitro Characterization of Bioactive Titanium Dioxide/Hydroxyapatite Surfaces Functionalized with BMP-2. *Journal of Biomedical Materials Research Part B-Applied Biomaterials* **2009,** *91B* (2), 780-787.
151. Jewell, C. M.; Zhang, J. T.; Fredin, N. J.; Wolff, M. R.; Hacker, T. A.; Lynn, D. M., Release of plasmid DNA from intravascular stents coated with ultrathin multilayered polyelectrolyte films. *Biomacromolecules* **2006,** *7* (9), 2483-2491.
152. Lynn, D. M.; Anderson, D. G.; Putnam, D.; Langer, R., Accelerated discovery of synthetic transfection vectors: Parallel synthesis and screening of degradable polymer library. *Journal of the American Chemical Society* **2001,** *123* (33), 8155-8156.
153. Gregory, C. A.; Gunn, W. G.; Peister, A.; Prockop, D. J., An Alizarin red-based assay of mineralization by adherent cells in culture: comparison with cetylpyridinium chloride extraction. *Analytical Biochemistry* **2004,** *329* (1), 77-84.
154. Yeo, A.; Rai, B.; Sju, E.; Cheong, J. J.; Teoh, S. H., The degradation profile of novel, bioresorbable PCL-TCP scaffolds: An in vitro and in vivo study. *J. Biomed. Mater. Res. Part A* **2008,** *84A* (1), 208-218.
155. van den Beucken, J. J. J. P.; Walboomers, X. F.; Boerman, O. C.; Vos, M. R. J.; Sommerdijk, N. A. J. M.; Hayakawa, T.; Fukushima, T.; Okahata, Y.; Nolte, R. J. M.; Jansen, J. A., Functionalization of multilayered DNA-coatings with bone morphogenetic protein 2. *Journal of Controlled Release* **2006,** *113* (1), 63-72.
156. Cheng, H. W.; Jiang, W.; Phillips, F. M.; Haydon, R. C.; Peng, Y.; Zhou, L.; Luu, H. H.; An, N. L.; Breyer, B.; Vanichakarn, P.; Szatkowski, J. P.; Park, J. Y.; He, T. C., Osteogenic activity of the fourteen types of human bone morphogenetic proteins (BMPs). *Journal of Bone and Joint Surgery-American Volume* **2003,** *85A* (8), 1544-1552.
157. Gazit, D.; Ebner, R.; Kahn, A. J.; Derynck, R., MODULATION OF EXPRESSION AND CELL-SURFACE BINDING OF MEMBERS OF THE TRANSFORMING GROWTH-FACTOR-BETA SUPERFAMILY DURING RETINOIC ACID-INDUCED OSTEOBLASTIC DIFFERENTIATION OF MULTIPOTENTIAL MESENCHYMAL CELLS. *Molecular Endocrinology* **1993,** *7* (2), 189-198.
158. Yamaguchi, A.; Katagiri, T.; Ikeda, T.; Wozney, J. M.; Rosen, V.; Wang, E. A.; Kahn, A. J.; Suda, T.; Yoshiki, S., RECOMBINANT HUMAN BONE MORPHOGENETIC PROTEIN-2

STIMULATES OSTEOBLASTIC MATURATION AND INHIBITS MYOGENIC DIFFERENTIATION INVITRO. *J. Cell Biol.* **1991,** *113* (3), 681-687.
159. Liu, Y.; de Groot, K.; Hunziker, E. B., BMP-2 liberated from biomimetic implant coatings induces and sustains direct ossification in an ectopic rat model. *Bone* **2005,** *36* (5), 745-757.
160. Strauss, P.; Closs, E.; Schmidt, J.; Erfle, V., Gene expression during osteogenic differentiation in mandibular condyles in vitro. *J. Cell Biol.* **1990,** *110* (4), 1369-1378.
161. Hillger, F.; Herr, G.; Rudolph, R.; Schwarz, E., Biophysical comparison of BMP-2, ProBMP-2, and the free pro-peptide reveals stabilization of the pro-peptide by the mature growth factor. *Journal of Biological Chemistry* **2005,** *280* (15), 14974-14980.
162. Rivron, N. C.; Liu, J.; Rouwkema, J.; de Boer, J.; van Blitterswijk, C. A., Engineering vascularised tissues in vitro. *European Cells & Materials* **2008,** *15*, 27-40.
163. Muschler, G. E.; Nakamoto, C.; Griffith, L. G., Engineering principles of clinical cell-based tissue engineering. *Journal of Bone and Joint Surgery-American Volume* **2004,** *86A* (7), 1541-1558.
164. Dunn, J. C. Y.; Chan, W. Y.; Cristini, V.; Kim, J. S.; Lowengrub, J.; Singh, S.; Wu, B. M., Analysis of cell growth in three-dimensional scaffolds. *Tissue Eng.* **2006,** *12* (4), 705-716.
165. Malda, J.; Klein, T. J.; Upton, Z., The roles of hypoxia in the In vitro engineering of tissues. *Tissue Eng.* **2007,** *13* (9), 2153-2162.
166. Malda, J.; Rouwkema, J.; Martens, D. E.; le Comte, E. P.; Kooy, F. K.; Tramper, J.; van Blitterswijk, C. A.; Riesle, J., Oxygen gradients in tissue-engineered PEGT/PBT cartilaginous constructs: Measurement and modeling. *Biotechnology and Bioengineering* **2004,** *86* (1), 9-18.
167. Wendt, D.; Stroebel, S.; Jakob, M.; John, G. T.; Martin, I. In *Uniform tissues engineered by seeding and culturing cells in 3D scaffolds under perfusion at defined oxygen tensions*, 4th International Symposium on Mechanobiology of Cartilage and Chondrocyte, Budapest, HUNGARY, May 20-22; Budapest, HUNGARY, 2006; pp 481-488.
168. Hussey, M. W., XiaoLian Han, Gregory Thomas, Anthony John Penington, Wayne Allan Morrison, Kenneth Ross Knight, Sandra Joy Feeney., Seeding of pancreatic islets into pre-vascularized tissue-engineering chambers. *Tissue Engineering Part A* **2009,** *DOI 10.1089/ten.TEA.2008.0682*.
169. Pelissier, P.; Villars, F.; Mathoulin-Pelissier, S.; Bareille, R.; Lafage-Proust, M. H.; Vilamitjana-Amedee, J. In *Influences of vascularization and osteogenic cells on heterotopic bone formation within a madreporic ceramic in rats*, 25th Annual Meeting of the Society-for-Biomaterials, Providence, Rhode Island, Apr 28-May 02; Lippincott Williams & Wilkins: Providence, Rhode Island, 1999; pp 1932-1941.
170. Levenberg, S.; Rouwkema, J.; Macdonald, M.; Garfein, E. S.; Kohane, D. S.; Darland, D. C.; Marini, R.; van Blitterswijk, C. A.; Mulligan, R. C.; D'Amore, P. A.; Langer, R., Engineering vascularized skeletal muscle tissue. *Nature biotechnology* **2005,** *23* (7), 879-84.

171. Red-Horse, K.; Crawford, Y.; Shojaei, F.; Ferrara, N., Endothelium-microenvironment interactions in the developing embryo and in the adult. *Developmental Cell* **2007,** *12* (2), 181-194.
172. Kaully, T.; Kaufman-Francis, K.; Lesman, A.; Levenberg, S., Vascularization-The Conduit to Viable Engineered Tissues. *Tissue Engineering Part B-Reviews* **2009,** *15* (2), 159-169.
173. Nahmias, Y.; Schwartz, R. E.; Hu, W. S.; Verfaillie, C. M.; Odde, D. J., Endothelium-mediated hepatocyte recruitment in the establishment of liver-like tissue in vitro. *Tissue Eng.* **2006,** *12* (6), 1627-1638.
174. Darland, D. C. a. D. A. P., TGF beta is required for the formation of capillary-like structures in three-dimensional cocultures of 10T1/2 and endothelial cells. *Angiogenesis* **2001,** *4* (1), 11-20.
175. Kumar, A.; Whitesides, G. M., Features of Gold Having Micrometer to Centimeter Dimensions Can Be Formed through a Combination of Stamping with an Elastomeric Stamp and an Alkanethiol Ink Followed by Chemical Etching. *Applied Physics Letters* **1993,** *63* (14), 2002-2004.
176. Jackman, R. J.; Wilbur, J. L.; Whitesides, G. M., Fabrication of Submicrometer Features on Curved Substrates by Microcontact Printing. *Science* **1995,** *269* (5224), 664-666.
177. Park, T. H.; Shuler, M. L., Integration of cell culture and microfabrication technology. *Biotechnol. Prog.* **2003,** *19* (2), 243-253.
178. Jiang, X. P.; Zheng, H. P.; Gourdin, S.; Hammond, P. T., Polymer-on-polymer stamping: Universal approaches to chemically patterned surfaces. *Langmuir* **2002,** *18* (7), 2607-2615.
179. Katanosaka, Y.; Bao, J. H.; Komatsu, T.; Suemori, T.; Yamada, A.; Mohri, S.; Naruse, K., Analysis of cyclic-stretching responses using cell-adhesion-patterned cells. *Journal of Biotechnology* **2008,** *133* (1), 82-89.
180. Pierschbacher, M. D.; Ruoslahti, E., Cell Attachment Activity of Fibronectin Can Be Duplicated by Small Synthetic Fragments of the Molecule. *Nature* **1984,** *309* (5963), 30-33.
181. Shen, J. Y.; Chan-Park, M. B.; Zhu, A. P.; Zhu, X.; Beuerman, R. W.; Yang, E. B.; Chen, W.; Chan, V., Three-dimensional microchannels in biodegradable polymeric films for control orientation and phenotype of vascular smooth muscle cells. *Tissue Eng.* **2006,** *12* (8), 2229-2240.
182. Feng, J.; Chan-Park, M. B.; Shen, J. Y.; Chan, V., Quick layer-by-layer assembly of aligned multilayers of vascular smooth muscle cells in deep microchannels. *Tissue Eng.* **2007,** *13* (5), 1003-1012.
183. Wood, K. C.; Zacharia, N. S.; Schmidt, D. J.; Wrightman, S. N.; Andaya, B. J.; Hammond, P. T., Electroactive controlled release thin films. *Proceedings of the National Academy of Sciences of the United States of America* **2008,** *105* (7), 2280-2285.